New Zealand Fisheries
Assessment Report
2009/34
July 2009
ISSN 1175-1584

The 2008 stock assessment of paua (*Haliotis iris*) in PAU 7

Andy McKenzie
Adam N. H. Smith

The 2008 stock assessment of paua (*Haliotis iris*) in PAU 7

Andy McKenzie
Adam N. H. Smith

NIWA
Private Bag 14901
Wellington 6241

New Zealand Fisheries Assessment Report 2009/34
July 2009

Published by Ministry of Fisheries
Wellington
2009

ISSN 1175-1584

McKenzie, A.; Smith, A.N.H. (2009).
The 2008 stock assessment of paua (*Haliotis iris*) in PAU 7.
New Zealand Fisheries Assessment Report 2009/34. 84 p.

This series continues the informal
New Zealand Fisheries Assessment Research Document series
which ceased at the end of 1999.

EXECUTIVE SUMMARY

McKenzie, A.; Smith, A.N.H. (2009). The 2008 stock assessment of paua (*Haliotis iris*) in PAU 7.

***New Zealand Fisheries Assessment Report 2009/34*. 84 p.**

A length-based stock assessment model was used to assess the PAU 7 paua (abalone, *Haliotis iris*) stock. The assessment used Bayesian techniques to estimate model parameters, the state of the stock, future states of the stock, and their uncertainties. Point estimates from the mode of the joint posterior distribution were used to explore sensitivity of the results to model assumptions and the input data; the assessment itself was based on marginal posterior distributions generated from Markov chain-Monte Carlo simulation.

The model was revised slightly from the 2005 assessment model used for PAU 7 by the inclusion of a common observation error term in the tag-recapture data likelihood, which is also in the other data likelihoods.

The model was fitted to seven datasets from areas 17 and 38 within PAU 7: two standardised CPUE series, a standardised index of relative abundance from research diver surveys, proportions-at-length from commercial catch sampling and research diver surveys, tag-recapture data, and maturity-at-length data.

Iterative re-weighting of the datasets produced a base case result in which the standard deviations of the normalised residuals were close to unity for most datasets. Model results for PAU 7 suggest a stock that is depleted: current levels of spawning and recruited biomass are below agreed reference levels from an earlier period in the fishery history. However, the current exploitation rate is moderate, at an estimated 37%.

The model projections, made for three years using recruitments re-sampled from the recent model estimates, suggest a very strong likelihood of rebuilding for both spawning and recruited biomass. Risks of decreased biomass are small.

1. INTRODUCTION

1.1 Overview

This document presents a Bayesian stock assessment of blackfoot paua (abalone, Haliotis iris) in PAU 7 (at the northern end of the South Island, Figure 1) using data to the end of 2007–08. The assessment is made with the length-based model first used in 1999 for PAU 5B (Breen et al. 2000a) and revised for subsequent assessments in PAU 5B (Stewart Island) and PAU 7 (Andrew et al. 2000a, Breen et al. 2000b, 2001, Breen & Kim 2003, 2005). Model revisions made for PAU 4 (Breen & Kim, 2004a) and PAU 5A (Breen & Kim 2004b) in 2004 were mostly discarded. The model was published by Breen et al. (2003).

Most catches have been taken from statistical areas 17 and 38. There is no time series of research diver surveys from outside these areas, and proportions-at-length from commercial catch sampling are very different from the other two areas, 18 and 36. Accordingly, Breen et al. (2001) and Breen & Kim (2003, 2005) based their assessments on areas 17 and 38 only. The Shellfish Fishery Assessment Working Group agreed to continue this practice for this assessment.

The seven sets of data fitted to in the assessment model were: (1) a standardised CPUE series covering 1983–2001 based on FSU/CELR data, (2) a standardised CPUE series covering 2002–2005 based on PCELR data, (3) a standardised research diver survey index (RDSI), (4) a research diver survey proportions-at-lengths series, (5) A commercial catch sampling length frequency series, (6) tag-recapture length increment data, and (7) maturity-at-length data. Catch history was an input to the model, encompassing commercial, recreational, customary, and illegal catch. Another document describes the datasets that are used in the stock assessment and the updates that were made for the 2008 assessment (McKenzie & Smith 2009).

The assessment was made in several steps. First, the model was fitted to the data with arbitrary weights on the various data sets. The weights were then iteratively adjusted to produce balanced residuals among the datasets. The fit obtained is the mode of the joint posterior distribution of parameters (MPD). Next, from the resulting fit, Markov chain-Monte Carlo (MCMC) simulations were made to obtain a large set of samples from the joint posterior distribution. From this set of samples, forward projections were made with different assumed catch levels and a set of agreed indicators was obtained. Sensitivity of the results was explored by comparing MPD fits made with datasets removed one at a time and by comparing MCMC retrospective analyses.

This document describes the model, assumptions made in fitting, the fit of the model to the data, projection results, and sensitivity trials.

1.2 Description of the fishery

The paua fishery was summarised by Schiel (1992), Annala et al. (2003), and in numerous previous assessment documents (e.g., Schiel 1989, McShane et al. 1994, 1996, Breen et al. 2000a, 2000b, 2001, Breen & Kim 2003, 2004a, 2004b). A further summary is not presented here.

The fishing year for paua is from 1 October to 30 September. In what follows we refer to fishing year by the second portion; thus we call the 1997–98 fishing year "1998".

2. MODEL

This section gives an overview of the model used for stock assessment of PAU 7 in 2008; for full details see Breen & Kim (2005). The model was developed for use in PAU 5B in 1999 and has been revised each year for subsequent assessments, in many cases echoing changes made to the rock lobster assessment model (Breen et al. 2002, Kim et al. 2004), which is a similar but more complex length-based Bayesian model. Only minor changes were made in 2008 to the 2005 assessment model (Breen & Kim 2005).

2.1 Changes to the 2005 assessment model

Only one minor change was made. Echoing a change made to the PAU 5B model, the common observation error component ($\tilde{\sigma}$) was introduced to the tag-recapture likelihood function:

$$-\ln(\mathbf{L})\left(\hat{d}_j \mid \theta\right) = \frac{\left(d_j - \hat{d}_j\right)^2}{2\left(\sigma_j^{tag}\right)^2} + \ln\left(\sigma_j^{tag}\right) + 0.5\ln\left(2\pi\right),$$

where

$$\sigma_j^{tag} = \tilde{\sigma} / \varpi^{tag} \sqrt{\sigma_{obs}{}^2 + \left(\sigma_j{}^d\right)^2}$$

Two further model changes were explored: (1) using a multinomial likelihood for the length-frequency data, and (2) using an inverse logistic growth curve instead of the exponential growth (Haddon et al. 2008). Neither of the changes improved the model, and were not used in final model runs.

2.2 Model description

The model (BLePSAM: Bayesian Length-based Paua Stock Assessment Model) does not use age; instead it uses a number of length bins (51 in this assessment), each of 2 mm shell length. The left-hand edge of the first bin is 70 mm and the largest bin is well above the maximum size observed. Sexes are not distinguished. The time step is one year for the main dynamics. There is no spatial structure within the area modelled. The model is implemented in AD Model Builder™ (Otter Research Ltd., http://otter-rsch.com/admodel.htm) version 6.2.1, compiled with the Borland 5.01 compiler.

2.2.1 Estimated parameters

Parameters estimated by the model are as follows. The parameter vector is referred to collectively as θ.

$\ln(R0)$	natural logarithm of base recruitment
M	instantaneous rate of natural mortality
g_α	expected annual growth increment at length α
g_β	expected annual growth increment at length β
ϕ	c.v. of the expected growth increment

q^I	scalar between recruited biomass and CPUE
X	coefficient of proportionality between q^I and q^{I2}, the scalar for PCPUE
q^J	scalar between numbers and the RDSI
L_{50}	length at which maturity is 50%
L_{95-50}	interval between L_{50} and L_{95}
T_{50}	length at which research diver selectivity is 50%
T_{95-50}	distance between T_{50} and T_{95}
D_{50}	length at which commercial diver selectivity is 50%
D_{95-50}	distance between D_{50} and D_{95}
$\tilde{\sigma}$	common component of error
h	shape of CPUE *vs.* biomass relation
ε	vector of annual recruitment deviations, estimated from 1977 to 2004

2.2.2 Constants

l_k	length of an abalone at the midpoint of the kth length class (l_k for class 1 is 71 mm, for class 2 is 73 mm and so on)
σ_{MIN}	minimum standard deviation of the expected growth increment (assumed to be 1 mm)
σ_{obs}	standard deviation of the observation error around the growth increment (assumed to be 0.25 mm)
MLS_t	minimum legal size in year t (assumed to be 125 mm for all years)
$P_{k,t}$	a switch based whether abalone in the kth length class in year t are above the minimum legal size (MLS) ($P_{k,t} = 1$) or below ($P_{k,t} = 0$)
a, b	constants for the length-weight relation, taken from Schiel & Breen (1991) (2.592E-08 and 3.322 respectively, giving weight in kg)
w_k	the weight of an abalone at length l_k
ϖ^I	relative weight assigned to the CPUE dataset. This and the following relative weights were varied between runs to find a basecase with balanced residuals
ϖ^{I2}	relative weight assigned to the PCPUE dataset.
ϖ^J	relative weight assigned to the RDSI dataset
ϖ^r	relative weight assigned to RDLF dataset
ϖ^s	relative weight assigned to CSLF dataset
ϖ^{mat}	relative weight assigned to maturity-at-length data
ϖ^{tag}	relative weight assigned to tag-recapture data
κ_t^s	normalised square root of the number measured greater than 113 mm in CSLF records for each year, normalised by the lowest year
κ_t^r	normalised square root of the number measured greater than 89 mm in RDLF records for each year, normalised by the lowest year
$U^{\max}$	exploitation rate above which a limiting function was invoked (0.80 for the base case)

μ_M	mean of the prior distribution for *M*, based on a literature review by Shepherd & Breen (1992)
σ_M	assumed standard deviation of the prior distribution for *M*
σ_ε	assumed standard deviation of recruitment deviations in log space (part of the prior for recruitment deviations)
n_ε	number of recruitment deviations
α	length associated with g_α (75 mm)
β	length associated with g_β (120 mm)

2.2.3 Observations

C_t	observed catch in year *t*
I_t	standardised CPUE in year *t*
$I2_t$	standardised PCPUE in year *t*
σ_t^I	standard deviation of the estimate of observed CPUE in year *t*, obtained from the standardisation model
σ_t^{I2}	standard deviation of the estimate of observed PCPUE in year *t*, obtained from the standardisation model
J_t	standardised RDSI in year *t*
σ_t^J	the standard deviation of the estimate of RDSI in year t, obtained from the standardisation model
$p_{k,t}^r$	observed proportion in the *k*th length class in year *t* in RDLF
$p_{k,t}^s$	observed proportion in the *k*th length class in year *t* in CSLF
l_j	initial length for the *j*th tag-recapture record
d_j	observed length increment of the *j*th tag-recapture record
Δt_j	time at liberty for the *j*th tag-recapture record
p_k^{mat}	observed proportion mature in the *k*th length class in the maturity dataset

2.2.4 Derived variables

R0	base number of annual recruits
$N_{k,t}$	number of abalone in the *k*th length class at the start of year *t*
$N_{k,t+0.5}$	number of abalone in the *k*th length class in the mid-season of year *t*
$R_{k,t}$	recruits to the model in the *k*th length class in year *t*
g_k	expected annual growth increment for abalone in the *k*th length class
σ^{g_k}	standard deviation of the expected growth increment for abalone in the *k*th length class, used in calculating $\mathbf{G}$
$\mathbf{G}$	growth transition matrix
B_t	biomass of abalone available to the commercial fishery at the beginning of year *t*

$B_{t+0.5}$ biomass of abalone above the MLS in the mid-season of year *t*

$S_{t+0.5}$ biomass of mature abalone in the mid-season of year *t*

U_t exploitation rate in year *t*

A_t the complement of exploitation rate

$SF_{k,t}$ finite rate of survival from fishing for abalone in the *k*th length class in year *t*

V_k^r relative selectivity of research divers for abalone in the *k*th length class

V_k^s relative selectivity of commercial divers for abalone in the *k*th length class

$\sigma_{k,t}^r$ error of the predicted proportion in the *k*th length class in year *t* in RDLF data

$\sigma_{k,t}^s$ error of the predicted proportion in the *k*th length class in year *t* in CSLF data

σ_j^d standard deviation of the predicted length increment for the *j*th tag-recapture record

σ_j^{tag} total error predicted for the *j*th tag-recapture record

σ_k^{mat} error of the proportion mature-at-length for the *k*th length class

$-\ln(\mathbf{L})$ negative log-likelihood

f total function value

2.2.5 Predictions

$\hat{I}_t$ predicted CPUE in year *t*

$\hat{I}2_t$ predicted PCPUE in year *t*

$\hat{J}_t$ predicted RDSI in year *t*

$\hat{p}_{k,t}^r$ predicted proportion in the *k*th length class in year *t* in research diver surveys

$\hat{p}_{k,t}^s$ predicted proportion in the *k*th length class in year *t* in commercial catch sampling

$\hat{d}_j$ predicted length increment of the *j*th tag-recapture record

$\hat{p}_k^{mat}$ predicted proportion mature in the *k*th length class

2.2.6 Initial conditions

The initial population is assumed to be in equilibrium with zero fishing mortality and the base recruitment. The model is run for 60 years with no fishing to obtain near-equilibrium in numbers-at-length. Recruitment is evenly divided among the first five length bins:

(1) $R_{k,t} = 0.2R0$ for $1 \le k \le 5$

(2) $R_{k,t} = 0$ for $k > 5$

A growth transition matrix is calculated inside the model from the estimated growth parameters. If the growth model is linear, the expected annual growth increment for the *k*th length class is

$$\Delta l_k = \left(\frac{\beta g_\alpha - \alpha g_\beta}{g_\alpha - g_\beta} - l_k \right) \left[1 - \left(1 + \frac{g_\alpha - g_\beta}{\alpha - \beta} \right) \right] \quad (3)$$

The model uses the AD Model Builder™ function *posfun*, with a dummy penalty, to ensure a positive expected increment at all lengths, using a smooth differentiable function. The *posfun* function is also used with a real penalty to force the quantity $\left(1 + \frac{g_\alpha - g_\beta}{\alpha - \beta} \right)$ to remain positive.

If the growth model is exponential (used for the base case), the expected annual growth increment for the *k*th length class is

$$\Delta l_k = g_\alpha \left(g_\beta / g_\alpha \right)^{(l_k - \alpha)/(\beta - \alpha)} \quad (4)$$

again using *posfun* with a dummy penalty to ensure a positive expected increment at all lengths.

The standard deviation of g_k is assumed to be proportional to g_k with minimum σ_{MIN}:

$$\sigma^{g_k} = \left(g_k \phi - \sigma_{MIN} \right) \left(\frac{1}{\pi} \tan^{-1} \left(10^6 \left(g_k \phi - \sigma_{MIN} \right) \right) + 0.5 \right) + \sigma_{MIN} \quad (5)$$

From the expected increment and standard deviation for each length class, the probability distribution of growth increments for an abalone of length l_k is calculated from the normal distribution and translated into the vector of probabilities of transition from the *k*th length bin to other length bins to form the growth transition matrix **G**. Zero and negative growth increments are permitted, i.e., the probability of staying in the same bin or moving to a smaller bin can be non-zero.

In the initialisation, the vector $\mathbf{N_t}$ of numbers-at-length is determined from numbers in the previous year, survival from natural mortality, the growth transition matrix **G,** and the vector of recruitment $\mathbf{R_t}$:

$$\mathbf{N_t} = \left(\mathbf{N_{t-1}} \, e^{-M} \right) \bullet \mathbf{G} + \mathbf{R_t} \quad (6)$$

where the dot (•) denotes matrix multiplication.

2.2.7 Dynamics

2.2.7.1 Sequence of operations

After initialising, the first model year is 1965 and the model is run through 2008. In the first 9 years the model is run with an assumed catch vector, because it is unrealistic to assume that the fishery was in a virgin state when the first catch data became available in 1974. The assumed catch vector rises linearly from zero to the 1974 catch. These years can be thought of as an additional part of the initialisation, but they use the dynamics described in this section.

Model dynamics are sequenced as follows:

- numbers at the beginning of year *t*-1 are subjected to fishing, then natural mortality, then growth to produce the numbers at the beginning of year *t*.
- recruitment is added to the numbers at the beginning of year *t*.
- biomass available to the fishery is calculated and, with catch, is used to calculate the exploitation rate, which is constrained if necessary.
- half the exploitation rate (but no natural mortality) is applied to obtain mid-season numbers, from which the predicted abundance indices and proportions-at-length are calculated. Mid-season numbers are not used further.

2.2.7.2 Main dynamics

For each year *t*, the model calculates the start-of-the-year biomass available to the commercial fishery. Biomass available to the commercial fishery is:

$$B_t = \sum_k N_{k,t} V_k^s w_k \tag{7}$$

where

$$V_k^s = \frac{1}{1+19^{-\left(\left(l_k - D_{50}\right)/D_{95-50}\right)}} \tag{8}$$

The observed catch is then used to calculate exploitation rate, constrained for all values above U^{max} with the *posfun* function of AD Model Builder™. If the ratio of catch to available biomass exceeds U^{max}, then exploitation rate is constrained and a penalty is added to the total negative log-likelihood function. Let minimum survival rate A_{min} be 1-U^{max} and survival rate A_t be 1-U_t:

$$A_t = 1 - \frac{C_t}{B_t} \quad \text{for} \quad \frac{C_t}{B_t} \le U^{\max} \tag{9}$$

$$A_t = 0.5 A_{\min}\left[1 + \left(3 - \frac{2\left(1 - \frac{C_t}{B_t}\right)}{A_{\min}}\right)^{-1}\right] \quad \text{for} \quad \frac{C_t}{B_t} > U^{\max} \tag{10}$$

The penalty invoked when the exploitation rate exceeds U^{max} is:

$$1000000\left(A_{\min} - \left(1 - \frac{C_t}{B_t}\right)\right)^2 \tag{11}$$

This prevents the model from exploring parameter combinations that give unrealistically high exploitation rates. Survival from fishing is calculated as:

$$SF_{k,t} = 1 - \left(1 - A_t\right) P_{k,t} \tag{12}$$

or

(13) $$SF_{k,t} = 1 - \left(1 - A_t\right) V_k^s$$

The vector of numbers-at-length in year *t* is calculated from numbers in the previous year:

(14) $$\mathbf{N_t} = \left(\left(\mathbf{SF_{t-1}} \otimes \mathbf{N_{t-1}}\right) \mathrm{e}^{-M}\right) \bullet \mathbf{G} + \mathbf{R_t}$$

where $\otimes$ denotes the element-by-element vector product. The vector of recruitment, $\mathbf{R_t}$, is determined from *R0* and the estimated recruitment deviations:

(15) $$R_{k,t} = 0.2R0e^{\left(\varepsilon_t - 0.5\sigma_\varepsilon^2\right)} \qquad \text{for } 1 \le k \le 5$$

(16) $$R_{k,t} = 0 \qquad \text{for } k > 5$$

The recruitment deviation parameters ε_t were estimated for all years from 1977; there was no constraint for deviations to have a mean of 1 in arithmetic space except for the constraint of the prior, which had a mean of zero in log space; and we assumed no stock recruitment relationship.

2.2.8 Model predictions

The model predicts CPUE in year *t* from mid-season recruited biomass, the scaling coefficient and the shape parameter:

(17) $$\hat{I}_t = q^I \left(B_{t+0.5}\right)^h$$

Available biomass $B_{t+0.5}$ is the mid-season vulnerable biomass after half the catch has been removed (no natural mortality is applied, because the time over which half the catch is removed might be short). It is calculated as in equation (7), but using the mid-year numbers, $N_{k,t+0.5}$:

(18) $$N_{k,t+0.5}^{vuln} = N_{k,t}\left(1 - \frac{\left(1 - A_t\right)}{2} V_k^s\right).$$

Similarly,

(19) $$\hat{I}2_t = q^{I2}\left(B_{t+0.5}\right)^h = Xq^I\left(B_{t+0.5}\right)^h$$

The same shape parameter *h* is used for both series: experiment outside the model showed that this was appropriate despite the different units of measurement for the two series. The predicted research diver survey index is calculated from mid-season model numbers in bins greater than 89 mm length, taking into account research diver selectivity-at-length:

(20) $$N_{k,t+0.5}^{res} = N_{k,t}\left(1 - \frac{\left(1 - A_t\right)}{2} V_k^r\right)$$

(21) $$\hat{J}_t = q^J \sum_{k=11}^{55} N^{res}_{k,t+0.5}$$

where the scalar is estimated and the research diver selectivity V^r_k is calculated from:

(22) $$V^r_k = \frac{1}{1+19^{-\left((l_k - T_{50})/T_{95-50}\right)}}$$

The model predicts proportions-at-length for the RDLF from numbers in each length class for lengths greater than 89 mm:

(23) $$\hat{p}^r_{k,t} = \frac{N^{res}_{k,t+0.5}}{\sum_{k=11}^{51} N^{res}_{k,t+0.5}} \qquad \text{for } 11 \le k < 51$$

Predicted proportions-at-length for CSLF are similar:

(24) $$\hat{p}^s_{k,t} = \frac{N^{vuln}_{k,t+0.5}}{\sum_{k=23}^{51} N^{vuln}_{k,t+0.5}} \qquad \text{for } 23 \le k < 51$$

The predicted increment for the *j*th tag-recapture record, using the linear model, is

(25) $$\hat{d}_j = \left(\frac{\beta g_\alpha - \alpha g_\beta}{g_\alpha - g_\beta} - L_j \right) \left[1 - \left(1 + \frac{g_\alpha - g_\beta}{\alpha - \beta} \right)^{\Delta t_j} \right]$$

where Δt_j is in years. For the exponential model (used in the base case) the expected increment is

(26) $$\hat{d}_j = \Delta t_j g_\alpha \left(g_\beta / g_\alpha \right)^{(L_j - \alpha)/(\beta - \alpha)}$$

The error around an expected increment is

(27) $$\sigma_j{}^d = \left(\hat{d}_j \phi - \sigma_{MIN} \right) \left(\frac{1}{\pi} \tan^{-1} \left(10^6 \left(\hat{d}_j \phi - \sigma_{MIN} \right) \right) + 0.5 \right) + \sigma_{MIN}$$

Predicted maturity-at-length is

(28) $$\hat{p}^{mat}_k = \frac{1}{1+19^{-\left((l_k - L_{50})/L_{95-50}\right)}}$$

2.2.9 Fitting

2.2.9.1 Likelihoods

The distribution of CPUE is assumed to be normal-log and the negative log-likelihood is:

$$-\ln(\mathbf{L})\left(\hat{I}_t \mid \theta\right) = \frac{\left(\ln\left(I_t\right) - \ln\left(\hat{I}_t\right)\right)^2}{2\left(\sigma_t^I \tilde{\sigma} / \varpi^I\right)^2} + \ln\left(\sigma_t^I \tilde{\sigma} / \varpi^I\right) + 0.5\ln\left(2\pi\right) \quad (29)$$

and similarly for PCPUE:

$$-\ln(\mathbf{L})\left(\hat{I}2_t \mid \theta\right) = \frac{\left(\ln\left(I2_t\right) - \ln\left(\hat{I}2_t\right)\right)^2}{2\left(\sigma_t^{I2} \tilde{\sigma} / \varpi^{I2}\right)^2} + \ln\left(\sigma_t^{I2} \tilde{\sigma} / \varpi^{I2}\right) + 0.5\ln\left(2\pi\right) \quad (30)$$

The distribution of the RDSI is also assumed to be normal-log and the negative log-likelihood is:

$$-\ln(\mathbf{L})\left(\hat{J}_t \mid \theta\right) = \frac{\left(\ln\left(J_t\right) - \ln\left(\hat{J}_t\right)\right)^2}{2\left(\sigma_t^J \tilde{\sigma} / \varpi^J\right)^2} + \ln\left(\sigma_t^J \tilde{\sigma} / \varpi^J\right) + 0.5\ln\left(2\pi\right) \quad (31)$$

The proportions-at-length from CSLF data are assumed to be normally distributed, with a standard deviation that depends on the proportion, the number measured, and the weight assigned to the data:

$$\sigma_{k,t}^s = \frac{\tilde{\sigma}}{\kappa_t^s \varpi^s \sqrt{p_{k,t}^s + 0.1}} \quad (32)$$

The negative log-likelihood is:

$$-\ln(\mathbf{L})\left(\hat{p}_{k,t}^s \mid \theta\right) = \frac{\left(p_{k,t}^s - \hat{p}_{k,t}^s\right)^2}{2\left(\sigma_{k,t}^s\right)^2} + \ln\left(\sigma_{k,t}^s\right) + 0.5\ln\left(2\pi\right) \quad (33)$$

The likelihood for research diver sampling is analogous. Errors in the tag-recapture dataset were also assumed to be normal. For the *j*th record, the total error is a function of the predicted standard deviation (equation (27)), observation error, and weight assigned to the data:

$$\sigma_j^{tag} = \tilde{\sigma} / \varpi^{tag} \sqrt{{\sigma_{obs}}^2 + \left({\sigma_j}^d\right)^2} \quad (34)$$

and the negative log-likelihood is:

$$-\ln(\mathbf{L})\left(\hat{d}_j \mid \theta\right) = \frac{\left(d_j - \hat{d}_j\right)^2}{2\left(\sigma_j^{tag}\right)^2} + \ln\left(\sigma_j^{tag}\right) + 0.5\ln\left(2\pi\right) \quad (35)$$

The proportion mature-at-length was assumed to be normally distributed, with standard deviation analogous to proportions-at-length:

$$\sigma_k^{mat} = \frac{\tilde{\sigma}}{\varpi^{mat}\sqrt{p_k^{mat} + 0.1}} \quad (36)$$

The negative log-likelihood is:

$$-\ln(\mathbf{L})\left(\hat{p}_k^{mat} \mid \theta\right) = \frac{\left(p_k^{mat} - \hat{p}_k^{mat}\right)^2}{2\left(\sigma_k^{mat}\right)^2} + \ln\left(\sigma_k^{mat}\right) + 0.5\ln\left(2\pi\right) \quad (37)$$

2.2.9.2 Normalised residuals

These are calculated as the residual divided by the relevant σ term used in the likelihood. For CPUE, the normalised residual is

$$\frac{\ln\left(I_t\right) - \ln\left(\hat{I}_t\right)}{\left(\sigma_t^I \tilde{\sigma} \Big/ \varpi^I\right)} \quad (38)$$

and similarly for PCPUE and RDSI. For the CSLF proportions-at-length, the residual is

$$\frac{p_{k,t}^s - \hat{p}_{k,t}^s}{\sigma_{k,t}^s} \quad (39)$$

and similarly for proportions-at-length from the RDLFs. Because the vectors of observed proportions contain many empty bins, the residuals for proportions-at-length include large numbers of small residuals, which distort the frequency distribution of residuals. When presenting normalised residuals from proportions-at-length, we arbitrarily ignore normalised residuals less than 0.05.

For tag-recapture data, the residual is

$$\frac{d_j - \hat{d}_j}{\sigma_j^{tag}} \quad (40)$$

and for the maturity-at-length data the residual is

$$\frac{p_k^{mat} - \hat{p}_k^{mat}}{\sigma_k^{mat}} \quad (41)$$

2.2.9.3 Dataset weights

Weights were chosen experimentally in choosing a base case, iteratively changing them to obtain standard deviations of the normalised residuals (*sdnr*) close to unity for each dataset.

2.2.9.4 Priors and bounds

Bayesian priors were established for all estimated parameters. Most were incorporated simply as uniform distributions with upper and lower bounds arbitrarily set wide so as not to constrain the estimation. The prior probability density for M was a normal-log distribution with mean μ_M and standard deviation σ_M. The contribution to the objective function of estimated $M = x$ is:

$$(42) \qquad -\ln(\mathbf{L})(x \mid \mu_M, \sigma_M) = \frac{\left(\ln(M) - \ln(\mu_M)\right)^2}{2\sigma_M{}^2} + \ln\left(\sigma_M \sqrt{2\pi}\right)$$

The prior probability density for the vector of estimated recruitment deviations, ε, was assumed to be normal with a mean of zero. The contribution to the objective function for the whole vector is:

$$(43) \qquad -\ln(\mathbf{L})(\varepsilon \mid \mu_\varepsilon, \sigma_\varepsilon) = \frac{\sum_{i=1}^{n_\varepsilon} (\varepsilon_i)^2}{2\sigma_\varepsilon{}^2} + \ln(\sigma_\varepsilon) + 0.5\ln(2\pi).$$

2.2.9.5 Penalty

A penalty is applied to exploitation rates higher than the assumed maximum (equation 10); it is added to the objective function after being multiplied by an arbitrary weight (1E6) determined by experiment.

AD Model Builder™ also has internal penalties that keep estimated parameters within their specified bounds, but these should have no effect on the final outcome, because choice of a base case excludes the situations where parameters are estimated at or near a bound.

2.2.10 Fishery indicators

The assessment is based on the following indicators calculated from their posterior distributions: the model's mid-season recruited and spawning biomass from 2008 (current biomass), from 2011 (projected biomass), from the nadir (lowest point) of the population trajectory (Bmin and Smin), and from a reference period, 1985–87. This was a period when the biomass was stable, production was good, and there was a subsequent period when the fishery flourished. The means of values from the three years were called Sav and Bav for spawning and recruited biomass respectively. We also used annual exploitation rate in 2008, U05, and in 2011, U11. Ratios of these reference points are also used.

Six additional indicators are calculated as the percentage of runs in which:

spawning biomass in 2011 had decreased from 2008: *S11<S08*
spawning biomass in 2011 was less than the reference level: *S11<Sav*

spawning biomass in 2011 was less than the nadir: *S11<Smin*
recruited biomass in 2011 had decreased from 2008: *B11<B08*
recruited biomass in 2011 was less than the reference level: *B11<Bav*
recruited biomass in 2011 was less than the nadir: *B11<Bmin*

2.2.11 Markov chain-Monte Carlo (MCMC) procedures

AD Model Builder™ uses the Metropolis-Hastings algorithm. The step size is based on the standard errors of the parameters and their covariance relationships, estimated from the Hessian matrix.

For the MCMCs in this assessment we ran single long chains that started at the MPD estimate. The base case was 5 million simulations long and we saved samples, regularly spaced by 5000. For sensitivities we made chains of 2.5 million, saving samples regularly spaced by 5000. In all MCMC trials we fixed the value of $\tilde{\sigma}$ to the estimated MPD value because it may be inappropriate to let a variance component change during the MCMC.

2.2.12 Sensitivity trials

These involved trials based on the MPD estimates and other trials based on full sets of MCMC simulations.

For the MPD trials, datasets were removed one at a time (seven trials), the model was fitted to a single CPUE series from 1983 to 2007, based on catch per diver day, and the inverse logistic model for growth was used. For the single CPUE series only, the data were iteratively re-weighted to balance the sdnrs; in all other trials the weights were left as in the base case.

The MCMC trials comprised retrospective trials in which data (except for tag-recapture data) were removed one year at a time for comparison with the base case. Two and half million MCMC simulations were made in each trial and 500 samples saved.

Two MCMC trials were made in which the assumed maximum exploitation rate, $U^{\max}$, was changed from 0.80 in the base case to 0.65 and 0.90.

2.2.13 Alternative non-commercial catch projections

Stochastic projections were made through 2008 by running the dynamics forward in time with each of the 500 parameter vectors, driving the model with a specified catch vector, this being the assumed catch for 2008 (202.1 t). The sequence of operations was as described for the main dynamics.

Recruitment in projections was stochastic, obtained by re-sampling the recruitments estimated from 1997 to 2006. Because the 2008 recruitment deviation is poorly determined by the data (it has no effect on any of the quantities being fitted), the estimated value is inappropriate for projections and was over-written with values obtained by re-sampling. Projected exploitation rate in projections is limited by simply truncating it at the specified maximum.

Two alternative projections were made with different assumptions for the non-commercial catch: (a) zero non-commercial catch and (b) the linear ramp in the non-commercial catch from 1974 to 2000 continued until 2011. The catches for the base case projection and alternative projections are summarised in Table 1.

2.2.14 Finding a base case

The base case was chosen by altering the relative weights of each dataset until the standard deviations of the normalised residuals were close to 1.0 for each dataset. The specifications for estimated parameters are shown in Table 2, with fixed values in Table 3.

2.3 MPD results

Base case parameter estimates and some indicators are shown in the first data column of Table 4, with the base case denoted as "001". The weights chosen gave standard deviations of normalised residuals that were very close to 1 for all data sets.

The MPD estimate of M was 0.15, somewhat larger than the assumed mean of the prior distribution, 0.10 (Table 4), but still within the prior.

The model estimated h as 0.730, giving a relation between CPUE and biomass with some hyperstability (Table 4). This is what one would expect from abalone populations, where divers can maintain high catch rates as the stock is fished down.

The base case model fits the two observed CPUE abundance indices credibly (Figure 2); though it is unable to fit the PCPUE index for 2006. The fit to the RDSI index is flatter then the general pattern of the index, though the fit does mirror the pattern of decrease to 2000 and subsequent increase (Figure 2). Residuals are reasonable given the sparse data (Figure 3), though those for the PCPUE index show that the fitted values are mostly below the observations. Further increasing the weight on the PCPUE index enables a more balanced residual pattern, but the fit to the CPUE index decreases in response and its residual pattern worsens. The fit to maturity-at-length is good (Figure 4).

Fits to proportions-at-length were reasonably good (Figure 5) and there was no consistent relation between the residuals and length (Figure 6). The means of residuals at length show some pattern (Figure 7), especially near the MLS. The q-q plot for normalised residuals from the RDLF data is a bit better formed than that from the CSLF (Figure 8), but both are reasonable between values of -2 and 2.

The fit to growth increment data (Figure 9) is generally acceptable except that where tags were not recovered until more than 600 days later, the model tended to over-estimate the increment. These tags were all from the same experiment at one site, so this could be a bias caused by the long time at liberty or could be caused by growth differences among sites. Figure 10 shows the q-q plot for normalised residuals for all datasets combined. The expected annual growth increment is also shown, with the standard deviations, in Figure 11 (top).

The midpoint of the research diver selectivity ogive (Figure 11, middle) was 104.8 mm, and the ogive was broad as in previous assessments. The midpoint of the commercial fishery selectivity (Figure 11, bottom) was 124.1 mm, just under the MLS, and this ogive was very narrow.

The model's MPD estimates of recruitment (Figure 12, top) were lower than average in the mid to late 1990s and about average in recent years.

Exploitation rate (Figure 12, bottom) increased steadily over the history of the fishery, reached the maximum of about 80% in 2000 and 2003, but shows a strong recent decline to 37% in 2008.

The unfished length frequency (Figure 13) has a mode at 80 mm and has substantial numbers of large paua. Recent proportions-at-length still have many small paua and far fewer larger paua

above the minimum length size of 125 mm. The model recruitment plotted against the model's spawning biomass two years earlier (Figure 14) shows no obvious relation.

The MPD biomass trajectories, the surplus production trajectories, and surplus production plotted against the recruited biomass are shown in Figure 15. Total biomass includes all animals. Recruited biomass involves those animals at or above the MLS. Available biomass involves those animals available to the commercial fishery. Estimated biomass decreased substantially from the 1965 estimate until the turn of the century, then recruited and available biomass show slight increases, with spawning biomass a somewhat more substantial increase. Surplus production increased as biomass decreased, to a maximum in the early 1990s, then declined to 2000 and shows a recent increase. Surplus production plotted against recruited biomass suggests a maximum near 500 t, at about one-sixth of the unfished recruited biomass, but this is based on a one-way trip and should be treated cautiously.

2.4 MPD sensitivity trials

Sensitivity trials based on MPD results involved removing the datasets one at a time to see how they affected the model's results, fitting to a single standardised CPUE series based on catch per diver day and making the growth model inverse logistic instead of exponential. Results are summarised in Table 4.

When the model was fitted to one data set at a time, recruitment estimates increased markedly when CPUE or tag-recapture data were removed. The *M* estimates increased slightly when CPUE was removed. Removal of tag data had the largest effect on the research diver selectivity estimates, and resulted in much lower estimates of growth parameters. Apart from these changes, sensitivity trials did not have much effect on parameter estimates, except where the data set removed contained the only information about the parameter. Indicators were remarkably stable in these trials. Using one continuous CPUE series led to less optimistic biomass ratio indicators, decreasing the percentage value by about 10, for those comparing the 2008 biomass to the reference period.

Using the inverse logistic growth to fit the growth increment data gave a better total likelihood by about 8 points, compared to the base model. However, the model took a very long time to converge, and the Hessian matrix at the MPD fit was not positive definite. Both of these problems are possibly due to correlation between the inverse logistic curve parameters. Because of these two problems the inverse logistic curve was not considered any further for model runs.

2.5 MCMC results

The MCMC traces (Figure 16) showed good mixing. The main diagnostic we used was to plot the running median and 5th and 95th quantiles of the posterior and the moving average calculated over 40 samples. Moving means for recruitment and *M* showed an excursion and return very late in the chain, along with one of the growth parameters and a research diver selectivity, but there is no strong evidence that the chain is not converged (Figure 17).

The MCMC parameter correlation matrix (Table 5) shows a high correlation between recruitment and *M*, as is usually seen; between the c.v. of growth and the other two growth parameters; between the two research diver selectivities; the two commercial selectivity parameters, between the first research diver selectivity parameter and recruitment and *M*; and among the abundance scalars and shape parameter. This list does not seem excessive.

2.6 Marginal posterior distributions and the Bayesian fit

Posteriors (Figure 18) were generally well formed and MPDs were mostly near the centres (but tended to be below the median of biomass posteriors). Posteriors of the sdnrs were mostly in the range from 0.8 to 1.2. The posteriors are summarised Table 6.

The posteriors of fits to CPUE (Figure 19) show that variation was greatest for the early years, where data are weakest, and was low for the recent years. Some years have predictions that do not encompass the observed values, but there is no pattern in the residuals. The posterior fits to PCPUE (Figure 20) and RDSI (Figure 21) also fit the data well, although the model is unable to fit the 2006 PCPUE observation, and seems unable to reproduce the range of variation seen in the RDSI data.

The posteriors of predicted CSLFs for 1999, when both CSLF and RDLF data were available, (Figure 22–23) were very tight and did not match the observed values for the peak size bins just above the MLS. The residual pattern was worse for RDLFs in the same year (Figure 22–23), although the overall fit was acceptable.

The posteriors of the fits to tagging data are difficult to show; instead we show the posterior of the q-q plot of the residuals (Figure 24), showing a moderately poor fit that is probably related to the influences of proportion-at-size datasets on the growth estimates.

The fit to maturity data (Figure 25) is tight because only this single data set contains any information about maturity.

The biomass trajectory posteriors (Figure 26) are widest for the earliest years, and for recruited biomass are very narrow near 2000, where the exploitation rate estimates were limited by the assumed maximum. All show recent and projected increases.

In all three biomass measures, the stock declined from 1965 to 2001. Recruited biomass then increased slightly to 2008. The projections at current assumed catch levels show a strong increase with increasing uncertainty over the three projection years. The recruited biomass trajectory is shown in more detail in Figure 27.

Exploitation rate (Figure 28, top) was similar to the MPD trajectory and shows a strong decrease in projections. Median recruitment (Figure 28, bottom) is also similar to the MPD, but individual estimates show high uncertainty (although higher or lower than average estimates are always higher or lower than average).

The surplus production trajectory (Figure 29) was similar to the MPD, with high variability in the 1980s and low variability near 2000. The posterior distribution of production as a function of recruited biomass (Figure 30) suggests high productivity at low stock size.

2.7 Comparison with 2005

Distributions of parameter estimates, for parameters common to both assessments (but excluding the recruitment deviations), are very similar (Table 7).

Biomass trajectories (Figure 31–32) and exploitation rates (Figure 33) are virtually identical. Estimated recruitment was slightly lower in 2005 than in 2008 (Figure 34), but had the same pattern.

This comparison shows that the 2008 assessment is not substantially different from the 2005 assessment, as might be expected: there are only slight changes in the data, two more years' data, and one small change to the model.

2.8 MCMC sensitivity trials

2.8.1 Retrospectives

In the retrospective MCMC sensitivity trials the data (except for tag-recapture data) were removed from the fitting one year at a time, from 2006 to 2004, for comparison with the base case, in which the last year of data was 2007.

The model results were generally stable to removal of data; all parameter values remained near the base case values (Table 8).

Consequently, biomass trajectories were similar (Figure 35), at least from 1985 forward. There are little data before then, and the sensitivity of early biomass estimates suggests that *B0* would be a poor reference point. Projections, shown in Figure 36, are similar among the trials though 2004 and 2005 show less of an increase. These results are mirrored in the exploitation rate trajectories (Figure 37). Recruitments (Figure 38–39) show similar patterns among the trials, albeit one noticeable pattern is that recruitment is less the further back a retrospective trial goes.

2.8.2 Maximum exploitation rate trials

When the assumed maximum exploitation rate was changed, substantial change occurred when 0.65 was assumed (Table 9); in particular, recruitment (Figure 40) and M were much larger and the fit to the data was worse, as reflected in the function value. Research divers were estimated to be much less sensitive to small paua. Absolute biomass indicators were all larger, as would be expected, though biomass indicator ratios were similar. Recruited biomass trajectories (Figure 41) were more complex: for 0.65 the historical biomass was much less than the base case; recent biomass was slightly higher. Projection indicators involving recruited biomass were similar to but less optimistic than the base case. Exploitation rates (Figure 42) followed similar patterns.

2.8.3 Alternative non-commercial catch projections

Projections were not strongly dependent on assumed value for the non-commercial catch. In the base case projection the spawning stock biomass in 2011 is estimated to be 8% higher then in 2008 (Table 10). In the zero and ramp non-commercial catch projections the spawning stock biomass is estimated to be 13% and 4% higher respectively. In the base case projection the probability that the 2011 spawning stock biomass is less then the reference spawning stock biomass is estimated at 0.48 (Table 10). In the zero and ramp projections this probability is estimated at 0.35 and 0.38 respectively.

3. DISCUSSION

3.1 Model performance

As there was only a slight change made to the model structure (introduction of the common error term to the tag-recapture data) and two more years of data added the diagnostics for this assessment were very similar to those for 2005 in being favourable. During searching for the base case MPD the model fitted the data comfortably and the residuals were balanced easily; there were no symptoms of trouble such as badly formed Hessians, or excessive numbers of function evaluations.

Sensitivity of the MPD indicators to dataset removal and other modelling choices was not great. M was sensitive to removal of the CPUE series (the longest abundance index series), but the indicators were not greatly affected. Growth estimates were sensitive to removal of the tag-recapture data set: the model estimated much slower growth when these data were absent, but again the indicators did not change much.

The MPD fit was best when higher values were assumed for maximum exploitation rate, and reducing the assumption to 0.65 led to a poor fit, unrealistically high M, and other symptoms of poor performance. This is the major source of uncertainty with respect to the MPD fits.

The diagnostics for MCMC simulations were acceptable. Retrospectives were generally stable until four years of data had been removed, when model predictions indicated greater recruitment and a lower exploitation rate. The 2006 data contain some significant information, which could either be the increase in PCPUE (see Figure 2) or the shift to the right of the commercial length frequency (see Figure 5).

As it was for the MPD, the assumed value of $U^{\max}$ is the major uncertainty. Increasing this from 0.80 to 0.90 has a small effect, but decreasing it to 0.65 increased M and made projection indicators less optimistic. Although the high M estimates appear to be unrealistic, the tendency for projected biomass increases to be weaker with decreased $U^{\max}$ must be noted.

3.2 PAU 7 assessment

It cannot hurt to repeat that the assessment addresses only areas 17 and 38 within PAU 7. These areas supported most of the catch until recently, and most of the data come from them, but the relation between this subset of PAU 7 and PAU 7 as a whole is uncertain.

The assessment shows a depleted stock. The current spawning and recruited biomass levels are both much lower than they were when the catch data begin in 1974 or CPUE data begin in 1983 (see Figure 26). Both are lower than the agreed target reference levels from 1985–87: spawning biomass has a median of 93%, with a 95% confidence interval of 79–114%; recruited biomass has a median of 54% (46–65%). Both are above the agreed limit biomass reference points. Current exploitation (poorly determined because it depends on the assumed value for $U^{\max}$) is estimated to be 37% (33–42%).

The tight ranges for most model estimates derive from the model's exploitation rate reaching its bound, $U^{\max}$. Sensitivity trials show that assuming other values for $U^{\max}$ has little effect on recent biomass estimates and trends, but assuming 0.65 leads to unrealistic M estimates and

quite different biomass trajectories. The target reference points are sensitive to $U^{\max}$ but the limit reference points are not. This is the major uncertainty of the assessment.

Although the stock is depleted, model projections show a very strong probability of increase in both spawning and recruited biomass (Table 10), even if the actual non-commercial catch is much higher then assumed in the base case. The risk of spawning biomass decrease would be 32% with a higher assumed non-commercial catch, but this nearly halves with catch at that assumed in the base case. In projections, the recruited biomass increases substantially in three years (at least 65%), across different assumptions made on the maximum exploitation rate and non-commercial catch. At current catch levels, the spawning stock biomass is estimated to be at the reference biomass levels in three years, and at 94% of the reference biomass level for recruited biomass.

3.3 Cautionary notes

The cautionary notes from the 2005 assessment are reiterated here (Breen & Kim 2005).

3.3.1 The MCMC process underestimates uncertainty

The base case assessment results described above have more uncertainty than that reflected in the posterior distributions. These results come from a single base case chosen from a wide range of possibilities, although the choice of a base case was reasonably objective. The most important uncertainty is the choice of $U^{\max}$, affecting both the estimated current status of the stock and the strength of rebuilding.

Another source of uncertainty outside the model is the 2008 catch. The assessment uses an estimate of the proportion of PAU 7 catch that comes from areas 17 and 38. Differences between the estimated and actual catch for 2008 in areas 17 and 38 could affect the strength of rebuilding predicted by the assessment. A further area of uncertainty is the non-commercial catch, which is not well known, though predicted rebuilding is not strongly dependent on the values assumed.

3.3.2 The data are not completely accurate

The next source of uncertainty comes from the data. The commercial catch before 1974 is unknown and, although we think the effect is minor, major differences may exist between the catches we assume and what was taken. In addition, non-commercial catch estimates are poorly determined and could be substantially different from what was assumed, and in recent years are estimated to be nearly 20% of the catch. The illegal catch is particularly suspect.

The tagging data may not reflect fully the average growth and range of growth in this population. Similarly, length frequency data collected from the commercial catch may not represent the commercial catch with high precision: after 2004 no paua have been measured from area 38 (McKenzie & Smith 2008, table 15).

The research diver data comprise seven surveys, but for some the standard errors are quite large (McKenzie & Smith 2008, figure 22) and length frequencies may not be fully representative of the population.

3.3.3 The model is homogeneous

The model treats the whole of the assessed substock of PAU 7 as if it were a single stock with homogeneous biology, habitat, and fishing pressures. This mean the model assumes homogeneity in recruitment, natural mortality which does not vary by size or year, and growth has the same mean and variance throughout the stock (we know this is violated because some areas are stunted and some are fast-growing).

To what extent does a homogenous model make biased predictions about a heterogeneous stock? Heterogeneity in growth can be a problem for this kind of model (Punt 2003). Variation in growth is addressed to some extent by having a stochastic growth transition matrix based on increments observed in several different places; similarly the length frequency data are integrated across samples from many places.

The effect is likely to make model results optimistic. For instance, if some local stocks are fished very hard and others not fished, recruitment failure can result because of the depletion of spawners, because spawners must breed close to each other and because the dispersal of larvae is unknown and may be limited. Recruitment failure is a common observation in overseas abalone fisheries. So local processes may decrease recruitment, which is an effect that the current model cannot account for.

3.3.4 The model assumptions may be violated

The most suspect assumption made by the model is that CPUE is an index of abundance. There is a large literature for abalone that suggests CPUE is difficult to use in abalone stock assessments because of serial depletion. This can happen when fishers can deplete unfished or lightly fished beds and maintain their catch rates. So CPUE stays high while the biomass is actually decreasing.

In fully developed fisheries such as PAU 7 this is not such a serious problem. In areas 17 and 38 the exploitation rate has been high and few undepleted areas are likely to remain. The main problem affects the model's estimates of the early fishery, but, in this assessment, the degree of hyperstability appeared reasonably well determined.

Another source of uncertainty is that fishing may cause spatial contraction of populations (e.g., Shepherd & Partington 1995), or that some populations become relatively unproductive after initial fishing (Gorfine & Dixon 2000). If this happens, the model will overestimate productivity in the population as a whole. Past recruitments estimated by the model might instead have been the result of serial depletion.

4. ACKNOWLEDGMENTS

This work was supported by a contract from the Ministry of Fisheries (PAU2007-04 Objective 1). Thank you to Paul Breen for developing the stock assessment model that was used in this assessment and for the use of major proportions of the 2005 report for this update.

5. REFERENCES

Andrew, N.L.; Breen, P.A.; Naylor, J.R.; Kendrick, T.H.; Gerring, P. (2000a). Stock assessment of paua (*Haliotis iris*) in PAU 7 in 1998–99. *New Zealand Fisheries Assessment Research Report 2000/49*. 40 p.

Annala, J.H.; Sullivan, K.J.; O'Brien, C.J.; Smith, N.W.McL.; Grayling, S.M. (comps.) (2003). Report from the Fishery Assessment Plenary, May 2003: Stock assessments and yield estimates. 616 p. (Unpublished report held in NIWA library, Wellington.)

Breen, P.A.; Andrew, N.L.; Kendrick, T.H. (2000a). Stock assessment of paua (*Haliotis iris*) in PAU 5B and PAU 5D using a new length-based model. *New Zealand Fisheries Assessment Report 2000/33*. 37 p.

Breen, P.A.; Andrew, N.L.; Kendrick, T.H. (2000b). The 2000 stock assessment of paua (*Haliotis iris*) in PAU 5B using an improved Bayesian length-based model. *New Zealand Fisheries Assessment Report 2000/48*. 36 p.

Breen, P.A.; Andrew, N.L.; Kim, S.W. (2001). The 2001 stock assessment of paua (*Haliotis iris*) in PAU 7. *New Zealand Fisheries Assessment Report 2001/55*. 53 p.

Breen, P.A.; Kim, S.W. (2003). The 2003 stock assessment of paua (*Haliotis iris*) in PAU 7. *New Zealand Fishery Assessment Report 2003/41*. 119 p.

Breen, P.A.; Kim, S.W. (2004a). The 2004 stock assessment of paua (*Haliotis iris*) in PAU 4. *New Zealand Fisheries Assessment Report 2004/55*. 79 p.

Breen, P.A.; Kim, S.W. (2004b). The 2004 stock assessment of paua (*Haliotis iris*) in PAU 5A. *New Zealand Fisheries Assessment Report 2004/40*. 86 p.

Breen, P.A.; Kim, S.W. (2005). The 2005 stock assessment of paua (*Haliotis iris*) in PAU 7. *New Zealand Fishery Assessment Report 2005/47*. 114 p.

Breen, P.A.; Kim, S.W.; Andrew, N.L. (2003). A length-based Bayesian stock assessment model for abalone. *Marine and Freshwater Research 54(5):* 619–634.

Breen, P.A.; Kim, S.W.; Starr, P.J.; Bentley, N. (2002). Assessment of the red rock lobsters (*Jasus edwardsii*) in area CRA 3 in 2001. *New Zealand Fisheries Assessment Report 2002/27*. 82 p.

Gorfine, H.K.; Dixon, C.D. (2000). A behavioural rather than resource-focused approach may be needed to ensure sustainability of quota managed abalone fisheries. *Journal of Shellfish Research 19*: 515–516.

Haddon, M.; Munday, C.; Tarbath, D. (2008). Using an inverse-logistic model to describe growth increments of blacklip abalone (*Haliotis rubra*) in Tasmania. *Fishery Bulletin 106*: 58–71.

Kim, S.W.; Bentley, N.; Starr, P.J.; Breen, P.A. (2004). Assessment of red rock lobsters (Jasus edwardsii) in CRA 4 and CRA 5 in 2003. *New Zealand Fisheries Assessment Report 2004/8*. 165 p.

McKenzie, A.; Smith, A.N.H. (2009). Data inputs for the PAU 7 stock assessment in 2008. *New Zealand Fisheries Assessment Report 2009/33.* 34 p.

Murray, T.; Akroyd, J. (1984). The New Zealand paua fishery: An update and review of biological considerations to be reconciled with management goals. New Zealand Ministry of Agriculture and Fisheries Research Centre Internal Report 5. 25 p. (Unpublished report held in NIWA library, Wellington.)

McShane, P.E.; Mercer, S.F.; Naylor, J.R. (1994). Spatial variation and commercial fishing of the New Zealand abalone (*Haliotis iris* and *H. australis*). *New Zealand Journal of Marine and Freshwater Research 28*: 345–355.

McShane, P.E.; Mercer, S.; Naylor, J.R.; Notman, P.R. (1996): Paua (*Haliotis iris*) fishery assessment in PAU 5, 6, and 7. New Zealand Fisheries Assessment Research Document 96/11. 35 p. (Unpublished report held in NIWA library, Wellington.)

Punt, A.E. (2003). The performance of a size-structured stock assessment method in the face of spatial heterogeneity in growth. *Fisheries Research 65:* 391–409.

Schiel, D.R. (1989). Paua fishery assessment 1989. New Zealand Fisheries Assessment Research Document 89/9: 20 p. (Unpublished report held in NIWA library, Wellington, New Zealand.)

Schiel, D.R. (1992). The paua (abalone) fishery of New Zealand. *In* Abalone of the world: Biology, fisheries and culture. Shepherd, S.A.; Tegner, M.J.; Guzman del Proo, S. (eds.) pp. 427–437. Blackwell Scientific, Oxford.

Schiel, D.R.; Breen, P.A. (1991). Population structure, ageing and fishing mortality of the New Zealand abalone *Haliotis iris*. *Fishery Bulletin 89*: 681–691.

Shepherd, S.A.; Breen, P.A. (1992). Mortality in abalone: its estimation, variability, and causes. *In* Abalone of the world: Biology, fisheries and culture. Shepherd, S.A.; Tegner, M.J.; Guzman del Proo, S. (eds.) pp. 276–304. Blackwell Scientific, Oxford.

Shepherd, S.A.; Partington, D. (1995). Studies on Southern Australian abalone (genus *Haliotis*). XVI. Recruitment, habitat and stock relations. *Marine and Freshwater Research 46:* 669–680.

Table 1: Total catches (kg) used for projections with alternative catches for the non-commercial catch. In the base scenario the non-commercial catch in the projection years is taken to equal that in 2008. For the zero scenario the non-commercial catch is taken to be zero in the projection years (2009, 2010, 2011). For the ramp scenario the linear ramp in the non-commercial catch from 1974 to 2000 is continued to 2011. For all scenarios the commercial catch in the projection years is equal to the estimated commercial catch in 2008.

Fishing Year	base	zero	ramp
2000	238 419	238 419	238 419
2001	180 731	180 731	184 056
2002	178 492	178 492	185 142
2003	204 755	204 755	214 730
2004	185 191	185 191	198 491
2005	183 568	183 568	200 193
2006	211 695	211 695	234 145
2007	196 968	196 968	225 243
2008	202 065	202 065	236 165
2009	202 065	169 565	237 365
2010	202 065	169 565	238 365
2011	202 065	169 565	239 565

Table 2: PAU 7 base case specifications: for estimated parameters, the phase of estimation, lower bound, upper bound, type of prior, (U, uniform; N, normal; LN = lognormal), mean and standard deviation of the prior.

Variable	Phase	LB	UB	Prior	Mean	Std. dev.
ln(*R0*)	1	5	50	U	–	–
M	3	0.01	0.5	LN	0.10	0.35
g_α	2	1	50	U	–	–
g_β	2	0.01	50	U	–	–
ϕ	2	0.001	1	U	–	–
q^I	1	-30	0	U	–	–
X	1	0.05	1	U	–	–
q^J	1	-30	0	U	–	–
L_{50}	1	70	145	U	–	–
L_{95-50}	1	1	50	U	–	–
T_{50}	2	70	125	U	–	–
T_{95-50}	2	0.001	50	U	–	–
D_{50}	2	70	145	U	–	–
D_{95-50}	2	0.01	50	U	–	–
$\ln(\tilde{\sigma})$	1	0.01	1	U	–	–
h	1	0.01	2	U	–	–
ε	3	-2.3	2.3	N	0	0.4

Table 3: Values for fixed quantities in the PAU 7 base case.

Variable	Value
α	75
β	120
ϖ^I	0.065
ϖ^{I2}	0.54
ϖ^J	0.138
ϖ^r	75.9
ϖ^s	36.4
ϖ^{tag}	0.189
ϖ^{mat}	5.53
$U^{\max}$	0.800
σ_{MIN}	1.0
σ_{obs}	0.25
a	2.59E-08
b	3.322

Table 4: MPD sensitivity trials for PAU 7. Columns "002" through "008" present results from trials in which one dataset was removed: CPUE, CSLF, RDLF, tag-recapture, maturity and PCPUE respectively; in the "009" trial a single CPUE dataset was used for 1985-2007; for '010" the growth model was inverse logistic. Sdnrs: standard deviations of the normalised residuals;. Shading indicates sdnrs inflated because they were not estimated, and likelihood contributions not used when datasets were removed. The parameter sigmatilde was not estimated in these runs, and was set to 0.267 as estimated in the base case. IL stands for inverse logistic.

	Base 001	No CPUE 002	No RDSI 003	No CSLF 004	No RDLF 005	No tags 006	No maturity 007	No PCPUE 008	One CPUE 009	IL growth 010
sdnrs										
sdnrCPUE	1.00	3.80	1.01	1.06	0.75	1.16	1.00	0.87	0.53	0.98
sdnrRDSI	0.97	1.07	2.41	0.97	1.50	1.03	0.97	1.06	1.05	0.97
sdnrCSLF	0.97	0.97	0.97	1.35	0.92	0.89	0.97	0.97	0.97	0.98
sdnrRDLF	0.99	0.97	0.99	0.93	12.04	0.99	0.99	0.97	0.97	1.00
sdnrMaturity	0.97	0.97	0.97	0.97	0.97	0.97	1.33	0.97	0.97	0.97
sdnrPCPUE	0.95	0.83	0.96	0.98	0.83	1.02	0.95	11.01	8.99	0.94
sdnrTags	1.01	1.01	1.01	1.01	1.03	3.69	1.01	1.01	1.01	1.00
Parameters										
ln(*R0*)	14.70	14.79	14.69	14.59	14.53	15.29	14.70	14.64	14.72	14.70
M	0.15	0.17	0.15	0.14	0.14	0.14	0.15	0.14	0.15	0.15
T_{50}	104.77	104.84	104.75	105.64	122.81	112.74	104.77	103.97	104.44	102.95
$T_{95\text{-}50}$	22.91	23.04	22.92	25.71	0.03	20.80	22.91	22.70	22.87	20.65
D_{50}	124.07	124.08	124.07	123.38	123.98	124.31	124.07	124.07	124.07	124.02
$D_{95\text{-}50}$	2.39	2.40	2.39	1.80	2.24	2.68	2.39	2.39	2.39	2.41
L_{50}	90.74	90.74	90.74	90.74	90.74	90.74	88.01	90.74	90.74	90.74
$L_{95\text{-}50}$	11.44	11.44	11.44	11.44	11.44	11.44	16.01	11.44	11.44	11.44
$\ln(q^I)$	-4.60	-8.60	-4.66	-4.30	-4.09	-5.93	-4.60	-2.97	-2.68	-4.39
X	0.198	0.052	0.199	0.195	0.183	0.201	0.198	0.525	0.525	0.196
$\ln(q^I)$	-15.29	-15.29	-13.00	-15.20	-14.06	-15.48	-15.29	-15.28	-15.28	-15.31
g_α	15.56	15.46	15.56	15.91	15.93	5.48	15.56	15.50	15.50	-
g_β	5.77	5.79	5.77	5.81	6.01	4.59	5.77	5.76	5.77	-
φ	0.425	0.424	0.425	0.416	0.400	0.190	0.425	0.425	0.425	-
h	0.730	1.175	0.734	0.706	0.693	0.821	0.730	0.604	0.570	0.712

Likelihoods										
CPUE	-12.2	2035.9	-12.1	-11.1	-16.5	-9.0	-12.2	-14.6	-9.5	-12.6
PCPUE	-4.8	-6.8	-4.7	-4.1	-6.8	-3.5	-4.8	1656.7	1306.0	-4.9
RDSI	-0.2	0.5	339.6	-0.2	4.3	0.2	-0.2	0.4	0.4	-0.2
CSLF	-1160.6	-1157.9	-1160.7	-983.1	-1180.4	-1189.6	-1160.6	-1159.1	-1158.9	-1155.1
RDLF	-1095.8	-1102.4	-1096.0	-1113.1	19584.8	-1095.2	-1095.8	-1100.8	-1101.8	-1092.2
Tags	2165.6	2165.2	2165.6	2165.2	2161.5	9701.6	2165.6	2165.9	2165.6	2148.8
Maturity	-30.6	-30.6	-30.6	-30.6	-30.6	-30.6	-18.0	-30.6	-30.6	-30.6
Prior on *M*	0.6	0.9	0.6	0.3	0.3	0.4	0.6	0.4	0.6	0.6
Prior on ε	5.5	5.0	5.5	4.3	7.0	6.2	5.5	5.3	5.1	5.5
ε	0.1	0.1	0.1	0.5	0.0	0.0	0.1	0.1	0.1	0.0
Total likelihood	-132.5	-126.1	-132.3	1011.2	938.8	-2321.1	-101.9	-133.1	-129.0	-140.9
Indicators										
max*Rdev*	1.637	1.531	1.618	1.536	1.606	1.823	1.637	1.548	1.538	1.568
min*Rdev*	0.495	0.485	0.495	0.497	0.503	0.606	0.495	0.500	0.489	0.488
U08	37%	47%	38%	37%	39%	37%	37%	46%	45%	36%
Smin	817	835	817	765	763	1735	832	804	821	780
Sav	1541	1571	1540	1523	1429	2671	1561	1535	1551	1521
S08	1438	1300	1426	1340	1094	2620	1455	1258	1298	1407
Bmin	106	107	106	97	102	144	106	107	107	105
Bav	639	544	638	655	646	712	639	685	615	666
B08	353	260	348	336	355	365	353	268	273	365
S08/Sav	93%	83%	93%	88%	77%	98%	93%	82%	84%	92%
B08/Bav	55%	48%	55%	51%	55%	51%	55%	39%	44%	55%
S08/Smin	176%	156%	174%	175%	143%	151%	175%	157%	158%	180%
B08/Bmin	334%	242%	330%	346%	349%	253%	334%	252%	256%	346%

Table 5: Correlations among estimated parameters in the PAU 7 MCMC. Boxes indicate absolute values greater than 0.50.

	ln(*R0*)	*M*	g_α	g_β	T_{50}	T_{95-50}	D_{50}	D_{95-50}	L_{50}	L_{95-50}	φ	ln(q^I)	*X*	ln(q^J)	*h*
ln(*R0*)	1.00														
M	0.96	1.00													
g_α	-0.13	-0.06	1.00												
g_β	0.40	0.50	0.18	1.00											
T_{50}	0.83	0.83	-0.40	0.32	1.00										
T_{95-50}	0.29	0.29	-0.16	-0.07	0.54	1.00									
D_{50}	0.33	0.29	-0.19	-0.34	0.28	0.17	1.00								
D_{95-50}	0.14	0.11	-0.01	-0.40	0.12	0.17	0.53	1.00							
L_{50}	0.00	0.00	0.00	0.00	0.00	0.00	0.00	0.00	1.00						
L_{95-50}	0.00	0.00	0.00	0.00	0.00	0.00	0.00	0.00	-0.45	1.00					
φ	-0.08	-0.15	-0.48	-0.59	0.04	0.12	0.28	0.13	0.00	0.00	1.00				
ln(q^I)	0.06	0.01	0.04	-0.05	0.06	-0.01	0.03	0.02	0.00	0.00	0.02	1.00			
X	0.04	0.06	-0.04	0.02	-0.02	0.01	0.04	0.01	0.00	0.00	-0.01	-0.75	1.00		
ln(q^J)	-0.01	0.00	-0.03	0.14	0.08	0.09	-0.12	-0.09	0.00	0.00	-0.06	-0.03	0.01	1.00	
h	-0.06	-0.01	-0.04	0.06	-0.06	0.00	-0.03	-0.02	0.00	0.00	-0.02	-1.00	0.72	0.03	1.00

Table 6 : Summary of the marginal posterior distributions from the MCMC chain from the base case for PAU 7. The projected catch is the estimated 2008 catch. The columns show the minimum values observed in the 500 samples, the maxima, the 5th and 95th percentiles, and the medians. The last few rows show the percentage of runs for which the indicator was true. Biomass is in tonnes.

	min	5%	median	95%	max
f	-132.5	-112.9	-104.9	-95.5	-84.5
ln(*R0*)	14.14	14.40	14.74	15.13	15.50
M	0.106	0.122	0.159	0.207	0.241
$g\alpha$	13.84	14.55	15.36	16.15	16.73
$g\beta$	5.27	5.47	5.70	5.91	6.16
D_{50}	123.9	124.0	124.1	124.2	124.3
T_{50}	101.9	103.1	105.4	107.9	109.7
$T_{95\text{-}50}$	19.65	21.08	23.21	25.33	27.38
$D_{95\text{-}50}$	2.12	2.24	2.41	2.59	2.75
L_{50}	88.79	89.93	90.70	91.50	92.55
$L_{95\text{-}50}$	8.69	9.65	11.56	13.41	14.94
φ	0.392	0.413	0.439	0.465	0.496
$\ln(q^I)$	-6.93	-5.68	-4.53	-3.43	-2.54
X	0.161	0.180	0.198	0.219	0.241
$\ln(q^J)$	-15.64	-15.46	-15.30	-15.15	-15.04
h	0.565	0.638	0.723	0.813	0.904
sdnrCPUE	0.784	0.890	1.037	1.227	1.560
sdnrPCPUE	0.779	0.862	0.990	1.184	1.389
sdnrRDSI	0.833	0.906	0.977	1.051	1.110
sdnrCSLF	0.948	0.959	0.975	0.993	1.011
sdnrRDLF	0.956	0.979	1.011	1.044	1.072
sdnrTags	0.903	0.947	0.987	1.029	1.080
sdnrMaturity	0.963	0.966	0.991	1.066	1.202
U08	28%	33%	37%	42%	46%
U11	15%	19%	25%	33%	41%
Smin	751	785	845	929	1045
Sav	1400	1465	1603	1812	2130
S08	1065	1230	1513	1908	2487
S09	1025	1230	1555	2021	2782
S10	973	1245	1591	2120	3086
S11	923	1237	1630	2206	3370
Bmin	99	103	107	112	116
Bav	506	564	662	764	876
B08	270	311	357	412	491
B09	336	389	467	554	720
B10	348	437	563	717	948
B11	334	450	619	859	1140
S08/Sav	70%	79%	93%	114%	134%
S08/Smin	134%	149%	177%	217%	259%
S11/Sav	62%	78%	101%	133%	194%
S11/S08	82%	95%	108%	124%	147%
B08/Bav	39%	46%	54%	65%	80%
B08/Bmin	256%	288%	334%	385%	471%
B11/Bav	51%	67%	94%	132%	175%
B11/B08	104%	134%	173%	229%	310%
S11<S08			18%		
S11<Sav			48%		
B11<Bav			62%		

Table 7: Comparison of the posterior distributions for parameters and two indicators between the 2005 and 2008 assessments. Only those variables common to the two assessments are shown.

	median		5%		95%	
	2005	2008	2005	2008	2005	2008
$\ln(R0)$	14.68	14.74	14.44	14.40	14.94	15.13
M	0.150	0.159	0.128	0.122	0.177	0.207
g_{α}	15.76	15.36	14.87	14.55	16.57	16.15
g_{β}	5.418	5.695	5.221	5.467	5.607	5.908
D_{50}	123.98	124.09	123.89	124.00	124.06	124.17
T_{50}	103.86	105.37	102.09	103.13	105.86	107.91
$T_{95\text{-}50}$	24.43	23.21	22.10	21.08	27.20	25.33
$D_{95\text{-}50}$	2.260	2.412	2.096	2.238	2.430	2.593
L_{50}	90.72	90.70	89.91	89.93	91.49	91.50
$L_{95\text{-}50}$	11.57	11.56	9.83	9.65	13.41	13.41
φ	0.609	0.439	0.575	0.413	0.648	0.465
$\ln(q^I)$	-3.479	-4.527	-4.596	-5.676	-2.384	-3.432
X	0.192	0.198	0.174	0.180	0.213	0.219
$\ln(q^J)$	-15.277	-15.301	-15.442	-15.457	-15.119	-15.154
h	0.642	0.723	0.558	0.638	0.729	0.813
Sav	1546	1603	1447	1465	1681	1812
Bav	673	662	589	564	765	764

Table 8 : Summary of parameter estimates and indicators from the retrospective MCMC sensitivity trials. Biomass indicators are in tonnes.

				median				5%				95%
Parameter	Base	2006	2005	2004	Base	2006	2005	2004	Base	2006	2005	2004
ln(*R0*)	14.7	14.7	14.7	14.5	14.4	14.5	14.4	14.3	15.1	15	14.9	14.8
M	0.159	0.153	0.151	0.134	0.122	0.133	0.126	0.116	0.207	0.177	0.177	0.159
g_α	15.4	15.3	15.2	15.4	14.5	14.5	14.4	14.6	16.1	16.2	16.1	16.2
g_β	5.695	5.763	5.727	5.74	5.467	5.548	5.525	5.528	5.908	5.95	5.904	5.958
D_{50}	124.1	124	123.9	123.9	124	123.9	123.9	123.8	124.2	124.1	124	124
$D_{95\text{-}50}$	2.412	2.345	2.389	2.33	2.238	2.147	2.389	2.123	2.593	2.533	2.389	2.527
T_{50}	105.4	105.2	104.6	103.8	103.1	103.5	102.9	102.1	107.9	107	106.5	105.7
$T_{95\text{-}50}$	23.2	22.9	23.1	23.8	21.1	21.1	21.1	21.4	25.3	25.2	25.5	27
L_{50}	90.7	90.7	90.7	90.7	89.9	89.9	89.9	89.8	91.5	91.4	91.4	91.5
$L_{95\text{-}50}$	11.6	11.6	11.6	11.5	9.6	10	9.9	9.7	13.4	13.4	13.5	13.5
φ	0.439	0.436	0.442	0.431	0.413	0.413	0.419	0.408	0.465	0.467	0.47	0.462
$\ln(q^I)$	-4.527	-4.736	-3.414	-2.988	-5.676	-5.872	-4.826	-4.336	-3.432	-3.578	-2.277	-1.698
X	0.198	0.199	0.18	0.165	0.18	0.178	0.161	0.144	0.219	0.22	0.203	0.187
$\ln(q^J)$	-15.301	-15.275	-15.268	-15.306	-15.457	-15.434	-15.428	-15.465	-15.154	-15.124	-15.121	-15.125
h	0.723	0.739	0.636	0.604	0.638	0.649	0.55	0.508	0.813	0.828	0.746	0.708
Smin	845	827	822	796	785	777	772	749	929	888	885	853
Sav	1603	1556	1564	1498	1465	1447	1455	1406	1812	1681	1692	1612
Bmin	107	106	107	107	103	102	102	103	112	112	113	115
Bav	662	639	669	674	564	547	575	578	764	729	766	770
sdnrCPUE	1.037	1.055	0.941	0.923	0.89	0.887	0.819	0.805	1.227	1.265	1.116	1.067
sdnrPCPUE	0.99	0.952	0.532	0.212	0.862	0.718	0.336	0.074	1.184	1.206	0.753	0.467
sdnrRDSI	0.977	0.97	1.093	1.083	0.906	0.896	0.988	0.983	1.051	1.055	1.195	1.181
sdnrCSLF	0.975	0.918	0.862	0.857	0.959	0.9	0.839	0.834	0.993	0.94	0.887	0.883
sdnrRDLF	1.011	1.016	0.988	0.916	0.979	0.982	0.957	0.886	1.044	1.048	1.025	0.954
sdnrTags	0.987	0.988	0.983	0.998	0.947	0.944	0.94	0.952	1.029	1.029	1.024	1.044
sdnrMaturity	0.991	0.989	0.988	0.99	0.966	0.965	0.965	0.966	1.066	1.069	1.066	1.074

Table 9: Summary of parameter estimates and indicators from the MCMC sensitivity trials in which maximum exploitation rate was varied to values indicated. Projected catches are the estimated 2008 catch. "*f*" indicates the function value. Biomass indicators are in tonnes.

	median			5%			95%		
	65%	base	90%	65%	base	90%	65%	base	90%
f	-70.4	-104.9	-114.6	-78.1	-112.9	-120.4	-60.7	-95.5	-103.5
ln(*R0*)	15.57	14.74	14.64	15.1	14.4	14.49	16.08	15.13	14.75
M	0.26	0.159	0.142	0.19	0.122	0.132	0.341	0.207	0.153
g_α	15.97	15.36	15.29	15.1	14.55	14.74	16.92	16.15	16.09
g_β	5.28	5.7	5.86	5.01	5.47	5.72	5.55	5.91	6.29
D_{50}	124.1	124.1	124	124	124	123.9	124.2	124.2	124.1
$D_{95\text{-}50}$	2.3	2.4	2.4	2.2	2.2	2.1	2.5	2.6	2.6
T_{50}	109.1	105.4	104.3	105.9	103.1	103.5	112.2	107.9	105.2
$T_{95\text{-}50}$	23.5	23.2	22.5	22	21.1	21	25.3	25.3	23.5
L_{50}	90.7	90.7	90.5	89.9	89.9	90	91.5	91.5	91
$L_{95\text{-}50}$	11.6	11.6	11.6	9.8	9.6	10.4	13.7	13.4	12.9
φ	0.442	0.439	0.421	0.417	0.413	0.401	0.47	0.465	0.44
$\ln(q^I)$	-5.02	-4.53	-4.45	-6.47	-5.68	-5.34	-3.84	-3.43	-3.39
X	0.196	0.198	0.196	0.177	0.18	0.18	0.216	0.219	0.215
$\ln(q^J)$	-15.53	-15.3	-15.26	-15.67	-15.46	-15.39	-15.38	-15.15	-15.15
h	0.746	0.723	0.721	0.655	0.638	0.638	0.857	0.813	0.791
sdnrCPUE	1.165	1.037	1.014	0.988	0.89	0.881	1.372	1.227	1.179
sdnrPCPUE	1.012	0.987	1.012	0.97	0.947	0.978	1.049	1.029	1.033
sdnrRDSI	1.025	0.99	0.976	0.874	0.862	0.848	1.24	1.184	1.16
sdnrCSLF	0.974	0.977	0.975	0.903	0.906	0.93	1.045	1.051	1.029
sdnrRDLF	0.961	0.975	0.989	0.942	0.959	0.973	0.982	0.993	1.005
sdnrMaturity	1.05	1.011	1.011	1.022	0.979	0.986	1.084	1.044	1.046
sdnrTags	0.991	0.991	0.987	0.966	0.966	0.966	1.08	1.066	1.024
U08	0.307	0.371	0.385	0.273	0.332	0.351	0.345	0.415	0.414
U11	0.216	0.253	0.249	0.166	0.189	0.192	0.275	0.333	0.297
Smin	1220	845	785	1073	785	737	1440	929	814
Sav	2537	1603	1484	2081	1465	1391	3220	1812	1552
S08	2324	1513	1419	1818	1230	1225	3072	1908	1676
S09	2341	1555	1465	1822	1230	1238	3197	2021	1748
S10	2352	1591	1501	1817	1245	1252	3249	2120	1845
S11	2355	1630	1538	1785	1237	1260	3294	2206	1928
Bmin	149	107	101	143	103	95	155	112	107
Bav	848	662	662	730	564	588	1028	764	719
B08	441	357	342	382	311	313	504	412	381
B09	561	467	460	470	389	399	659	554	538
B10	662	563	565	536	437	467	817	717	723
B11	721	619	635	547	450	515	960	859	858
S08/Sav	92%	93%	95%	77%	79%	86%	113%	114%	111%
S08/Smin	190%	177%	180%	158%	149%	164%	237%	217%	211%
S11/Sav	93%	101%	104%	73%	78%	87%	123%	133%	130%
S11/S08	102%	108%	108%	88%	95%	98%	118%	124%	122%
B08/Bav	51%	54%	52%	43%	46%	45%	62%	65%	59%
B08/Bmin	297%	334%	338%	255%	288%	307%	338%	385%	382%
B11/Bav	85%	94%	99%	62%	67%	76%	113%	132%	131%
B11/B08	165%	173%	188%	129%	134%	156%	210%	229%	242%
S11<S08	0.426	0.178	0.11						
S11<Sav	0.672	0.478	0.386						
B11<Bav	0.814	0.622	0.508						

Table 10: Summary of results from projections using alternative maximum exploitation rates and non-commercial catches. Median values are shown for the exploitation rate in 2011 (U11) and biomass ratios. In all runs, the median biomass exceeded Bmin and Smin.

	U11	S11/Sav	S11/S08	P(S11 < S_{AV})	P(S11 < S08)	B11/B_{AV}	B11/B08	P(B11 < B_{AV})
base	0.25	1.01	1.08	0.48	0.18	0.94	1.73	0.62
zero	0.20	1.06	1.13	0.35	0.05	1.05	1.94	0.41
ramp	0.30	1.04	1.04	0.38	0.32	0.92	1.63	0.63

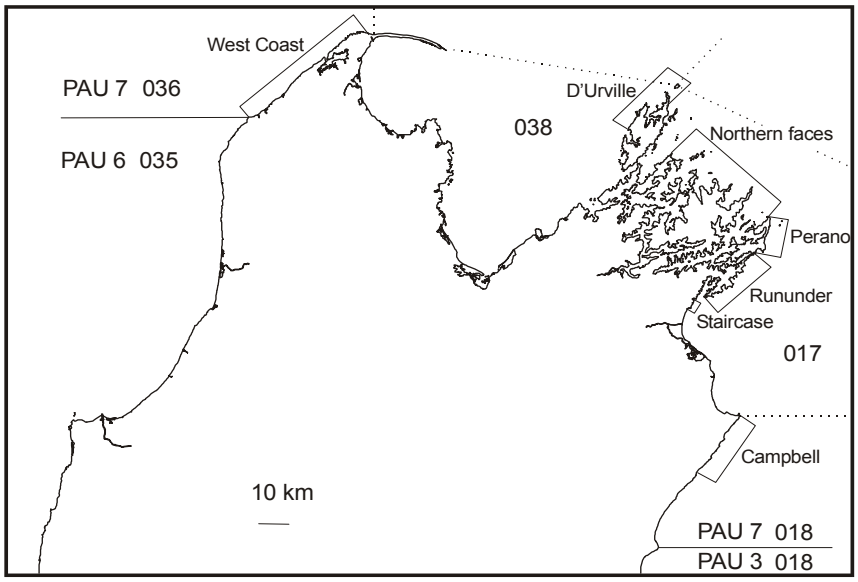

Figure 1: Boundaries of PAU 7, statistical areas and research survey strata.

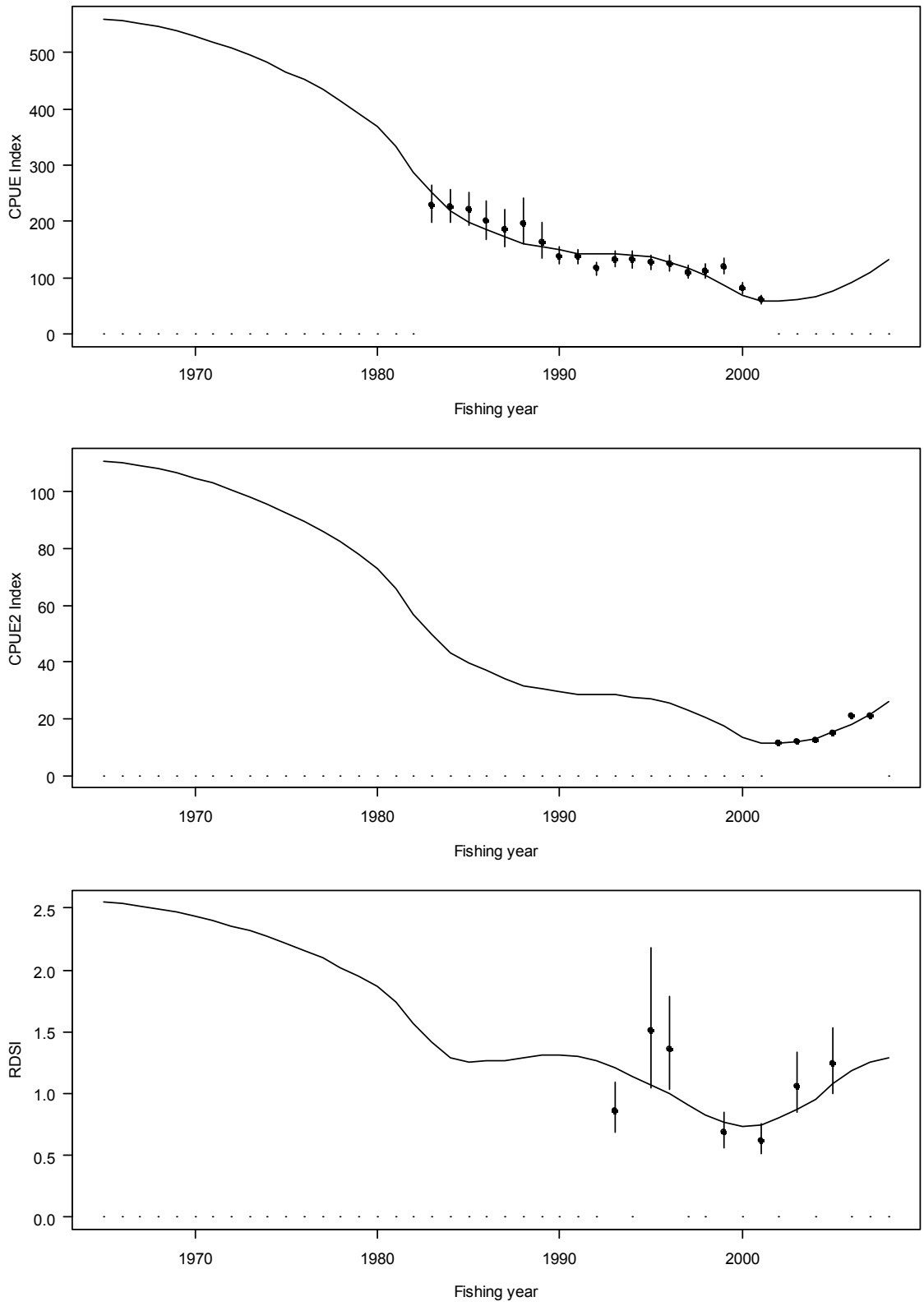

Figure 2: Observed (dots) and predicted (solid line) CPUE (top), PCPUE (middle) and RDSI (bottom) for the base case MPD fit for PAU 7. Error bars show the standard error term used by the model in fitting, including the effects of the common error term and the dataset weights.

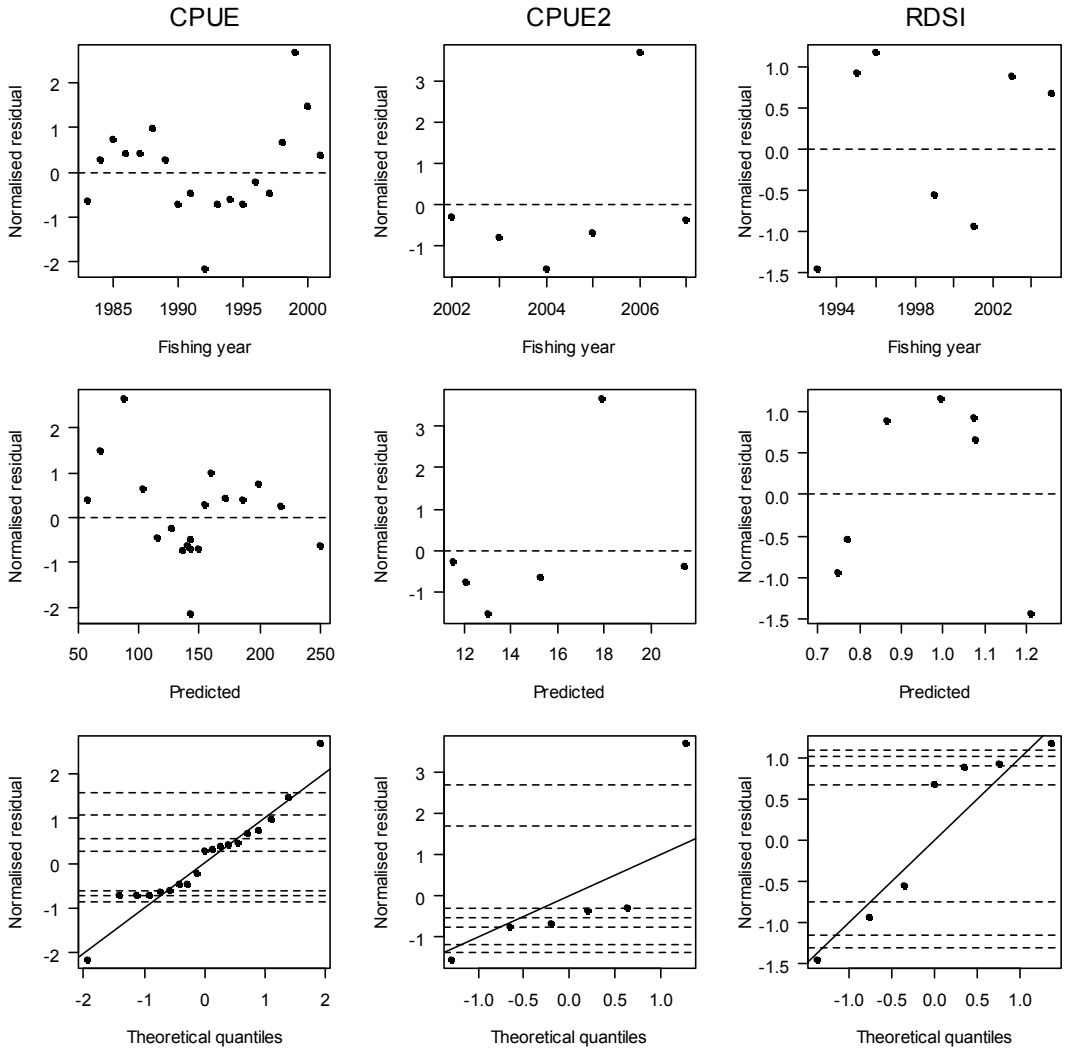

Figure 3: Normalised residuals for CPUE (left), PCPUE (middle) and RDSI (right) for the base case MPD fit for PAU 7. The horizontal lines in bottom plots are 5, 10, 25, 50, 75, 90, 95th percentiles.

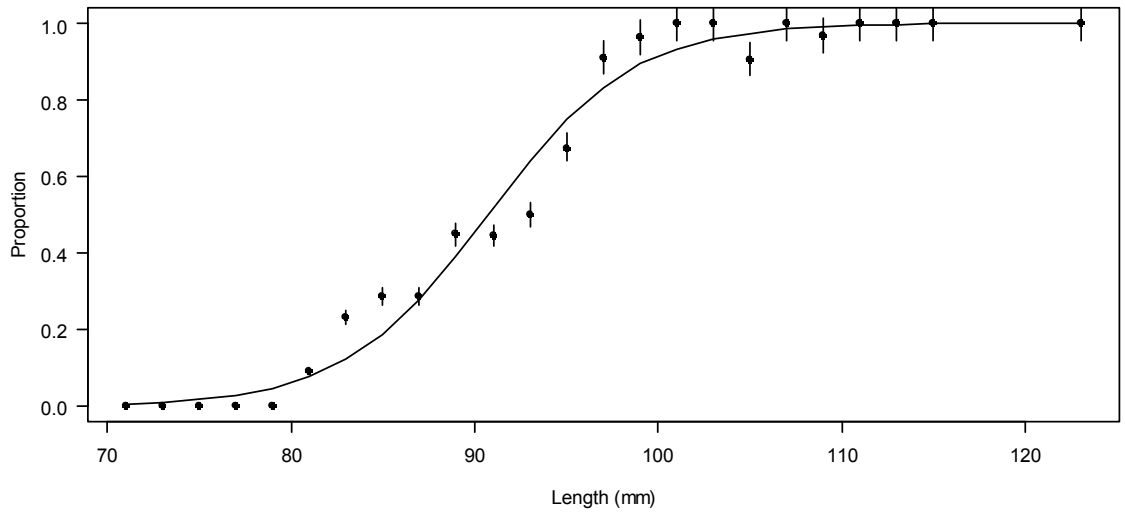

Figure 4: Observed (dots) and predicted (line) proportions of maturity-at-length.

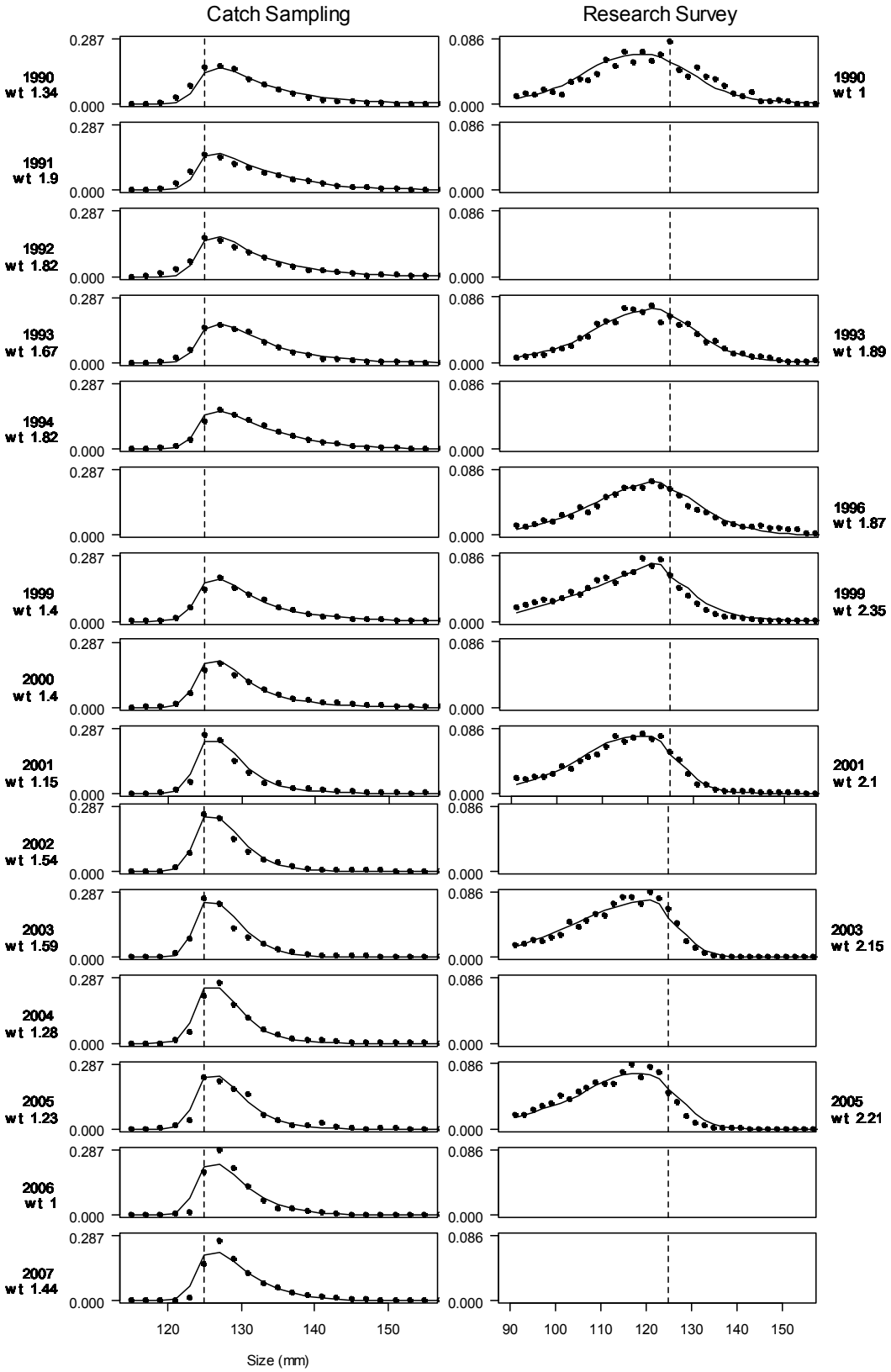

Figure 5: Observed (dots) and predicted (lines) proportions-at-length from commercial catch sampling (left) (CSLF) and research diver surveys (right) (RDLF) for the base case MPD fit for PAU 7. The number under each year is the relative weight given to the dataset, based on the number of paua measured.

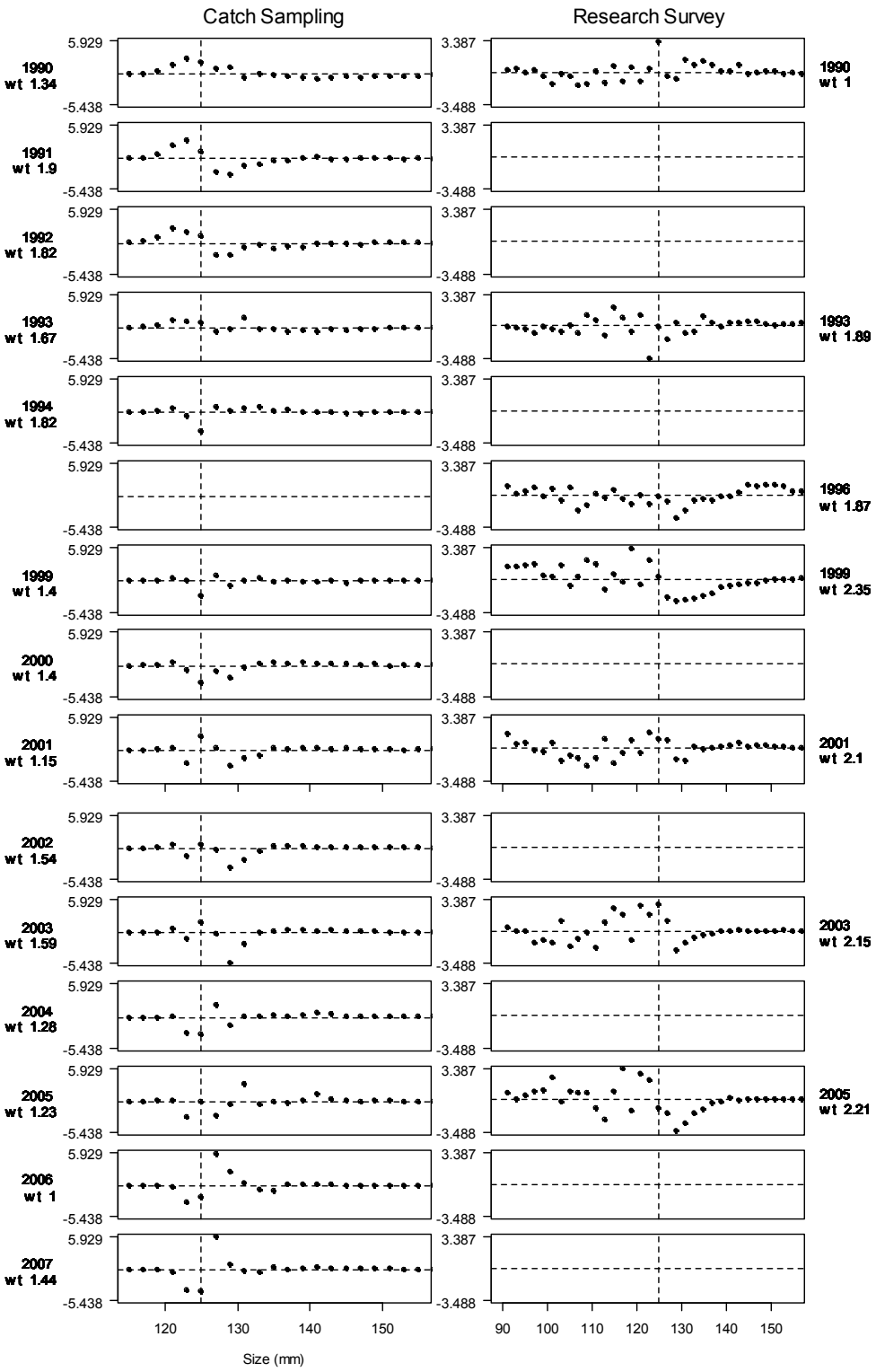

Figure 6: Residuals from base case MPD fits to CSLF (left) and RDLF (right) data seen in Figure 5.

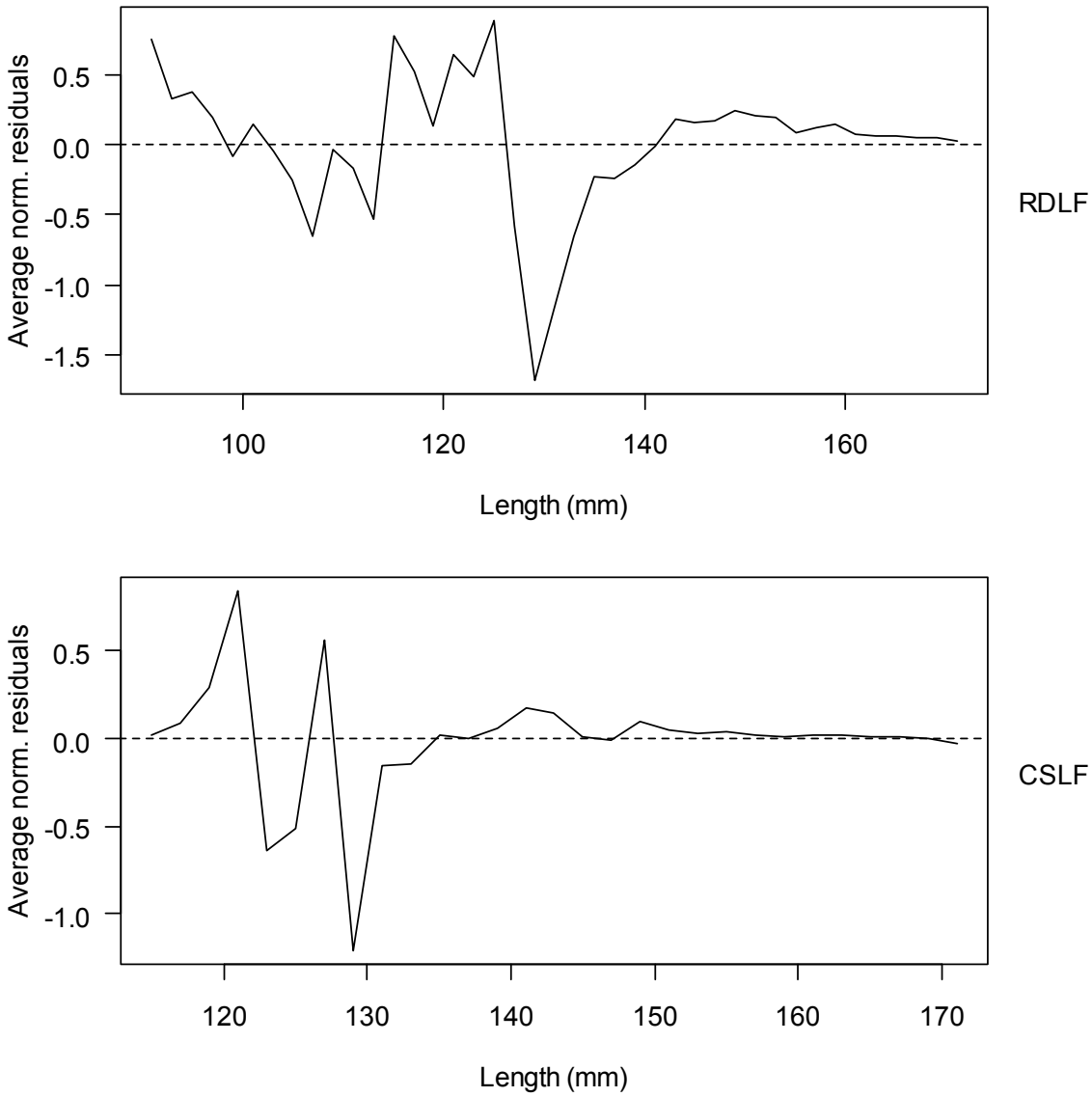

Figure 7: Means of normalised residuals at each length for the fits to the RDLF (upper) and CSLF datasets.

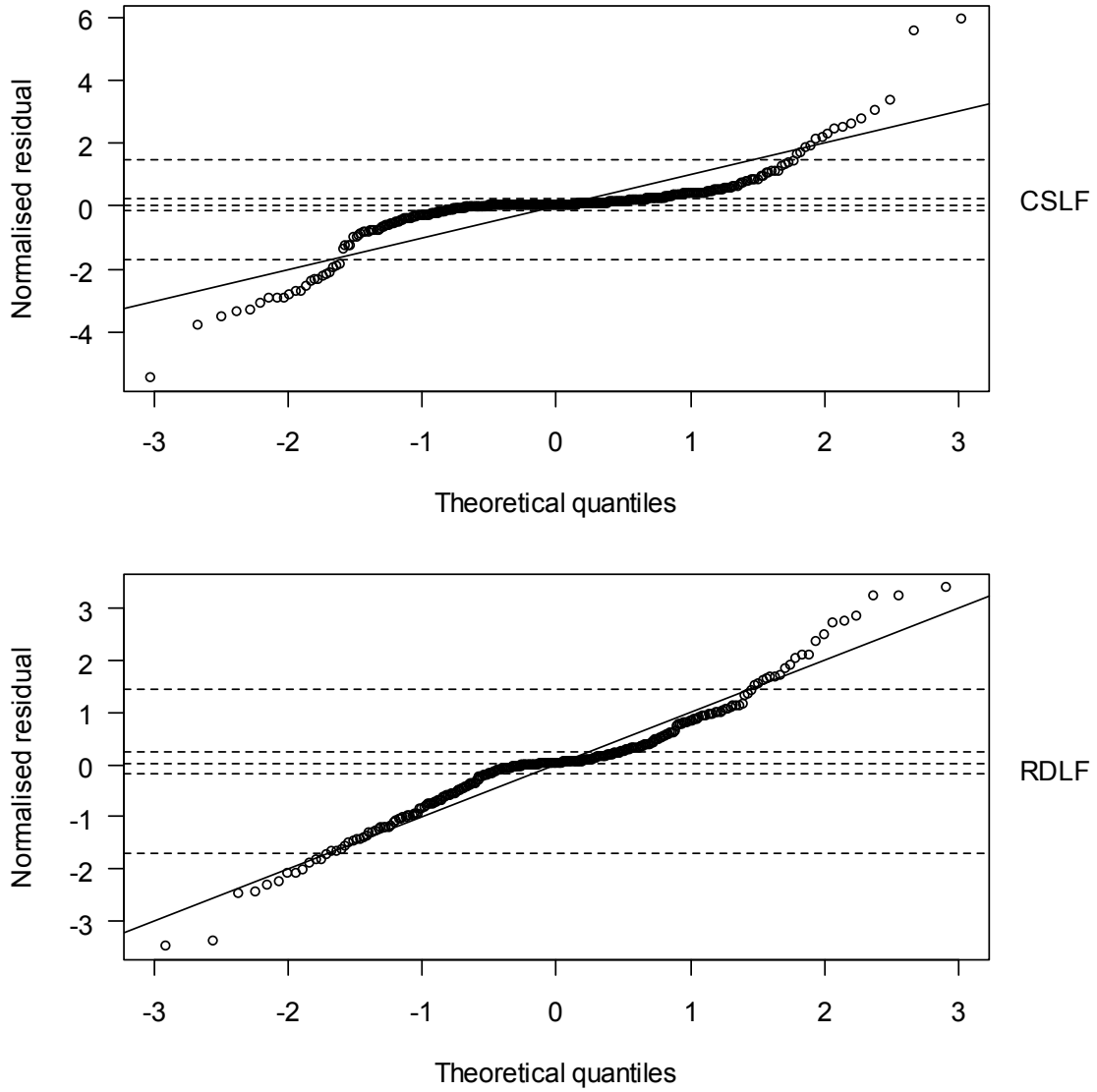

Figure 8: Q-Q plot of residuals for the fits to proportions-at-length from commercial catch sampling (top) and research diver surveys (bottom) from the base case MPD fit for PAU 7.

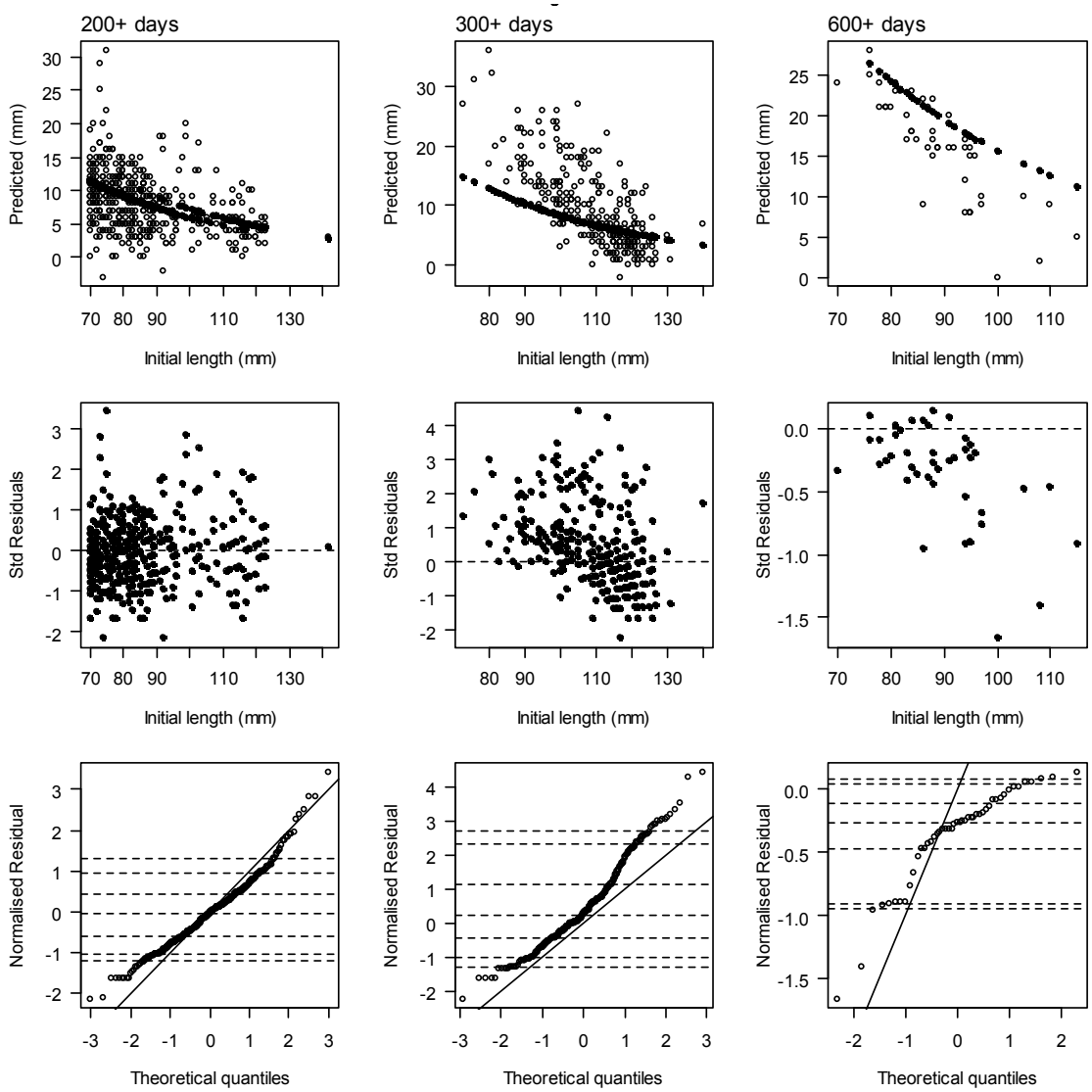

Figure 9: Top: predicted (closed circles) and observed (open circles) increments plotted against initial length of tagged paua from the base case MPD fit for PAU 7; middle: standardised residuals plotted against initial length; bottom: Q-Q plot of standardised residuals. Among the columns, the data have been divided based on the approximate time-at-liberty, which varied among experiments, animals within each experiment having almost the same time-at-liberty.

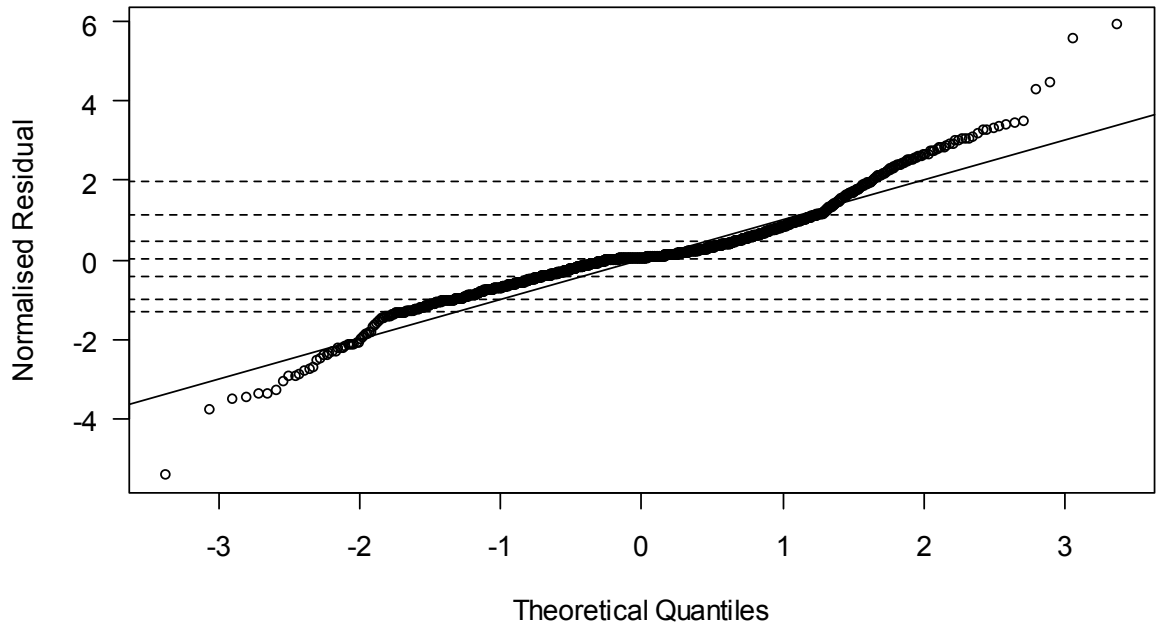

Figure 10: Q-Q plot of the normalised residuals from all datasets used by the model in the base case MPD fit.

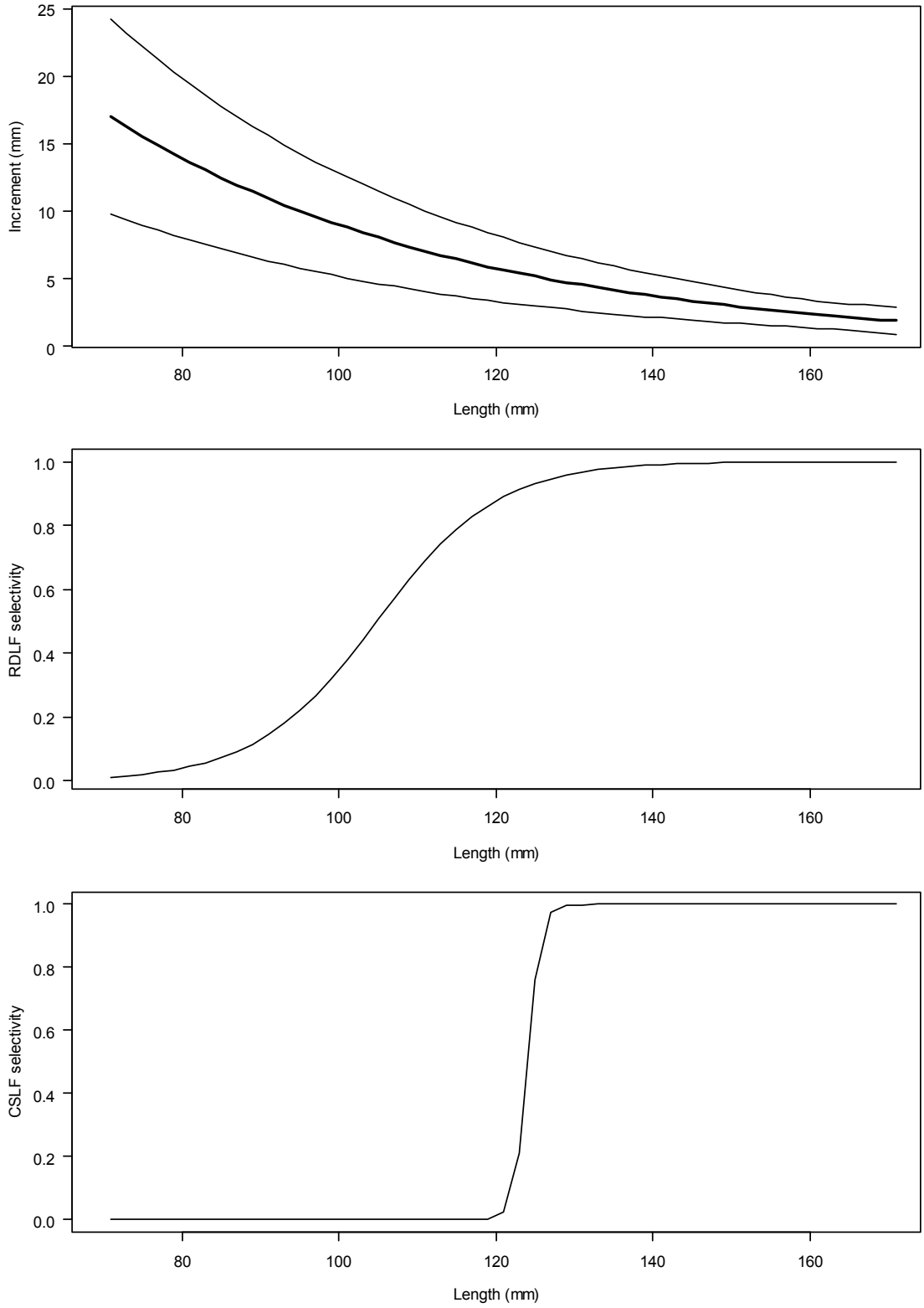

Figure 11: Top: predicted annual growth increment (thick line) *vs.* initial length of paua, shown with one standard deviation around the increment (thin line); middle: estimated research diver survey selectivity; bottom: estimated commercial catch sampling selectivity.

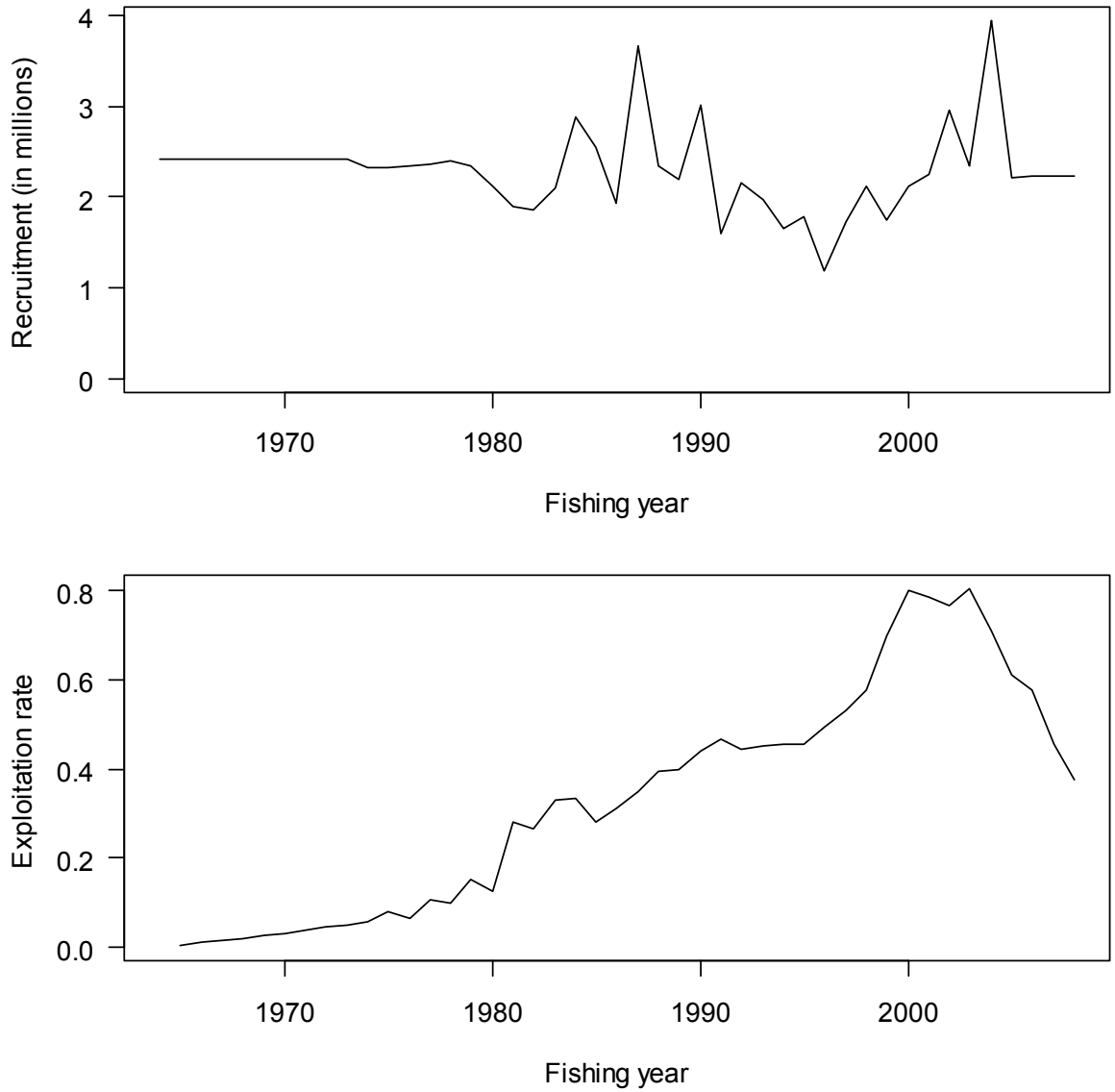

Figure 12: Recruitment to the model (top) and exploitation rate (bottom) from the base case MPD fit in PAU 7.

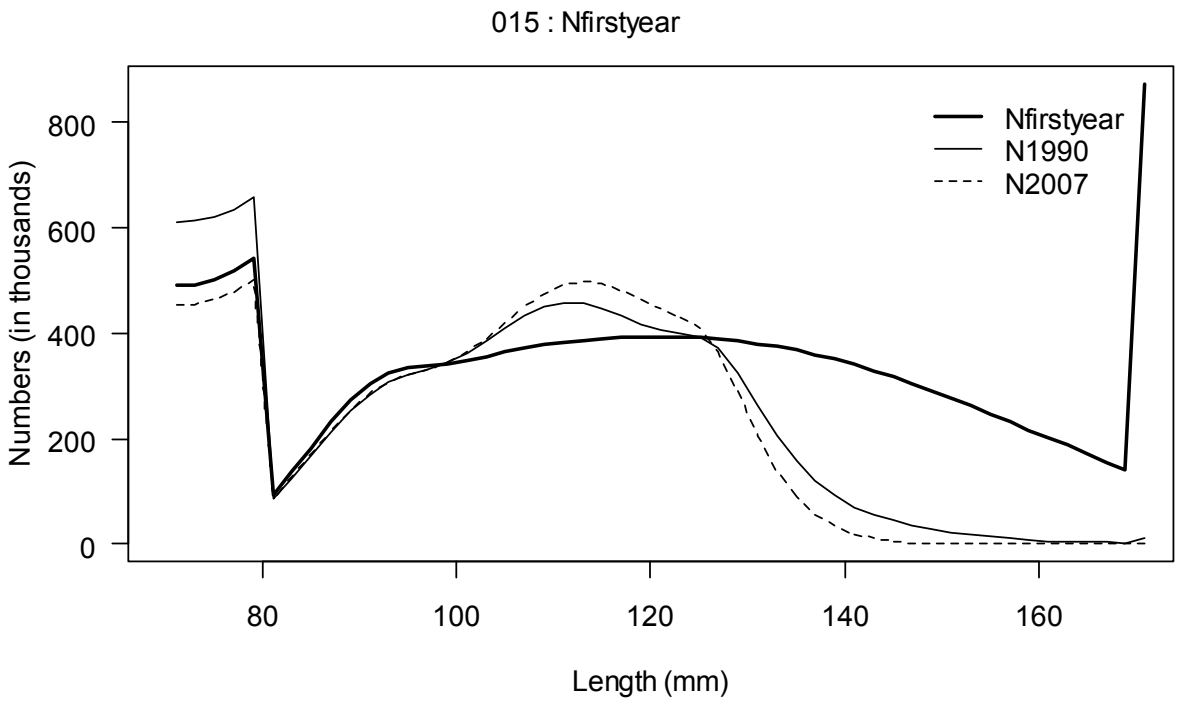

Figure 13: Comparison of size structures in the unfished population (heavy line) and the populations in 1990 (thin line) and 2007 (dashed line) from the base case MPD fit in PAU 7.

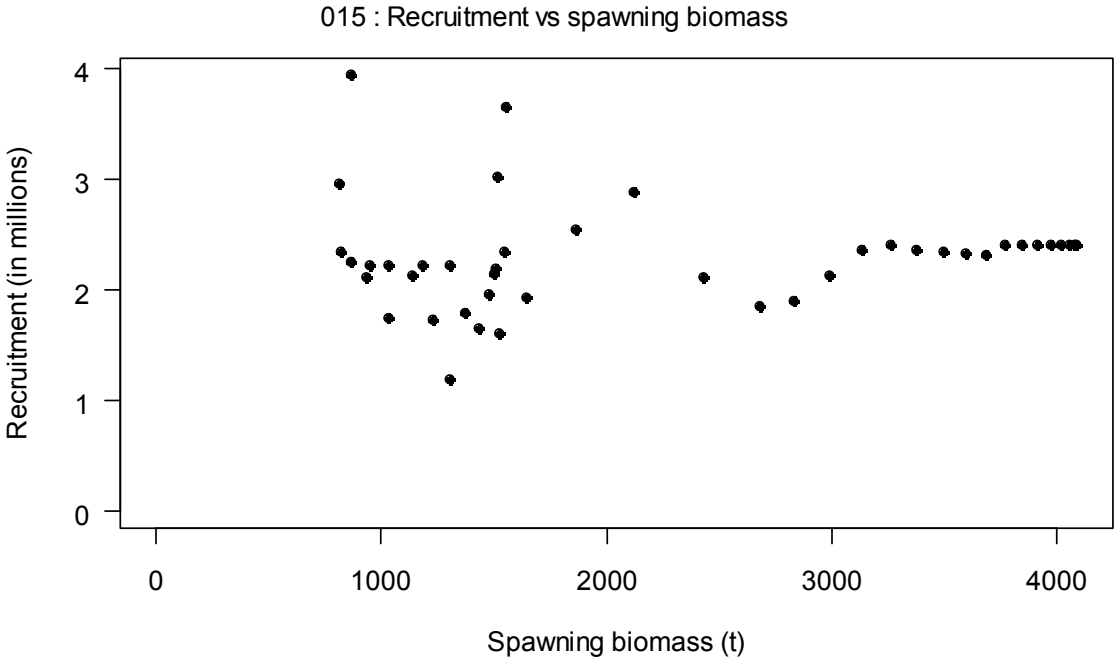

Figure 14: Recruitment plotted against spawning biomass two years earlier from the base case MPD fit in PAU 7.

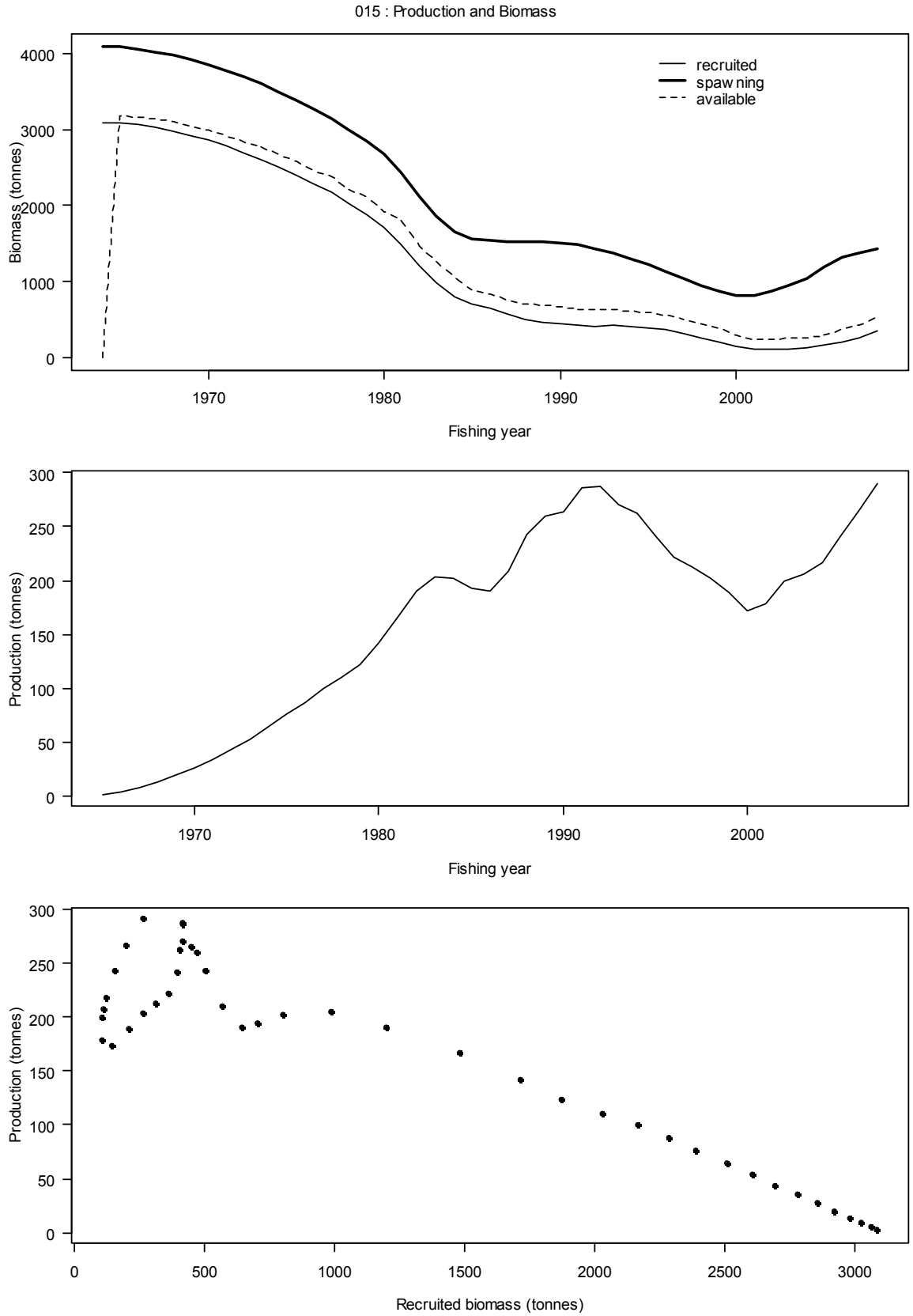

Figure 15: Recruited, spawning, and available biomass trajectories (top), the surplus production trajectory (middle) and surplus production plotted against recruited biomass (bottom), all from the base case MPD fit for PAU 7.

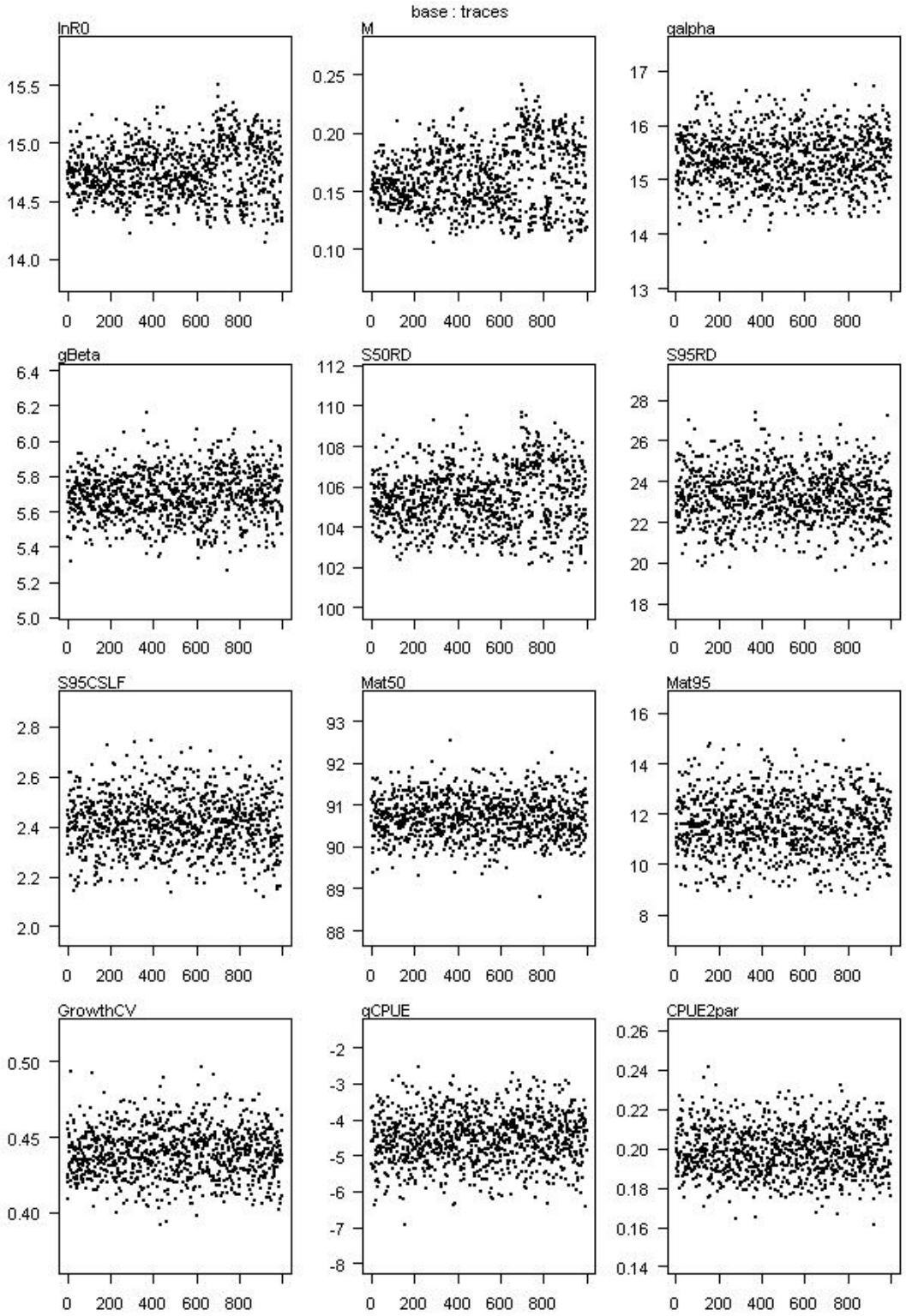

Figure 16: Traces from the PAU 7 base case MCMC.

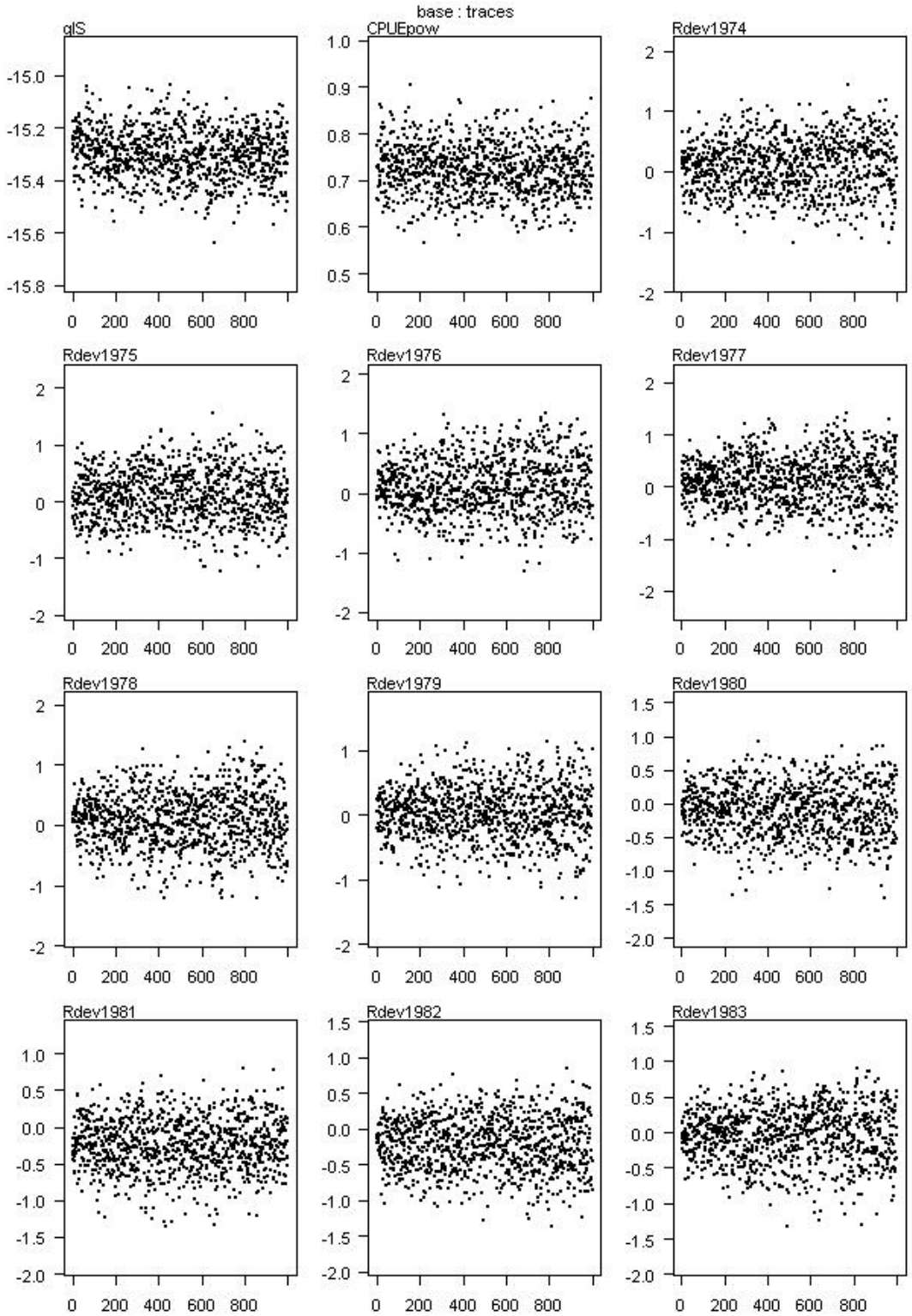

Figure 16 continued.

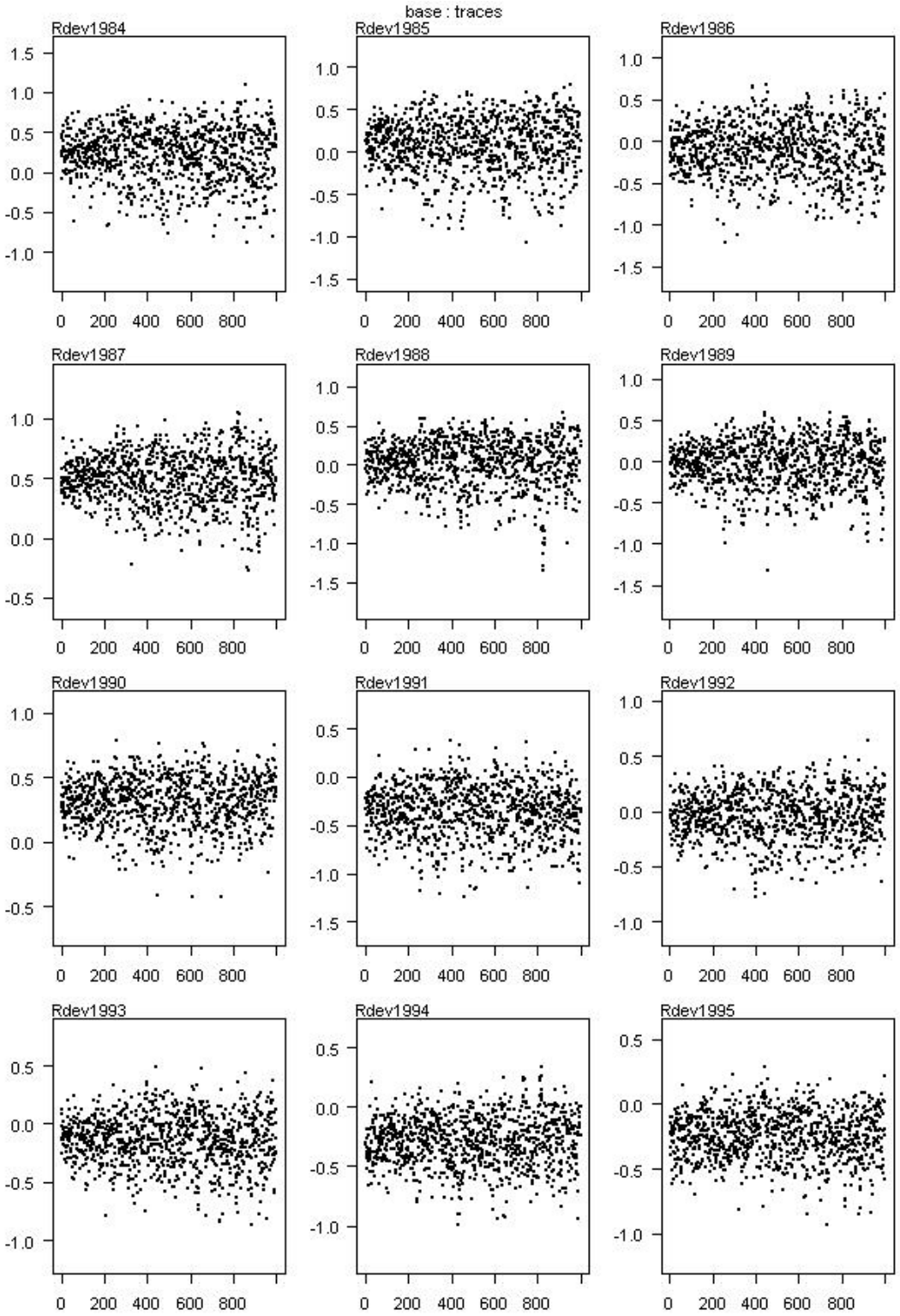

Figure 16 continued.

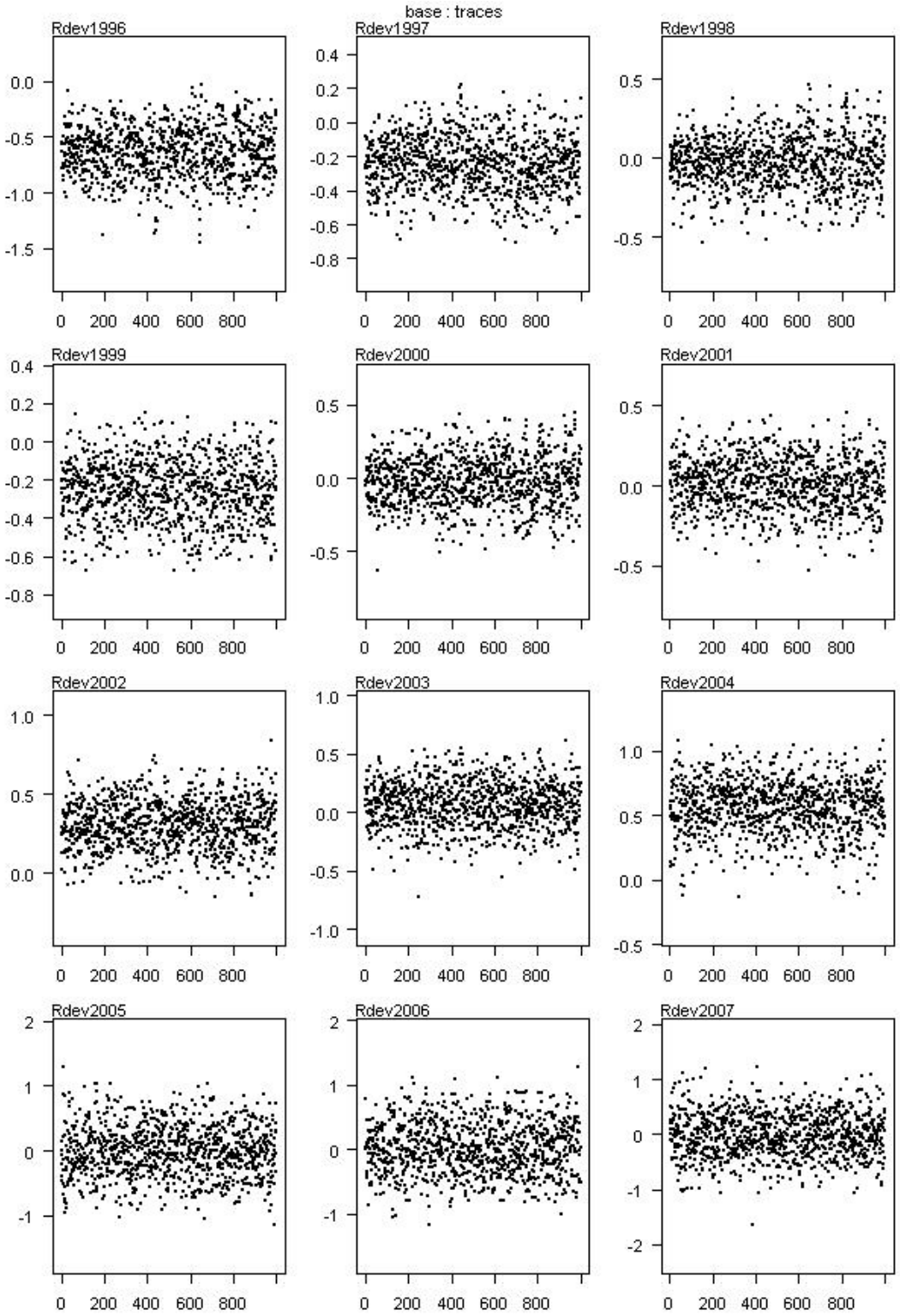

Figure 16 continued.

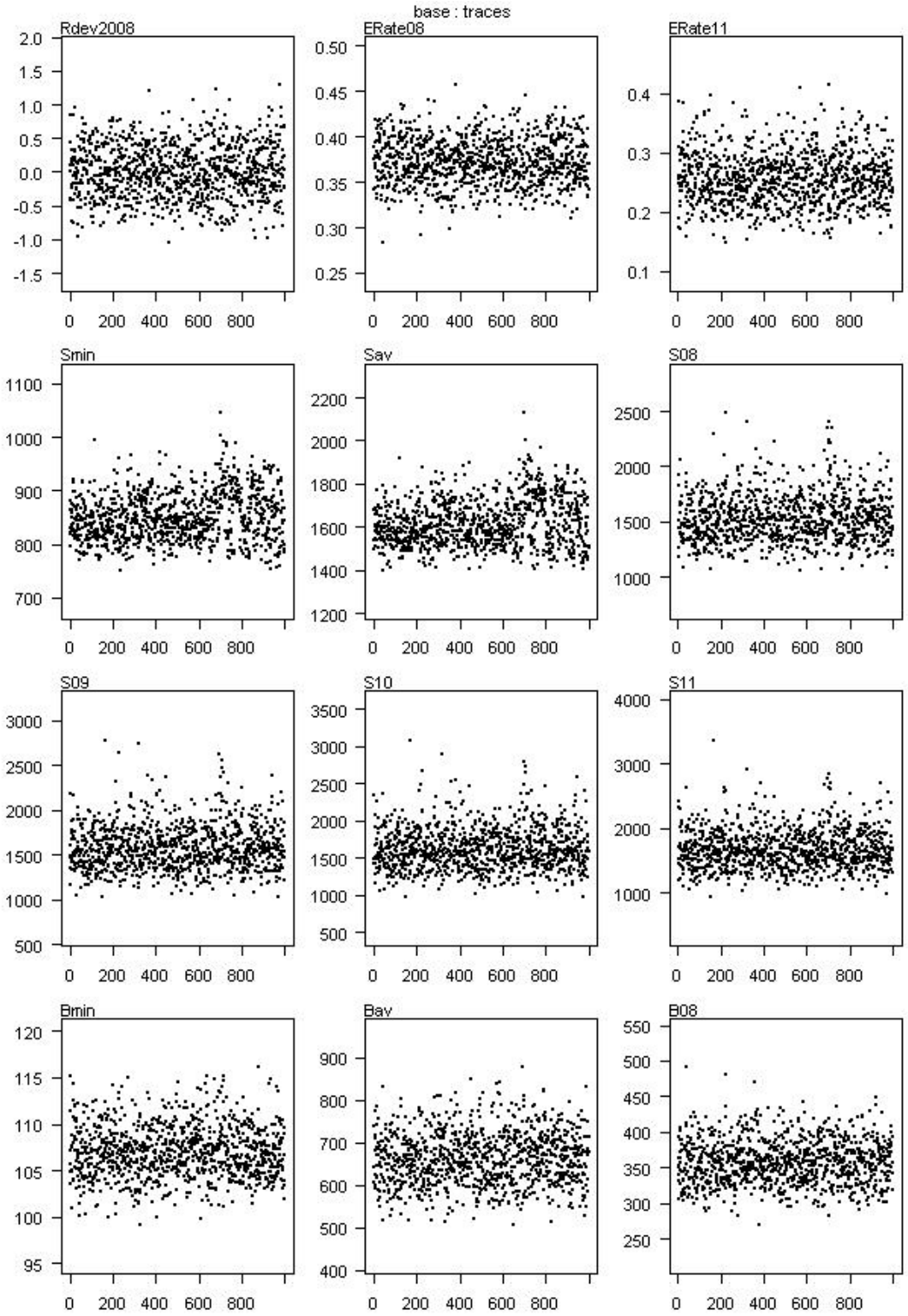

Figure 16 continued.

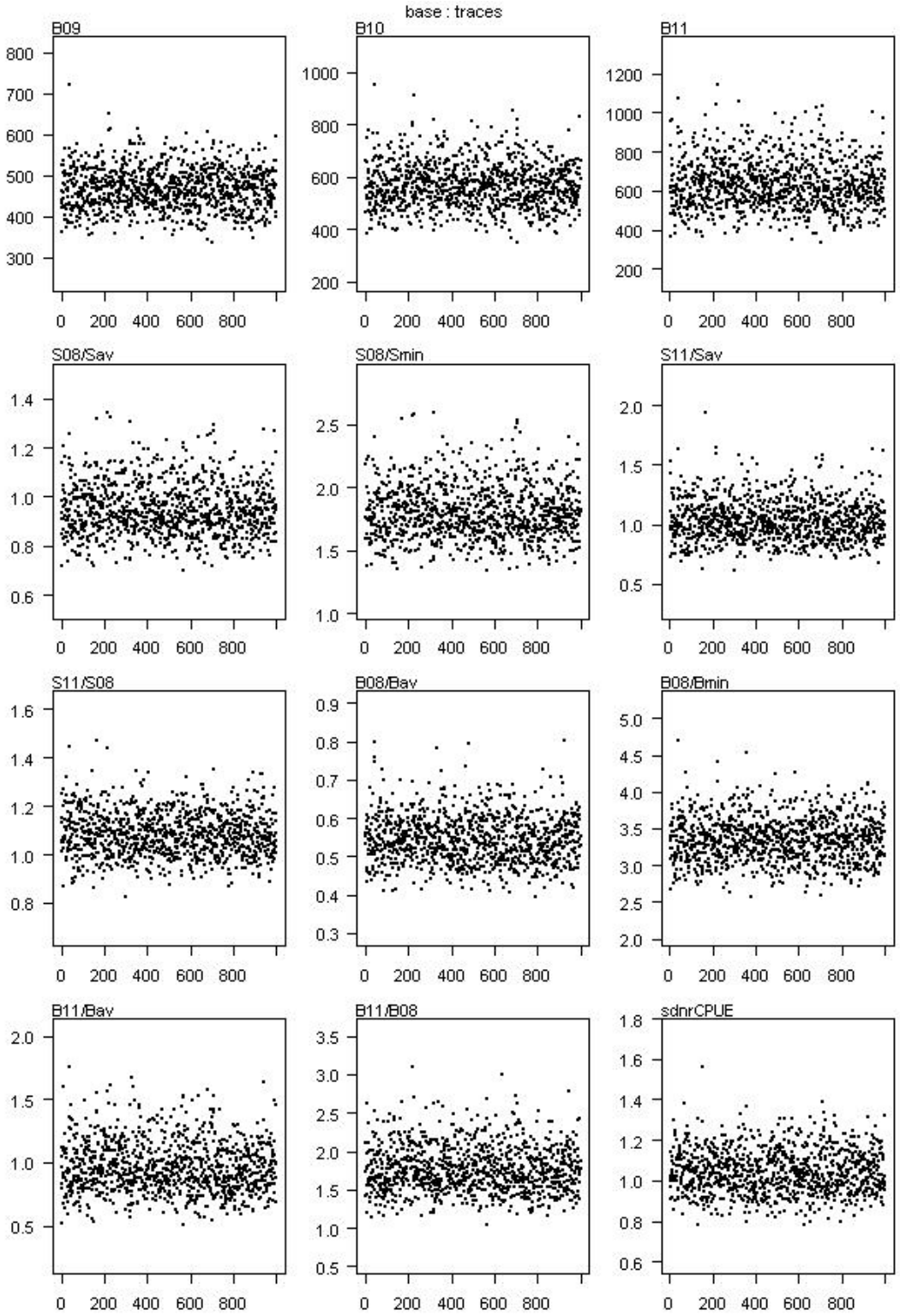

Figure 16 continued.

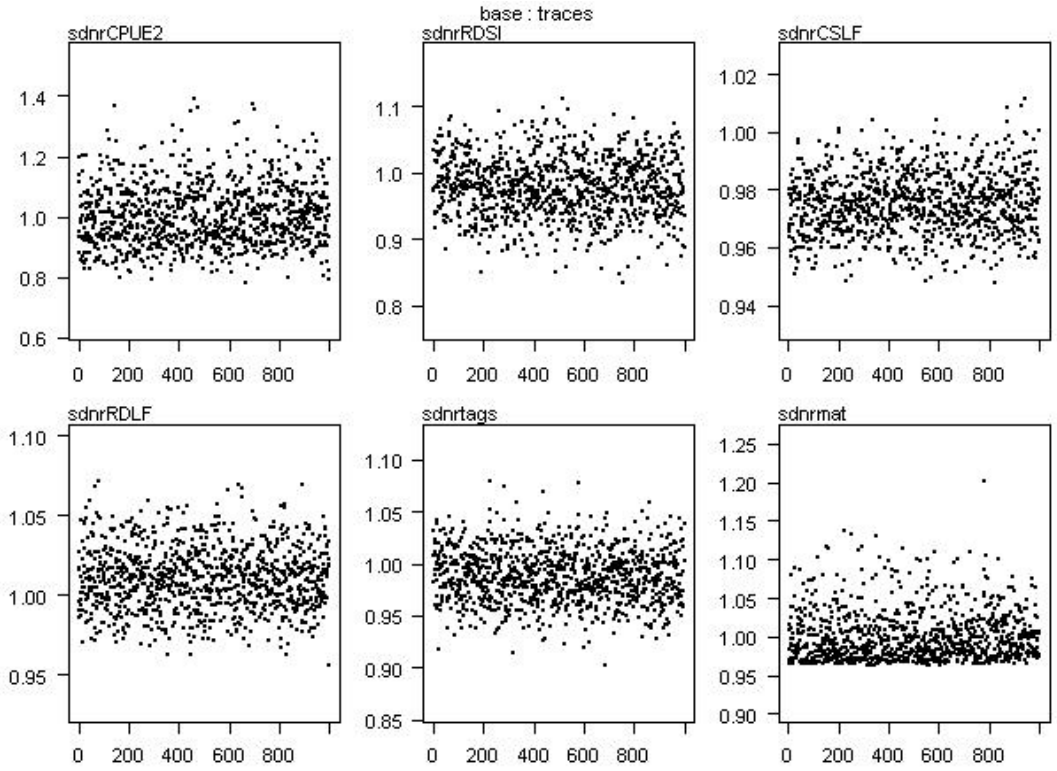

Figure 16 continued.

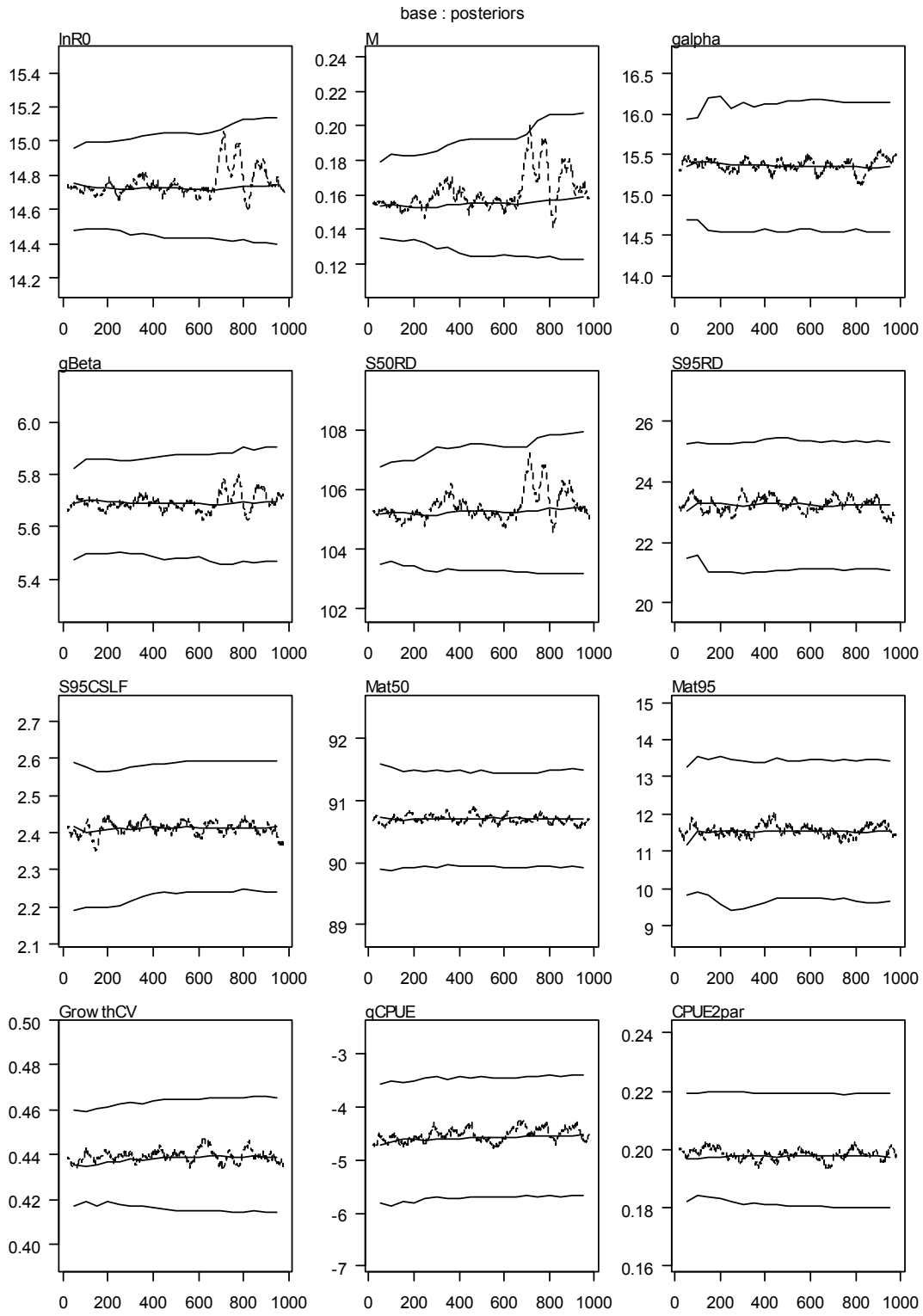

Figure 17: Diagnostic plots on the traces from the base case PAU 7 MCMC simulations. The central line is the running median; the upper and lower lines are the running 5th and 95th quantiles; the central dots show a moving average over 40 samples.

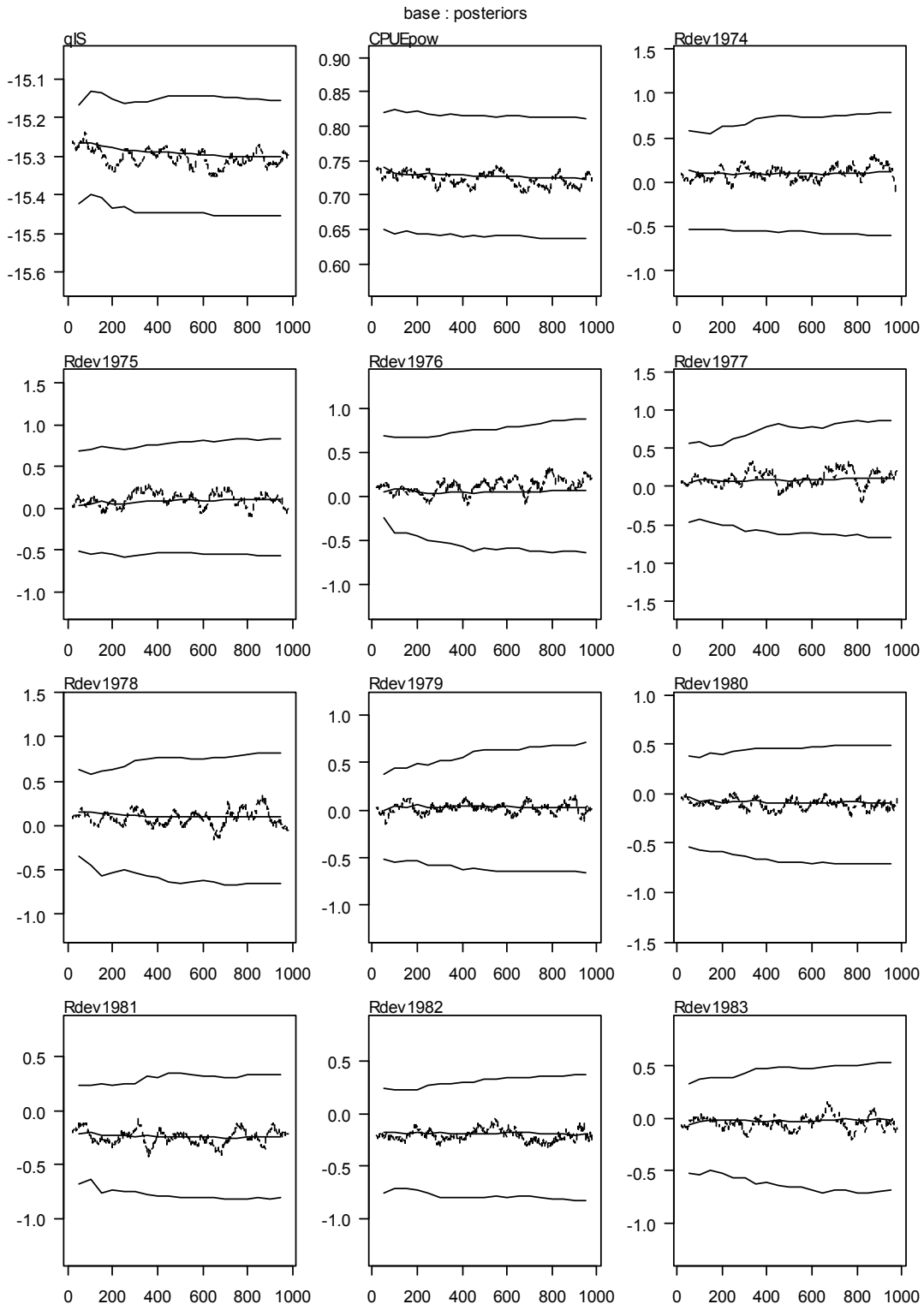

Figure 17 continued.

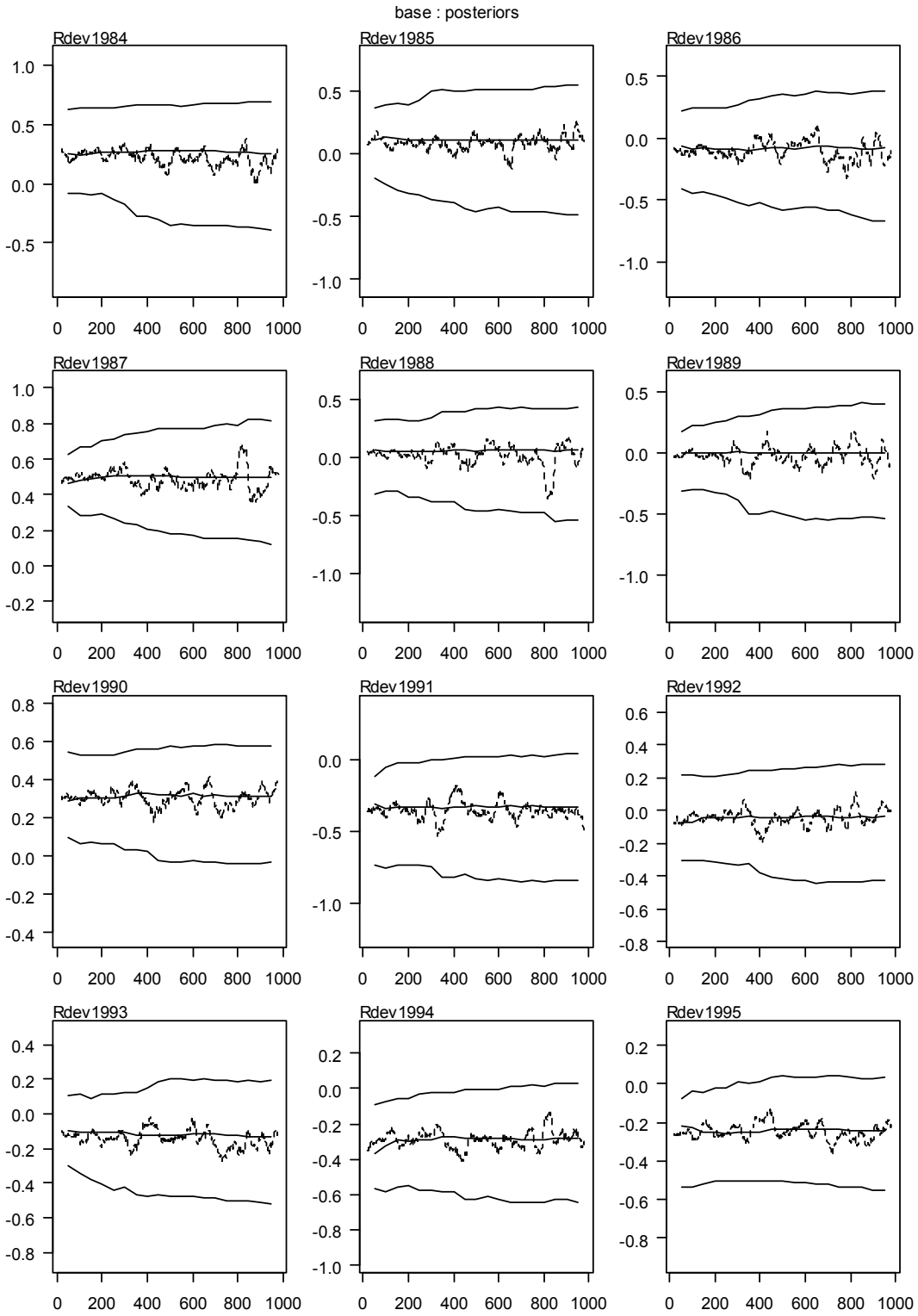

Figure 17 continued.

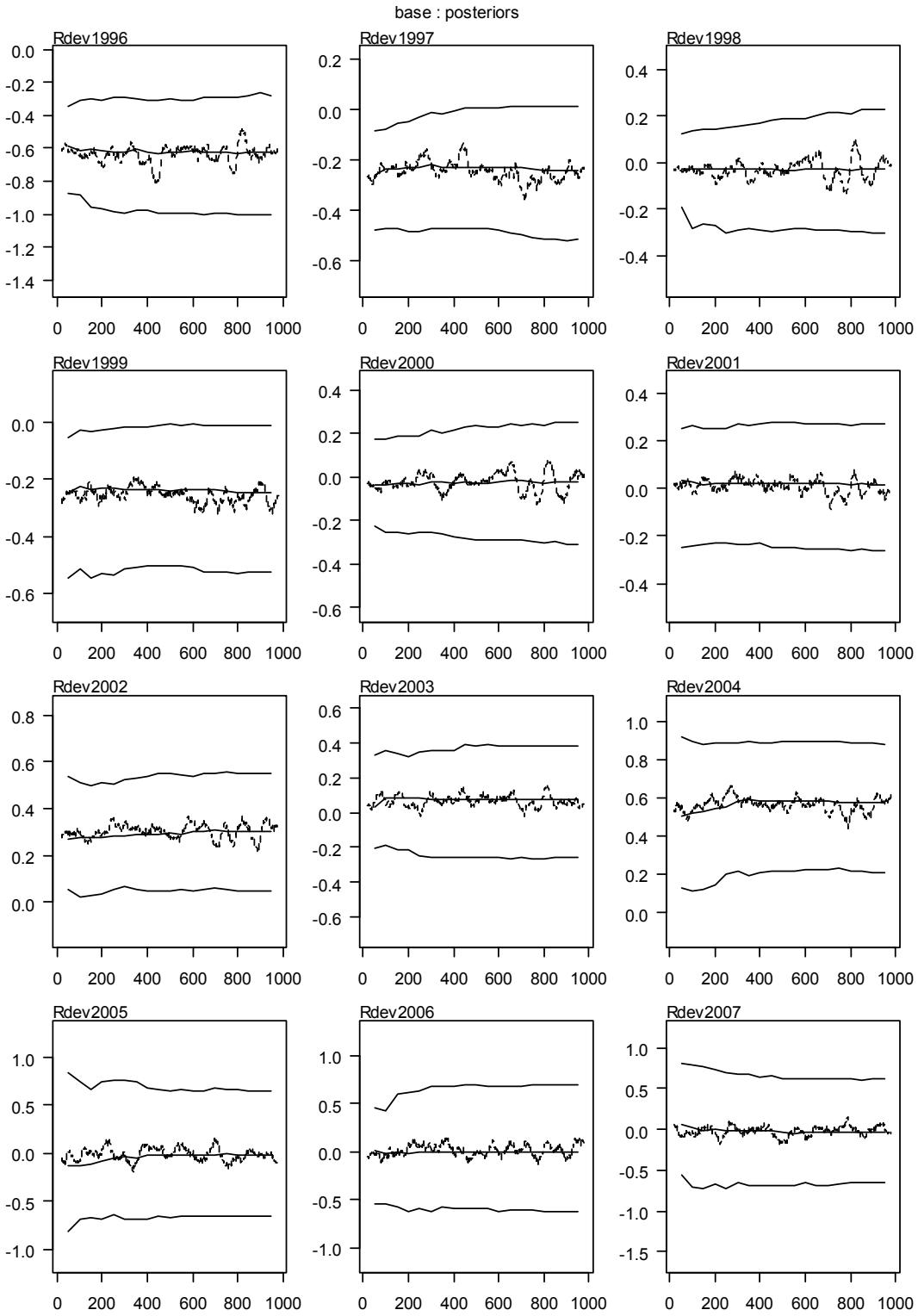

Figure 17 continued.

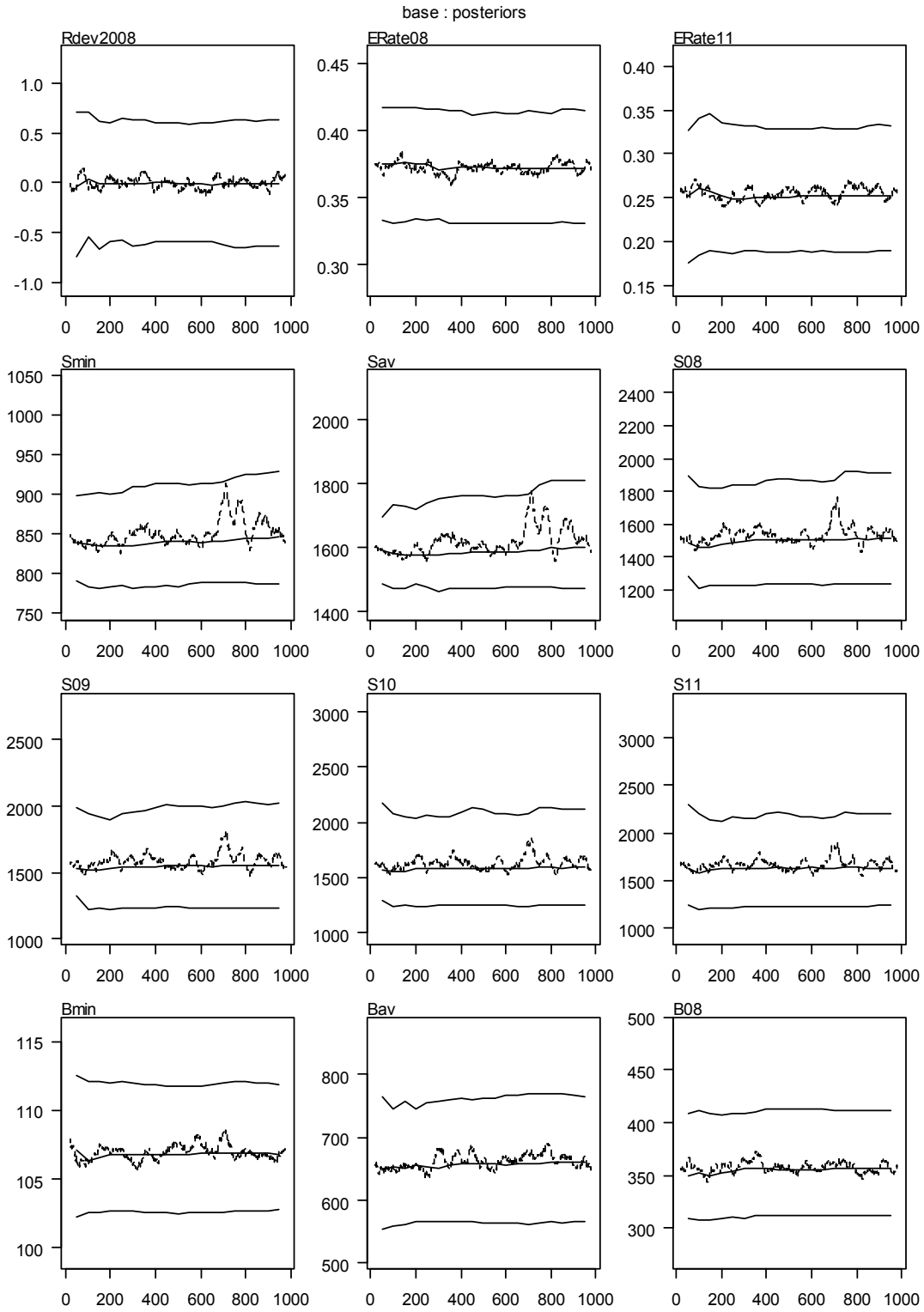

Figure 17 continued.

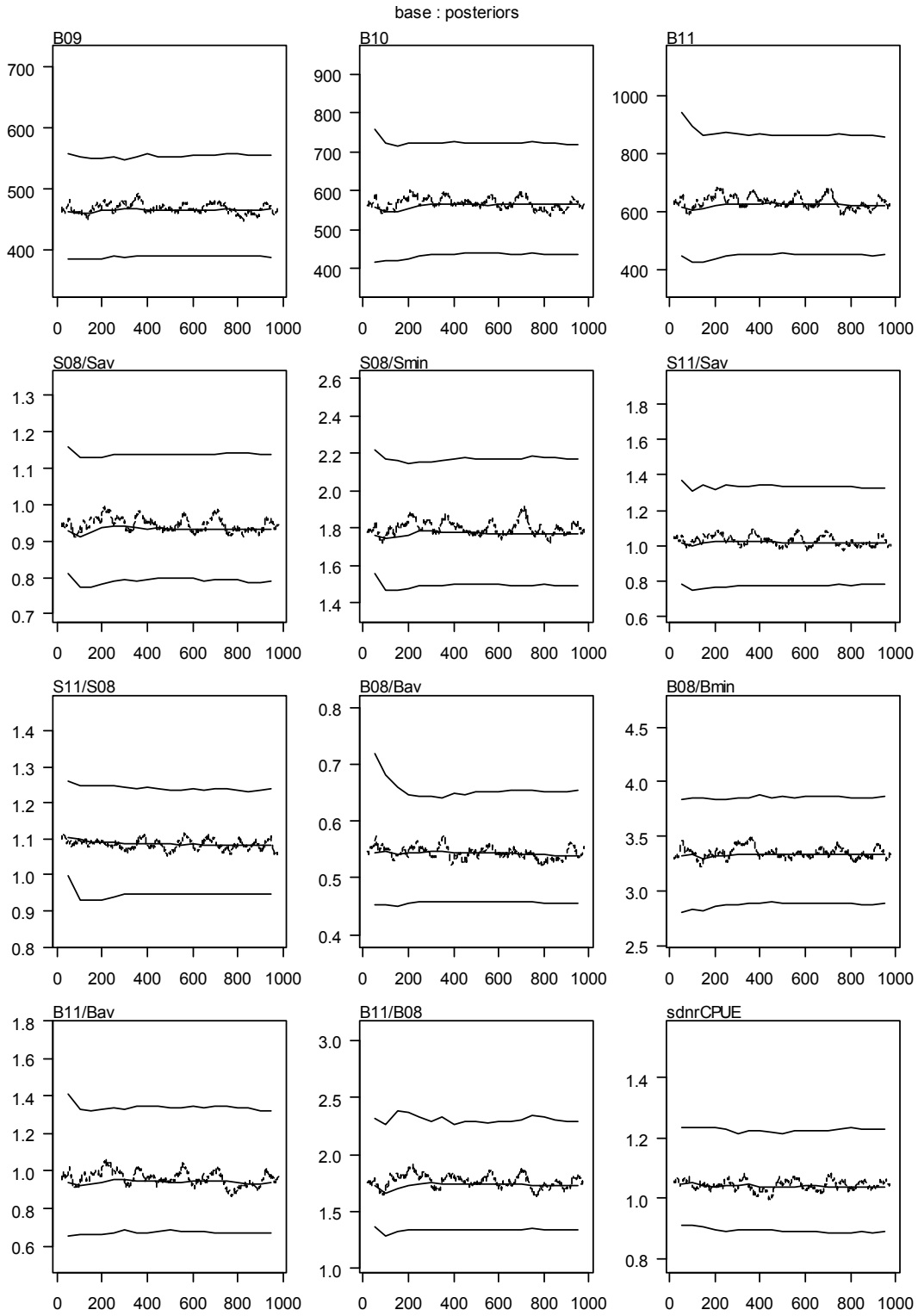

Figure 17 continued.

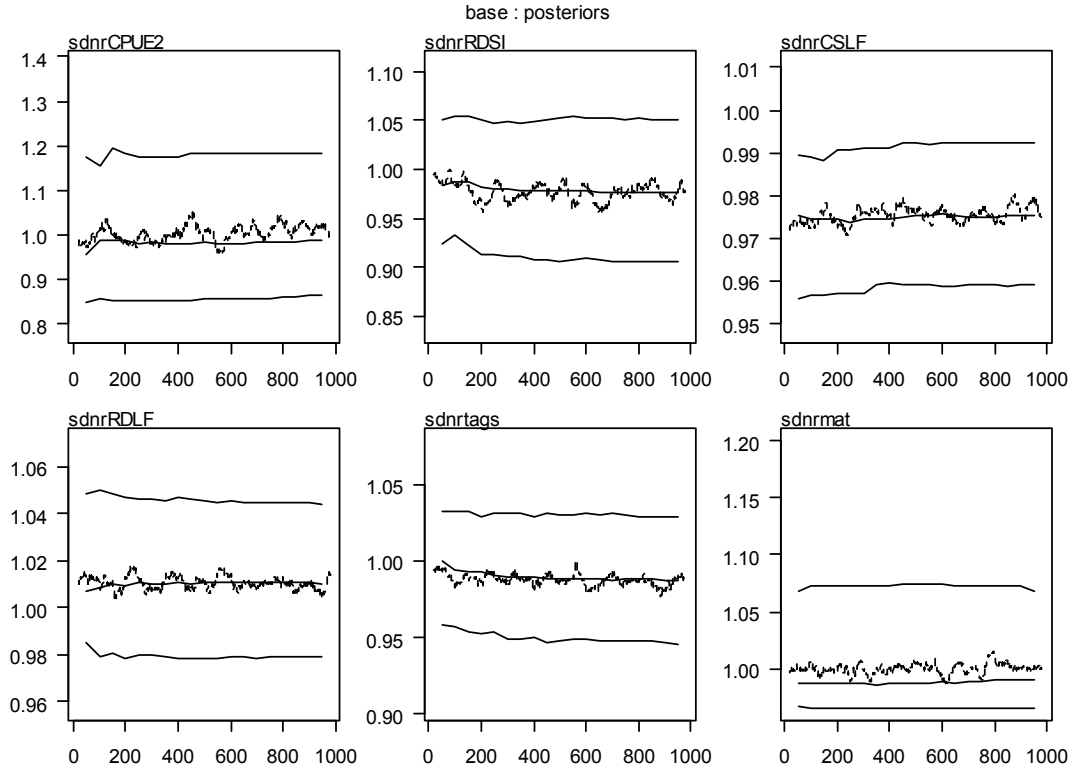

Figure 17 continued.

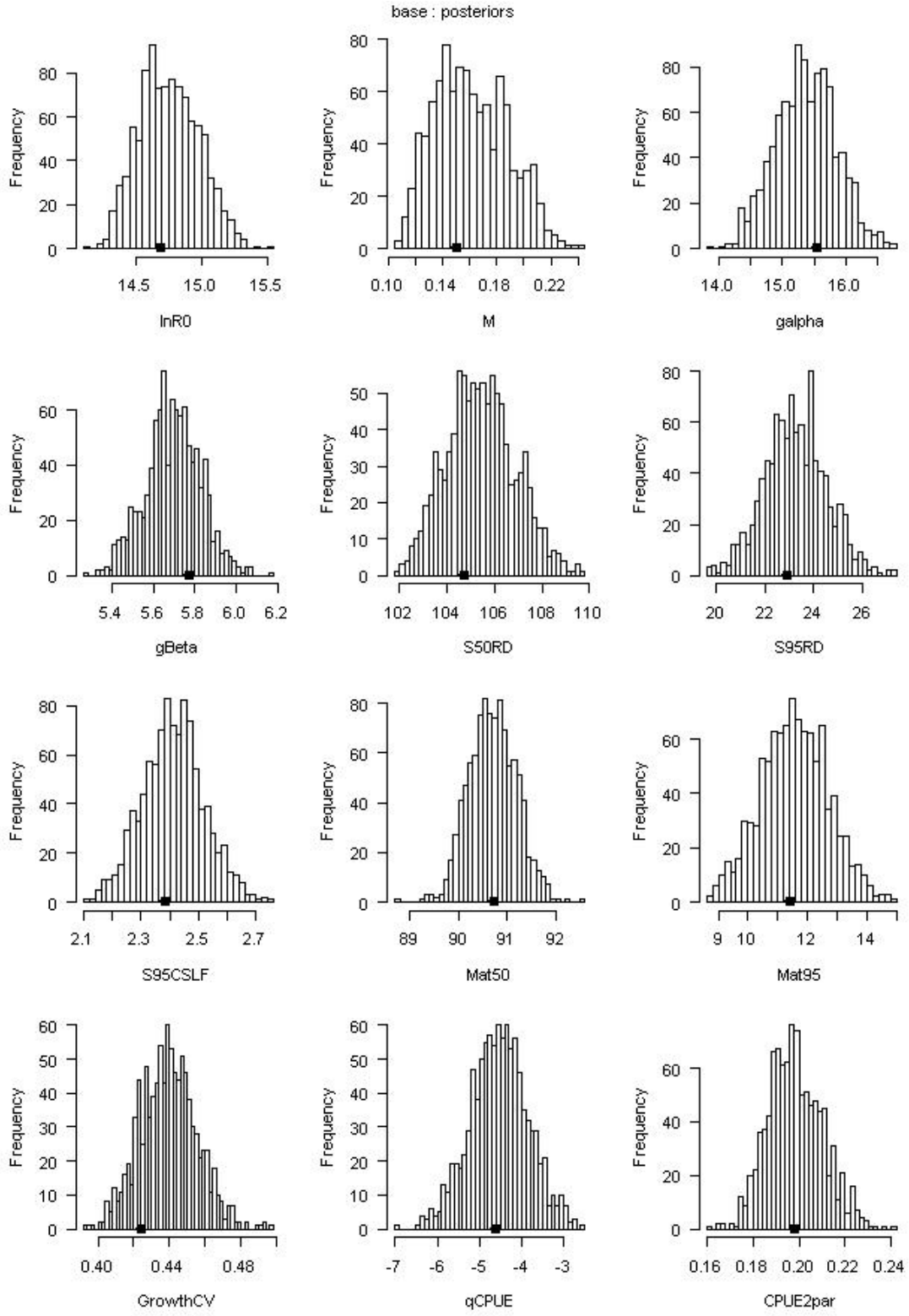

Figure 18: Posterior distributions of parameters and indicators from base case PAU 7 MCMC. Dots on the x-axis show the MPD estimate.

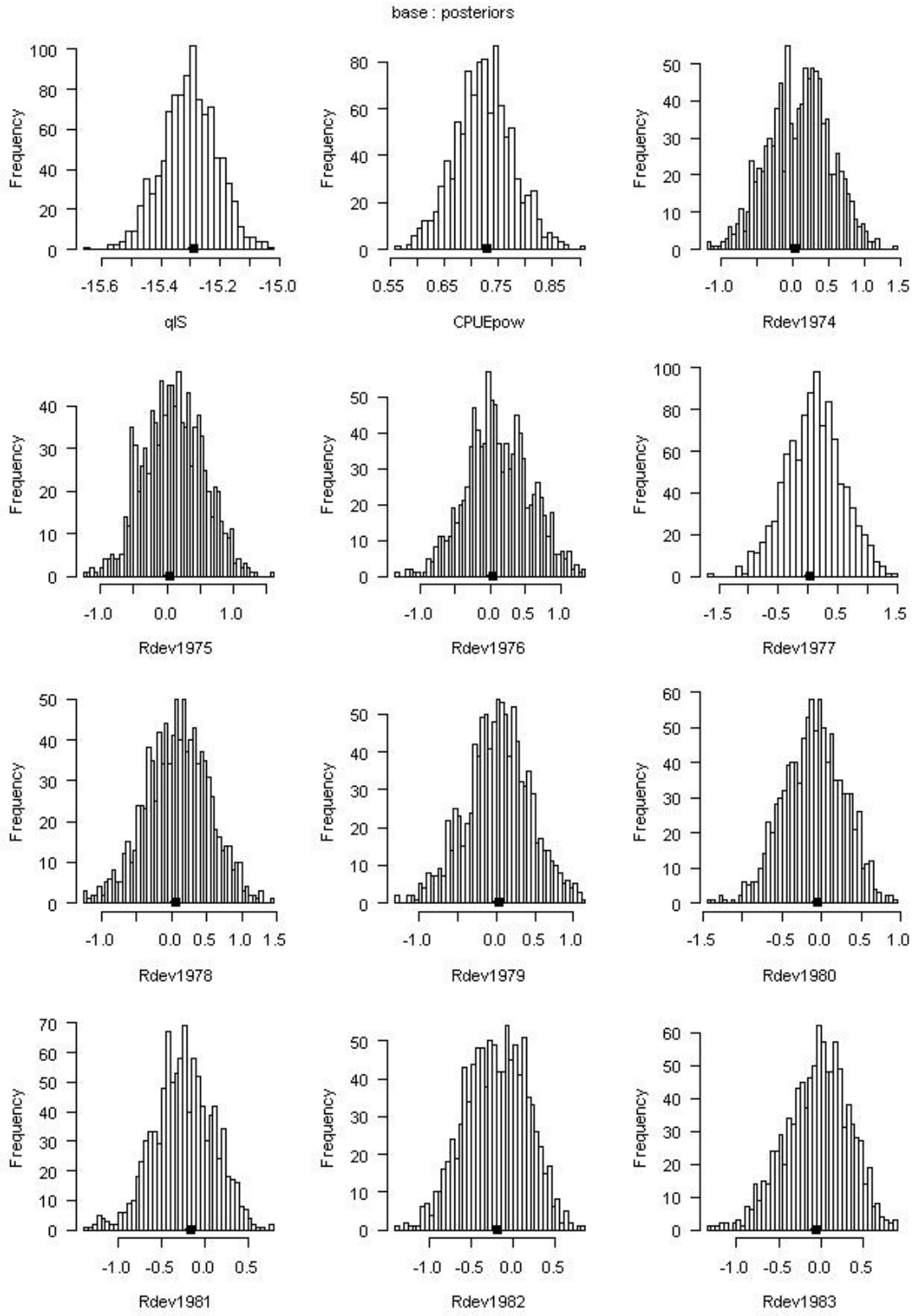

Figure 18 continued.

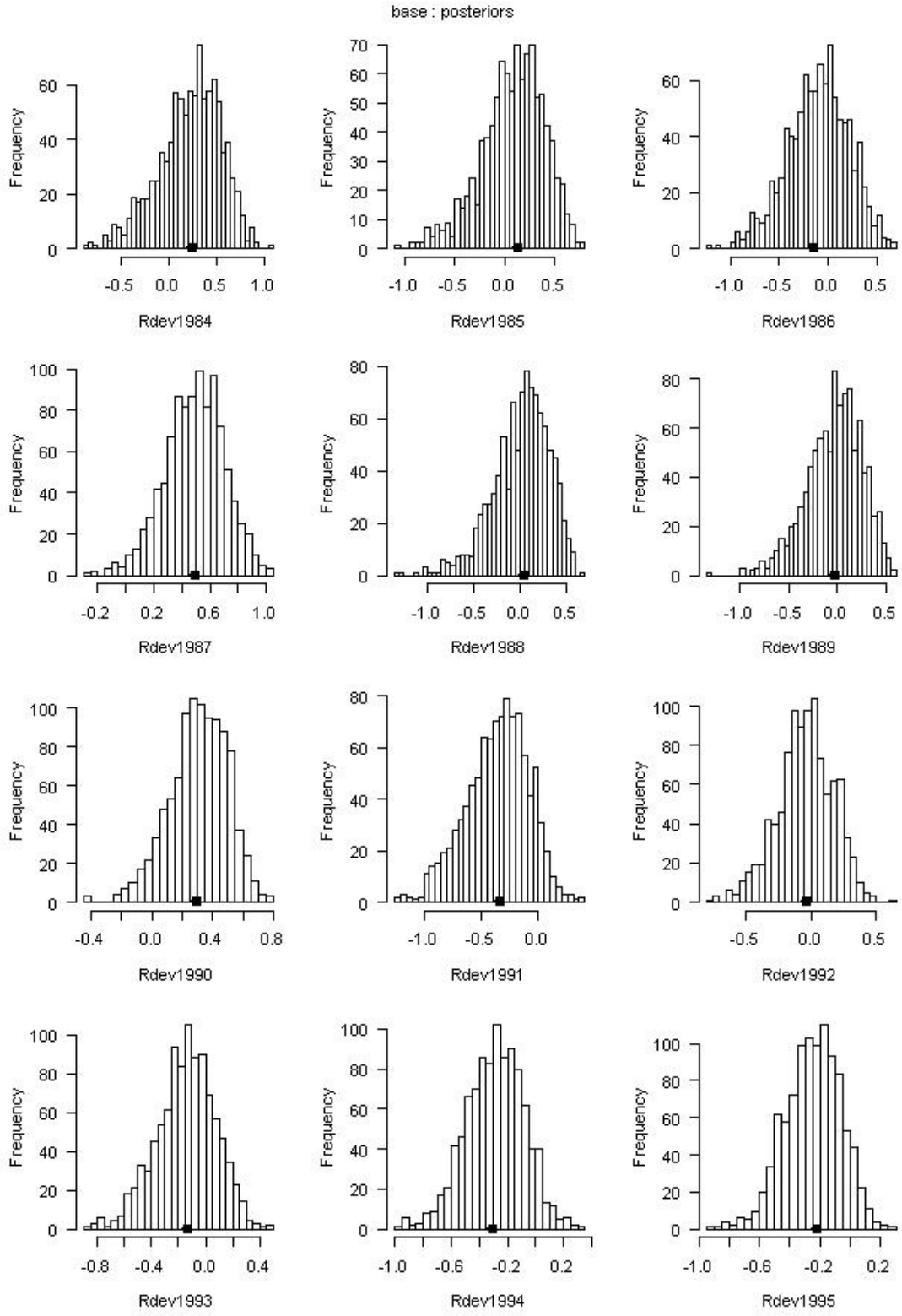

Figure 18 continued.

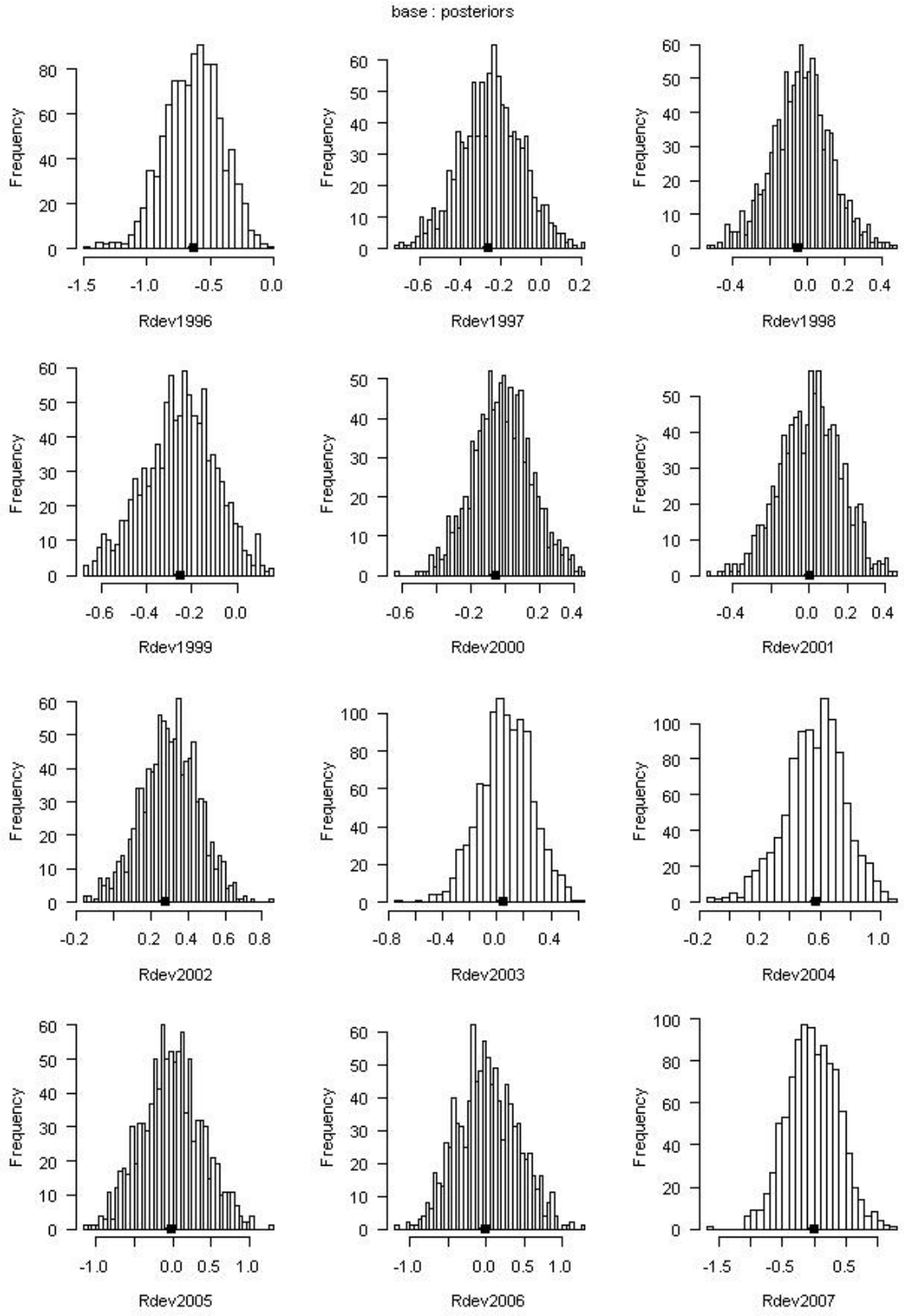

Figure 18 continued.

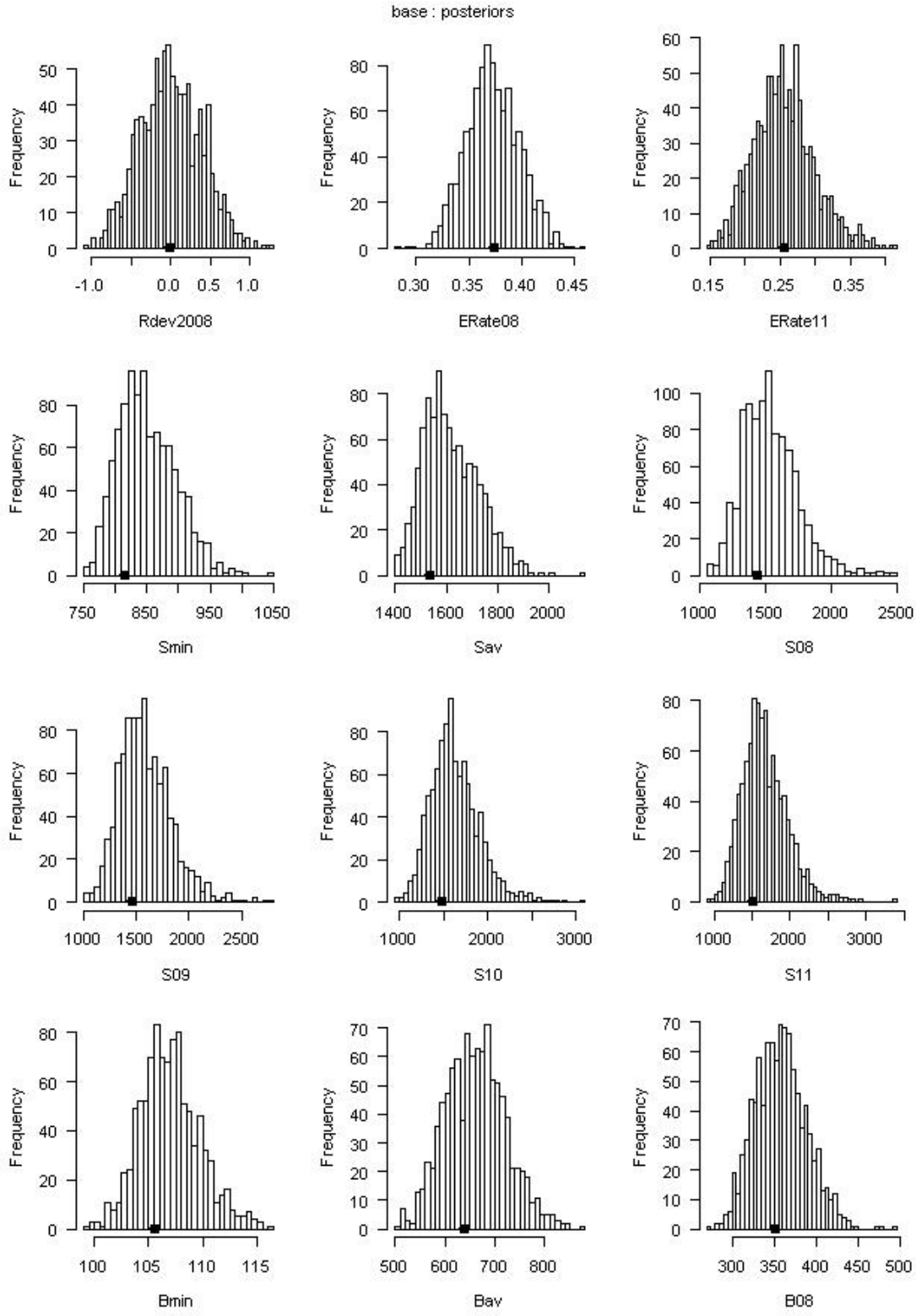

Figure 18 continued.

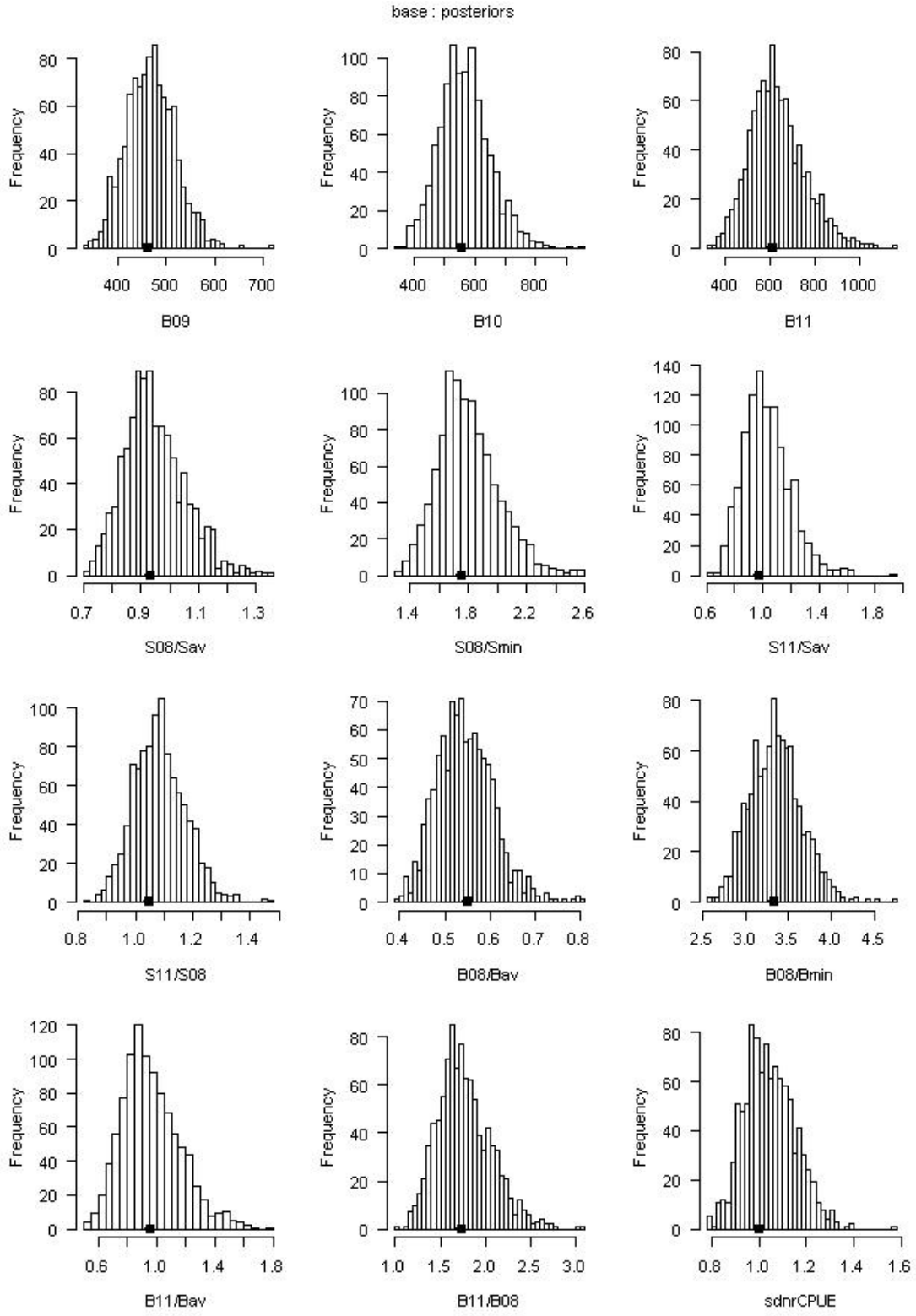

Figure 18 continued.

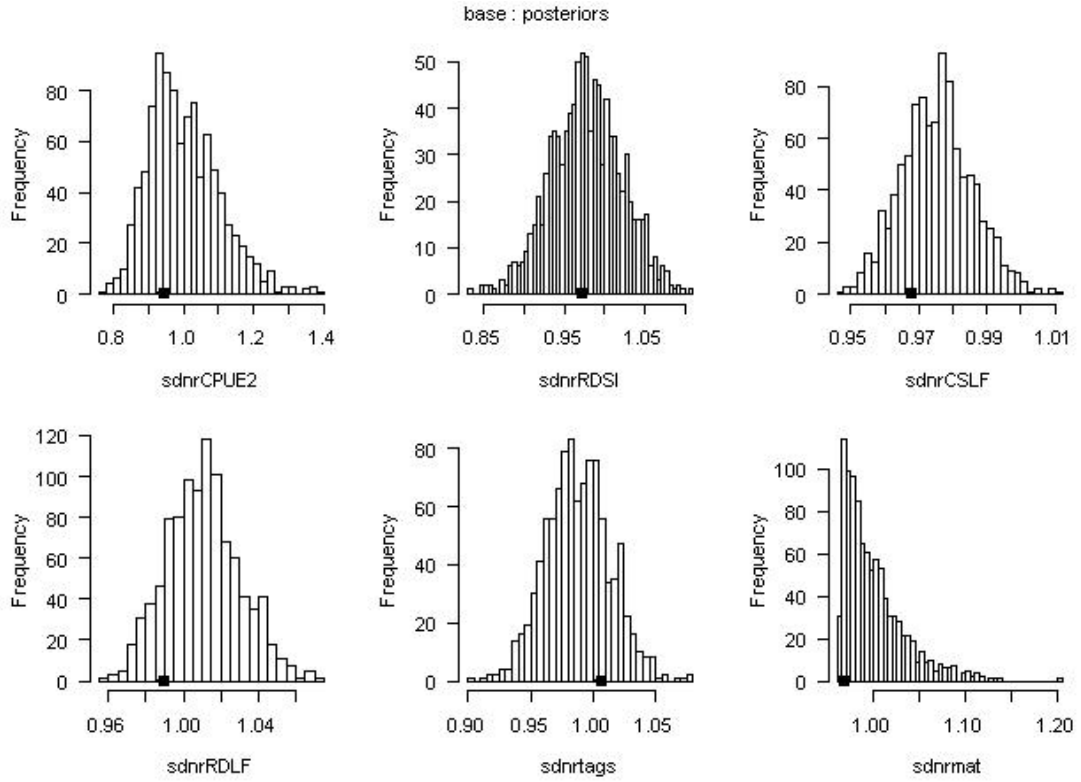

Figure 18 continued.

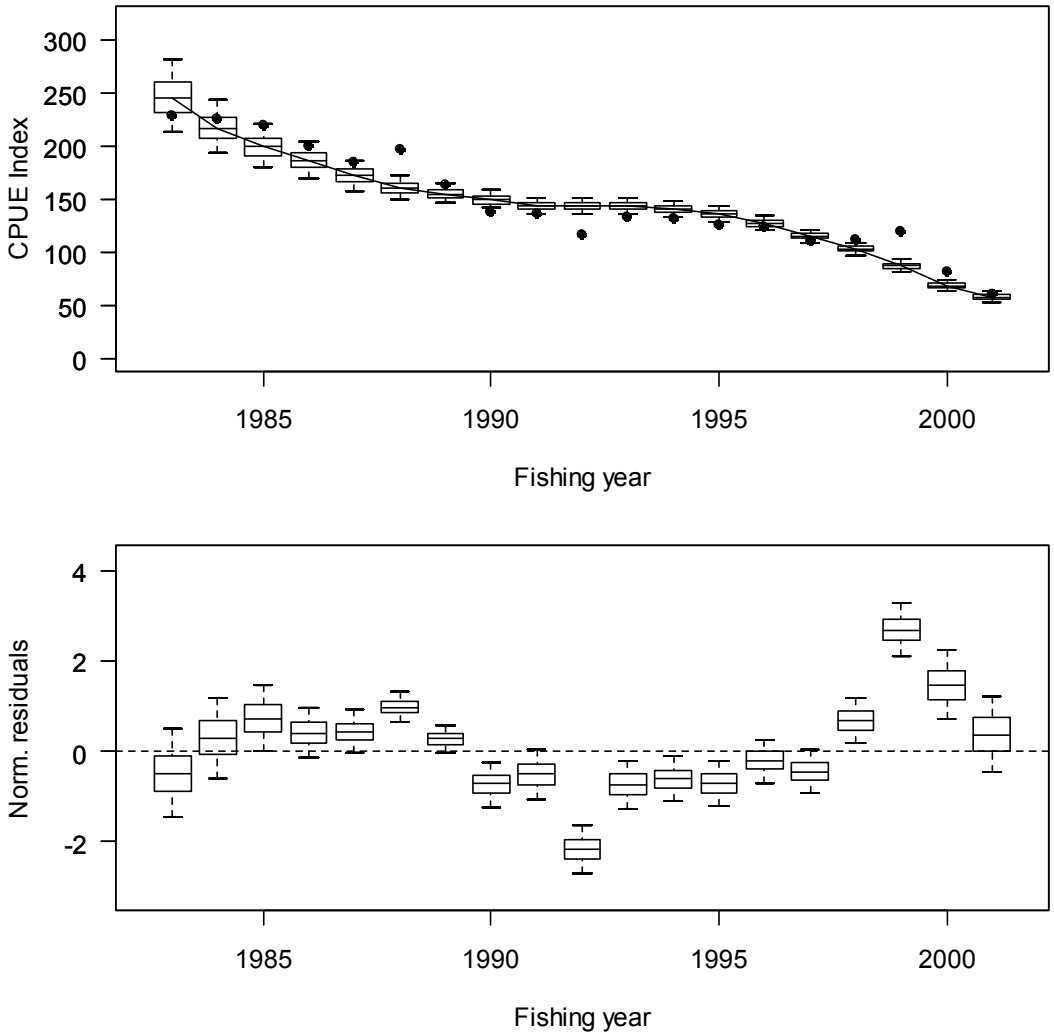

Figure 19: The posterior distributions of the fits to CPUE data (top) and the posterior distributions of the normalised residuals from the base case MCMC for PAU 7. In the upper plot, black dots show the observations. For each year, the figure shows the median of the posterior distribution (horizontal bar), the 25th and 75th percentiles (box) and 5th and 95th percentiles of the posterior.

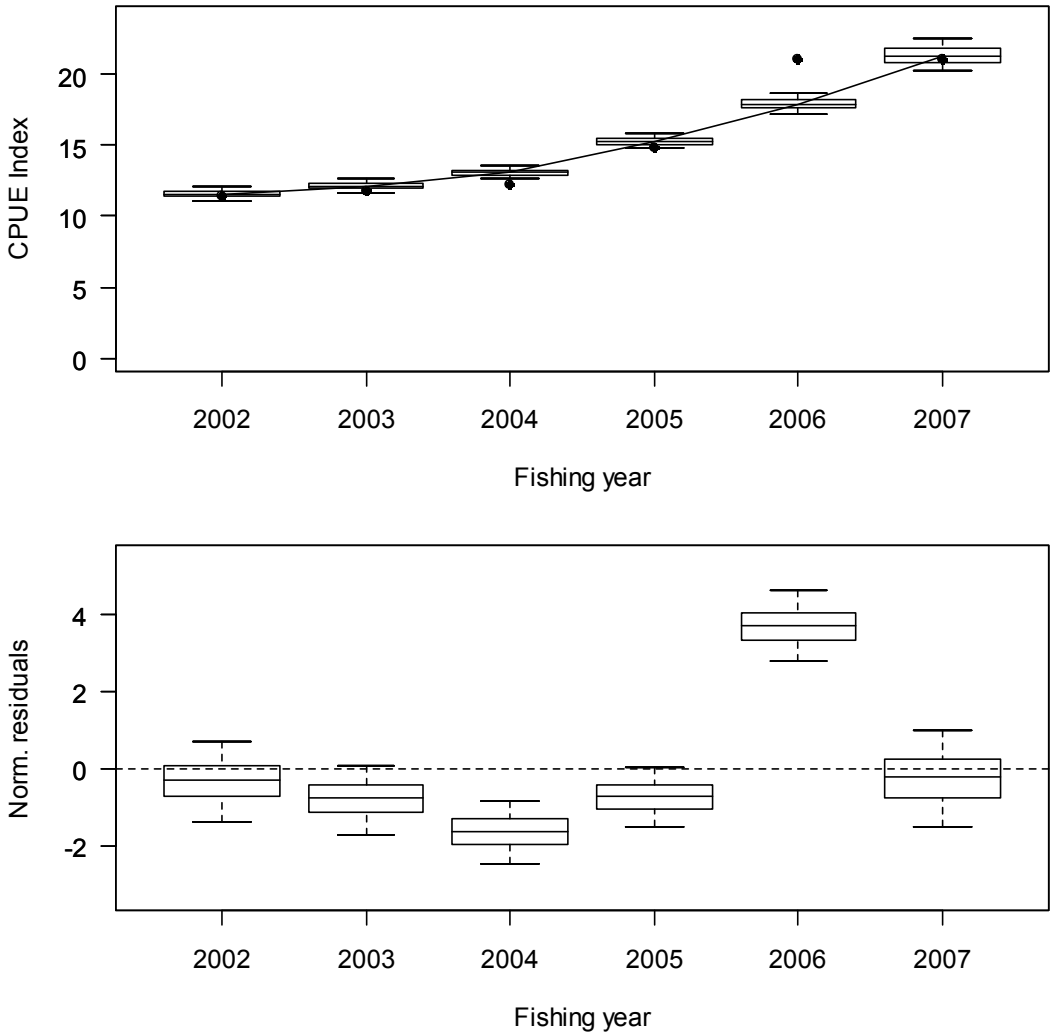

Figure 20 : The posterior distributions of the fits to PCPUE data (top) and the posterior distributions of the normalised residuals from the base case MCMC for PAU 7. In the upper plot, black dots show the observations. For each year, the figure shows the median of the posterior distribution (horizontal bar), the 25th and 75th percentiles (box) and 5th and 95th percentiles of the posterior.

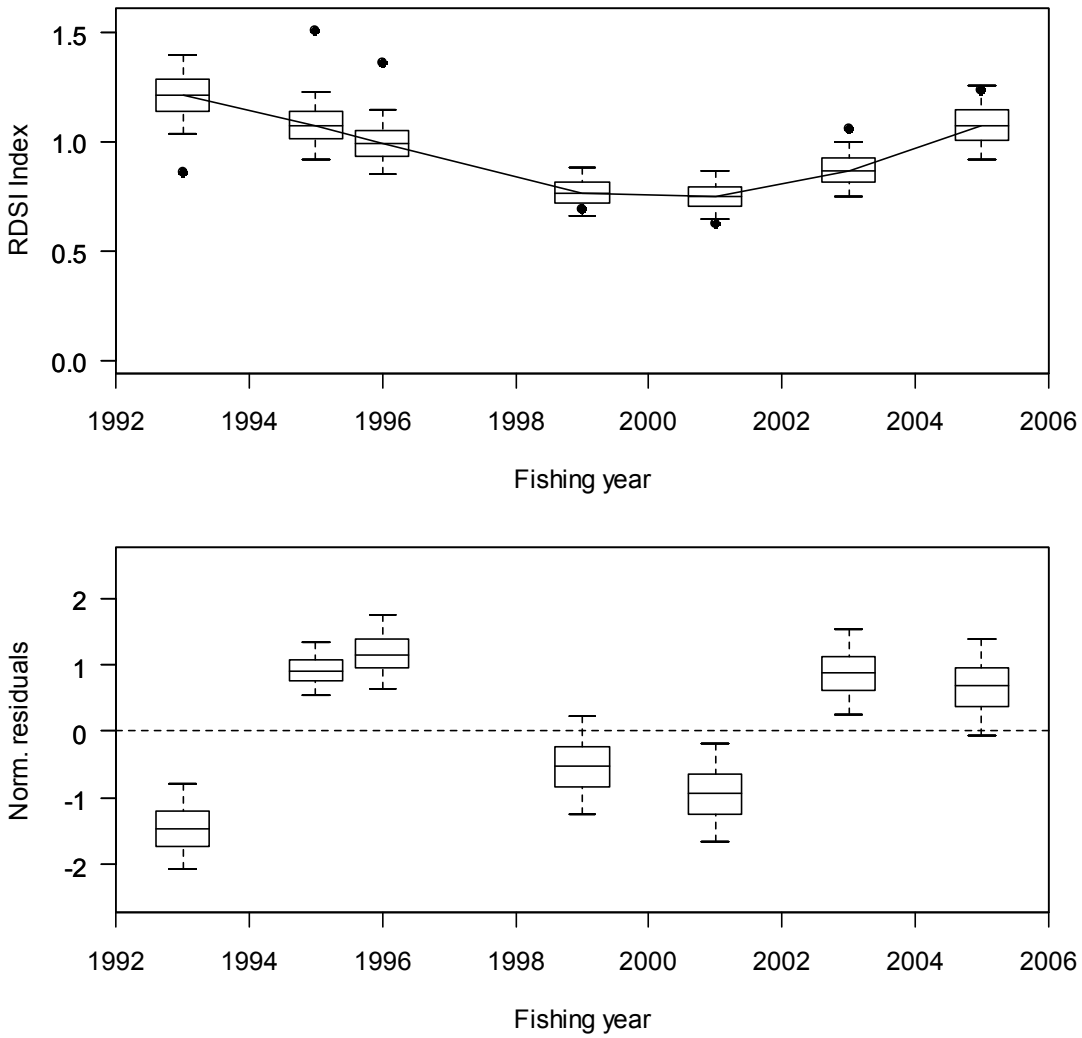

Figure 21: The posterior distributions of the fits to RDSI data (top) and the posterior distributions of the normalised residuals from the base case MCMC for PAU 7. In the upper plot, black dots show the observations. For each year, the figure shows the median of the posterior distribution (horizontal bar), the 25th and 75th percentiles (box) and 5th and 95th percentiles of the posterior.

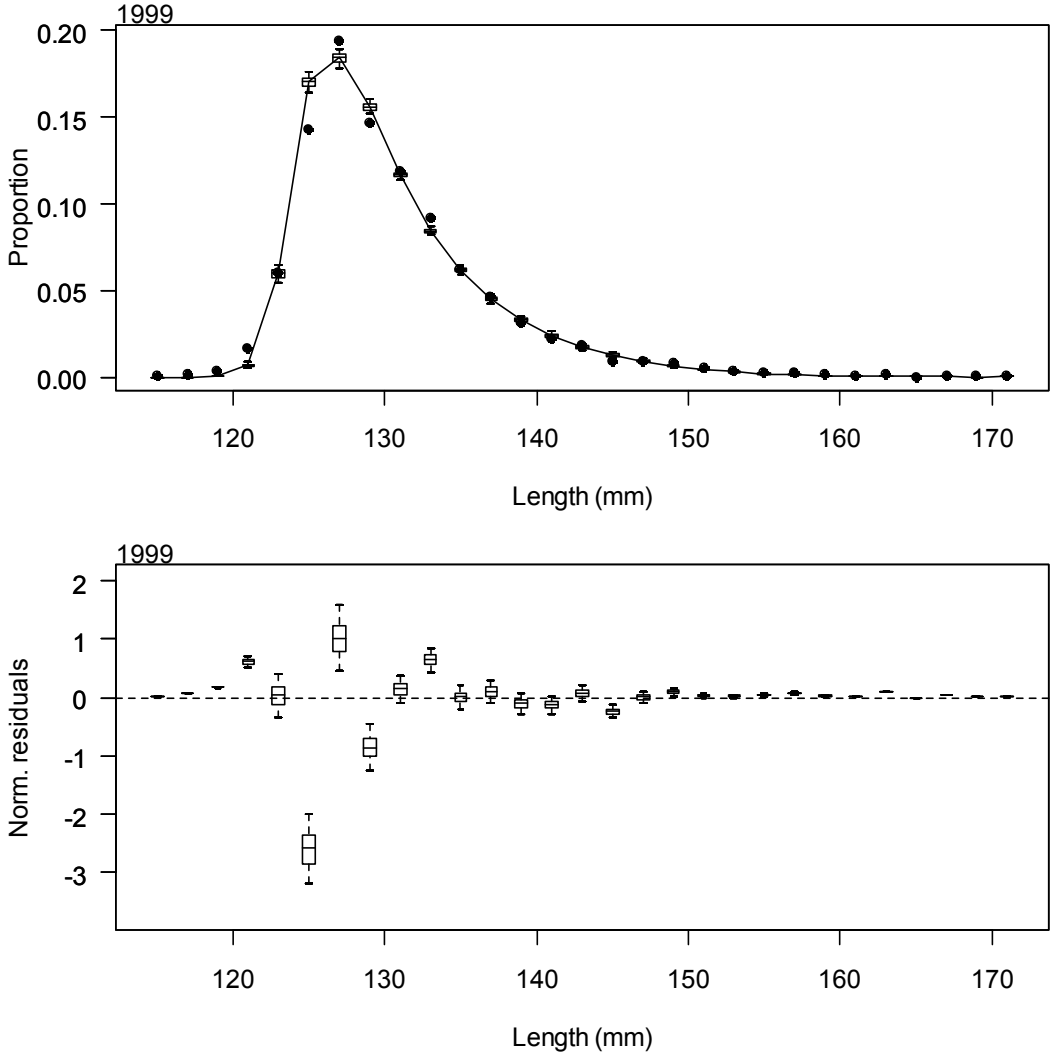

Figure 22 : The posterior distribution of the base case MCMC fit to the CSLF data from 1999 (top) and the posterior distributions of the normalised residuals.

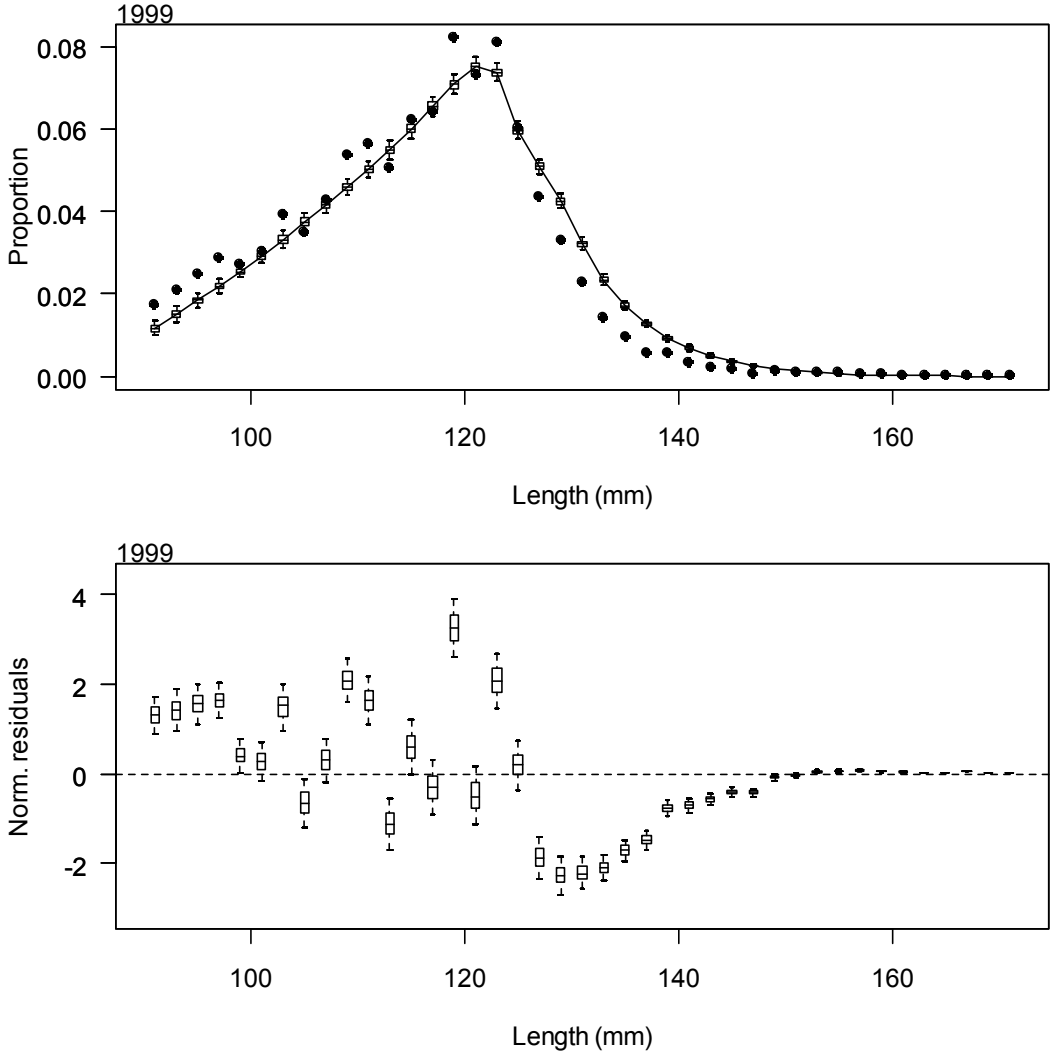

Figure 23: The posterior distributions of the base case MCMC fit to the RDLF data from 1999 (top) and the posterior distributions of the normalised residuals.

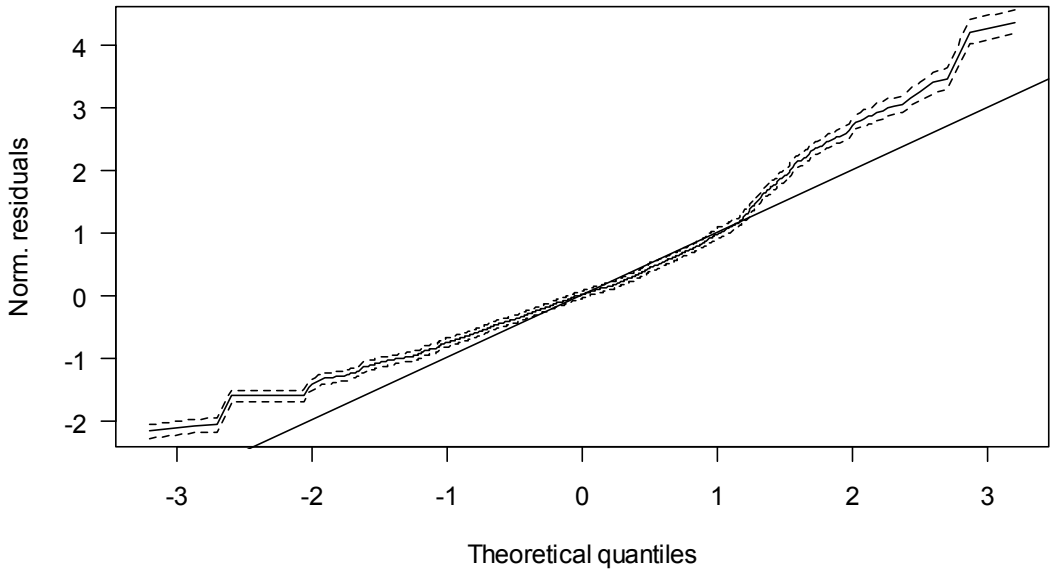

Figure 24: Q-Q plot of the normalised residuals from the posterior distributions of the base case MCMC fits to the tag-recapture data.

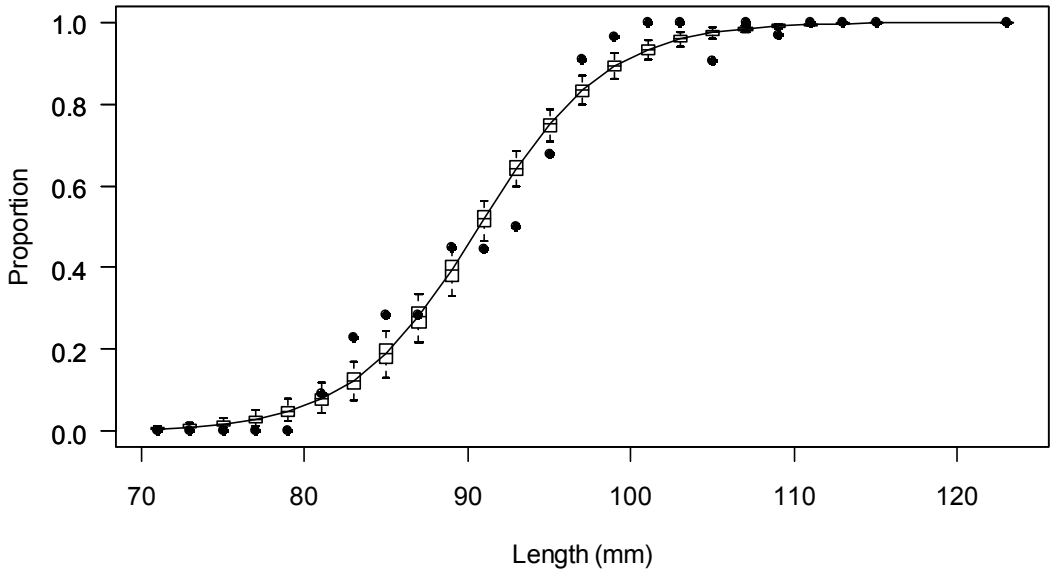

Figure 25 : The posterior distribution of the base case MCMC fit to maturity-at-length for PAU 7. Dots show the observations and the box plots summarise the posterior as in previous captions.

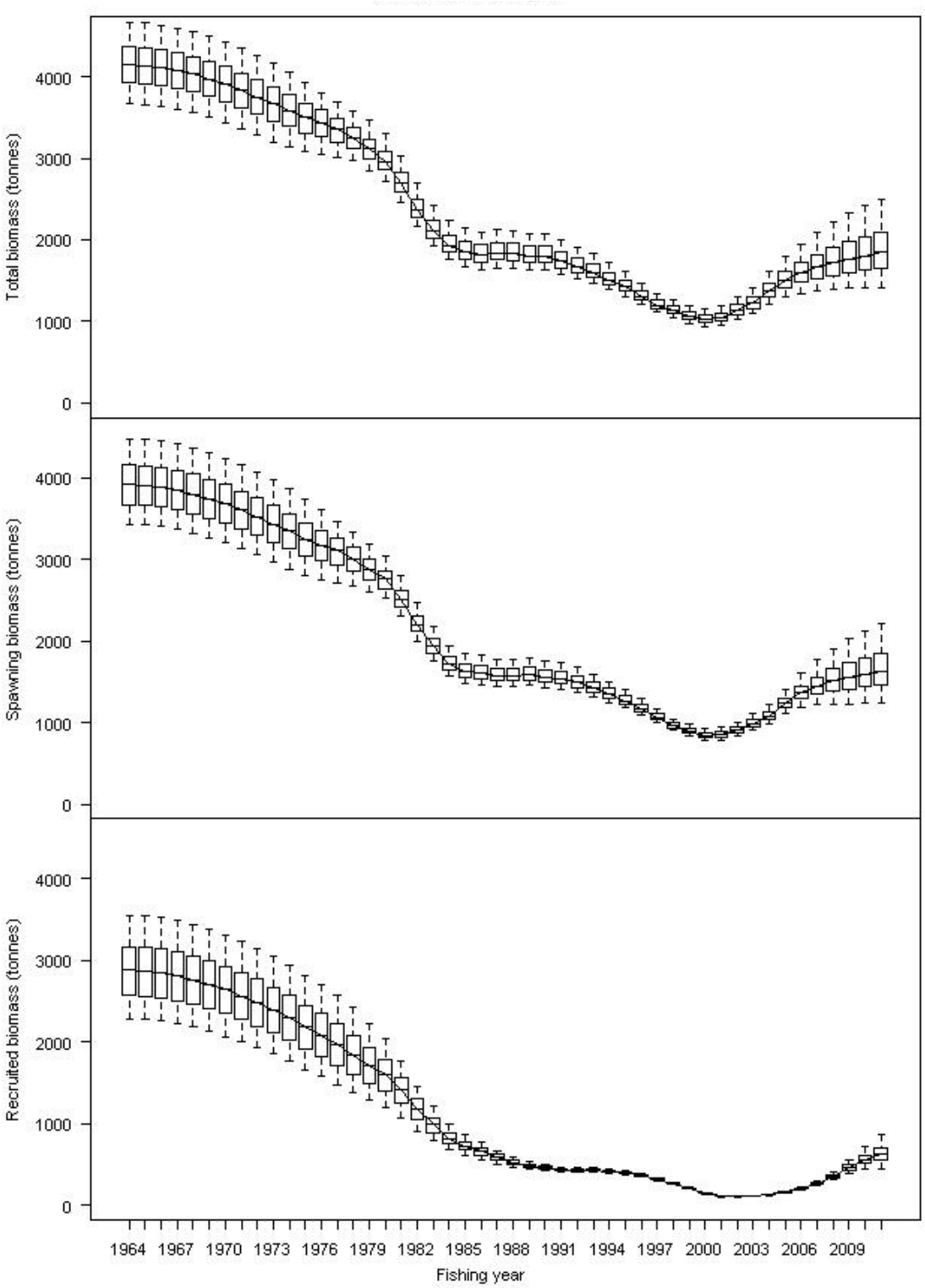

Figure 26: The posterior biomass trajectories from the base case MCMC for PAU 7: total biomass (top), spawning biomass (middle) and recruited biomass (bottom). Box plots summarise the posterior distribution for each year as described in previous captions.

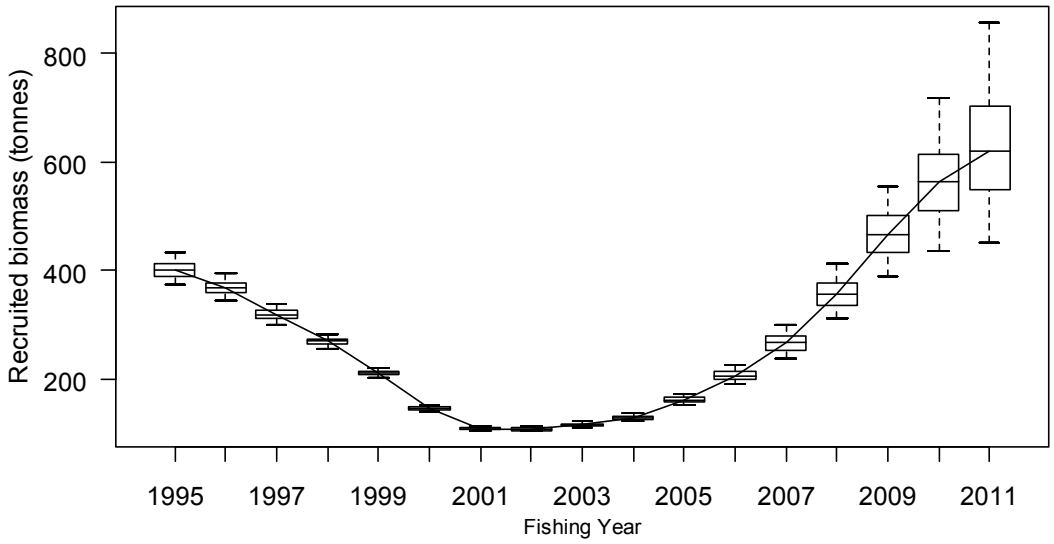

Figure 27: The posterior distribution of the base case MCMC recruited biomass trajectory from 1995 onwards.

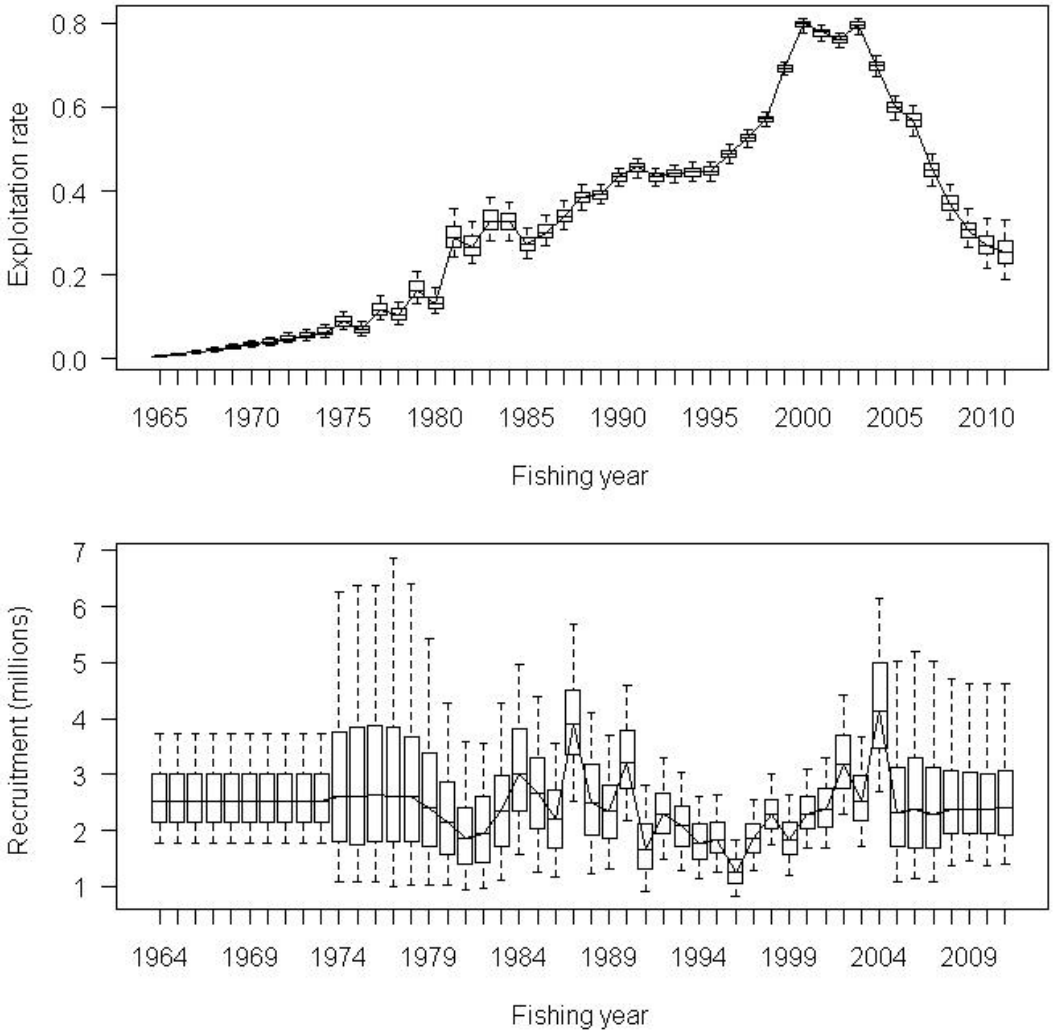

Figure 28: The posterior trajectories of exploitation rate (upper) and recruitment (lower) for the base case MCMC for PAU 7.

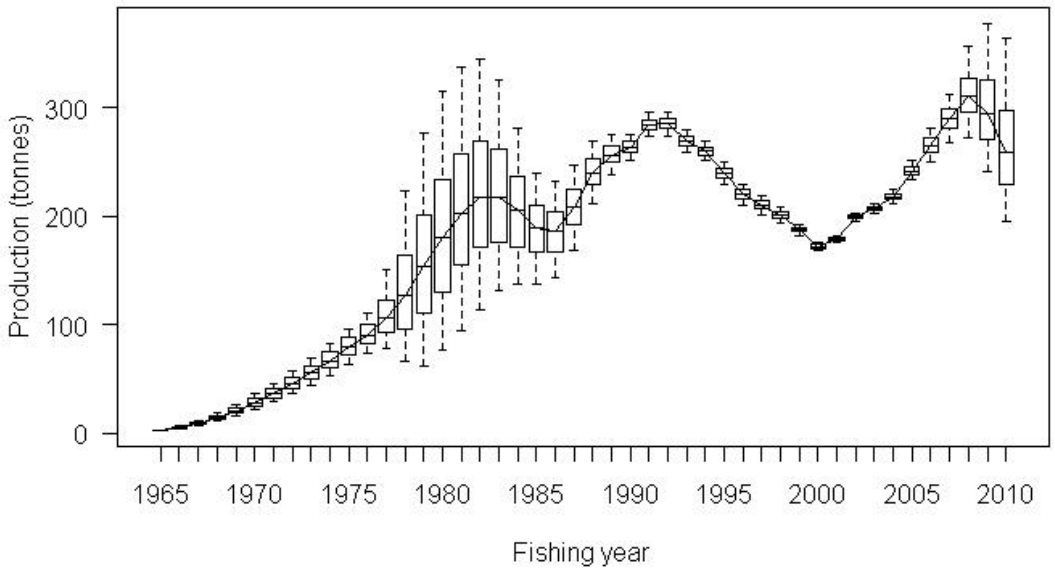

Figure 29: The posterior trajectory of estimated surplus production from the base case MCMC for PAU 7.

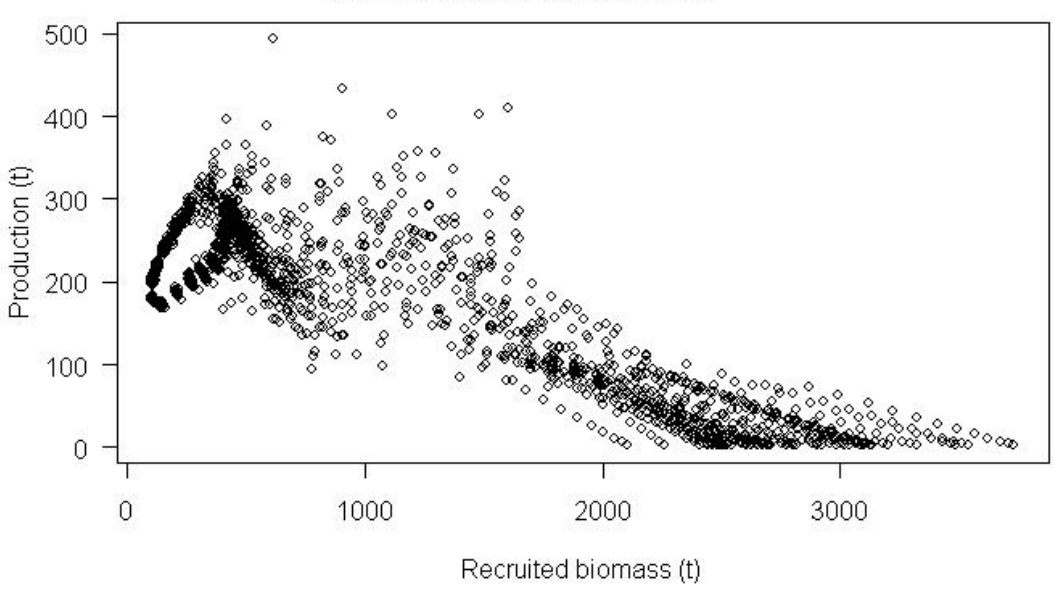

Figure 30: Surplus production plotted against mid-year recruited biomass from the base case MCMC for PAU 7. Each point represents one year in one sample from the joint posterior distribution. For this plot, samples were uniformly thinned to 4% of the total sample.

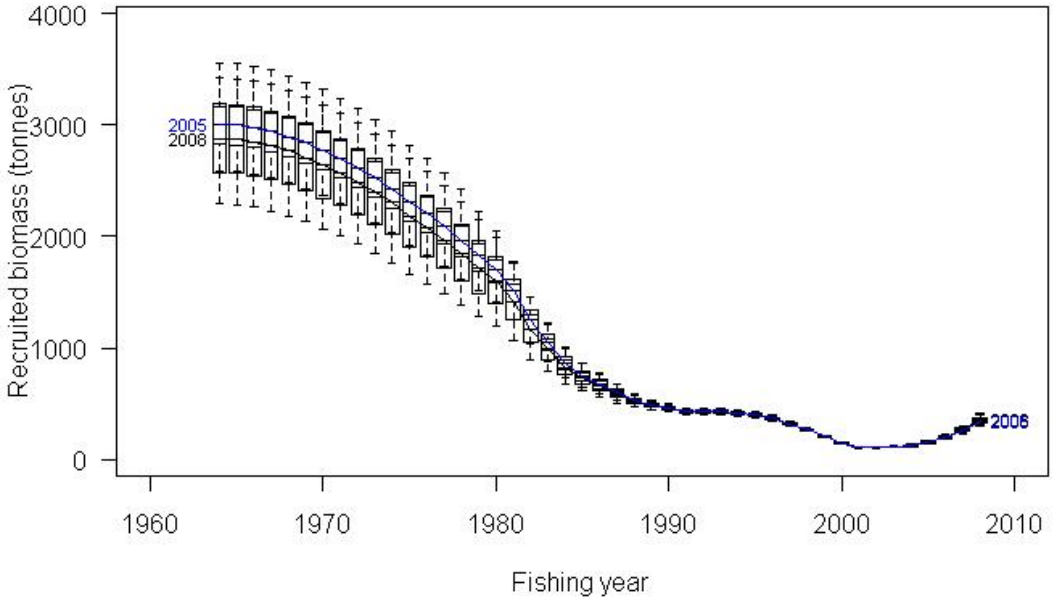

Figure 31: Comparison of recruited biomass from the 2005 and 2008 stock assessments.

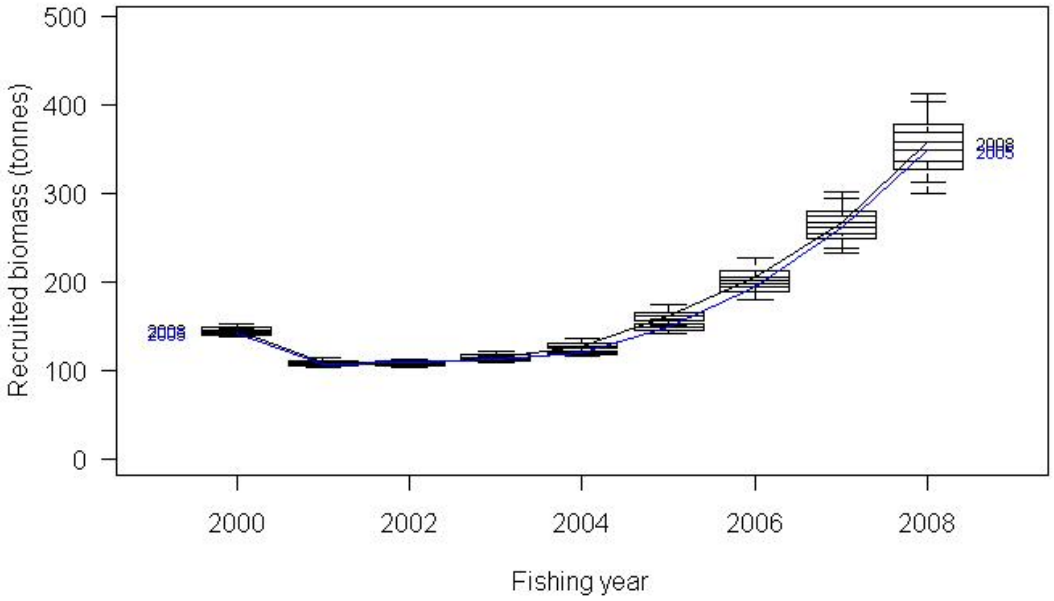

Figure 32 : Comparison of recruited biomass from the 2005 and 2008 stock assessments from 2000-2008.

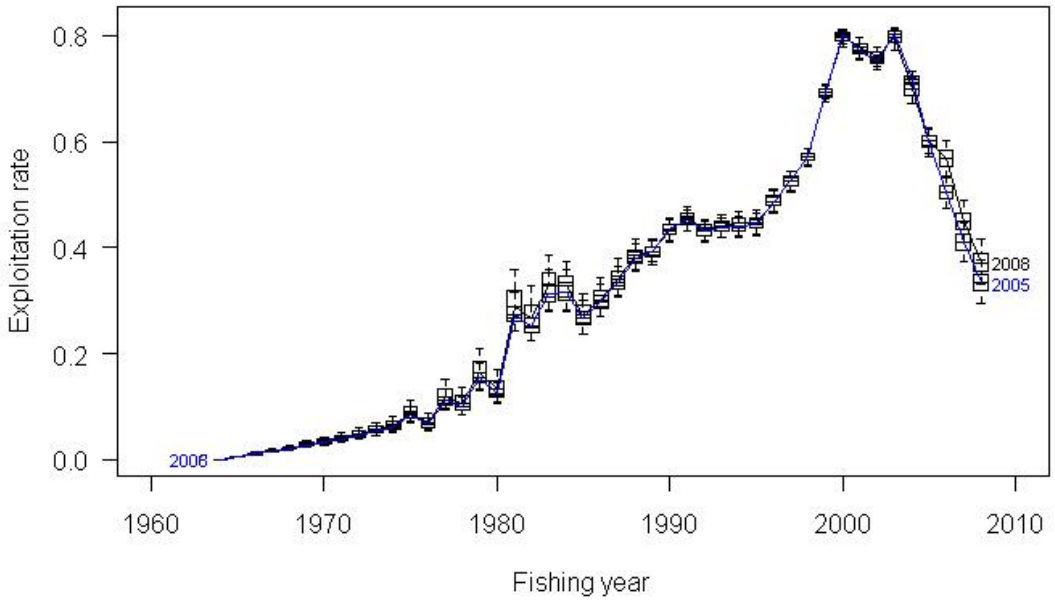

Figure 33: Comparison of exploitation rate from the 2005 and 2008 stock assessments.

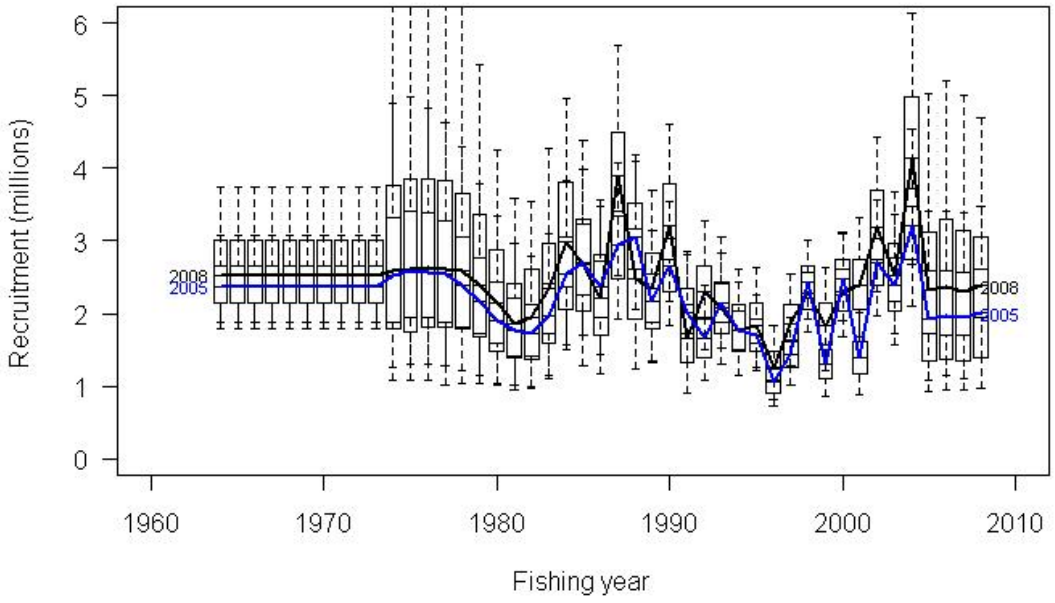

Figure 34: Comparison of recruitment from the 2005 and 2008 stock assessments.

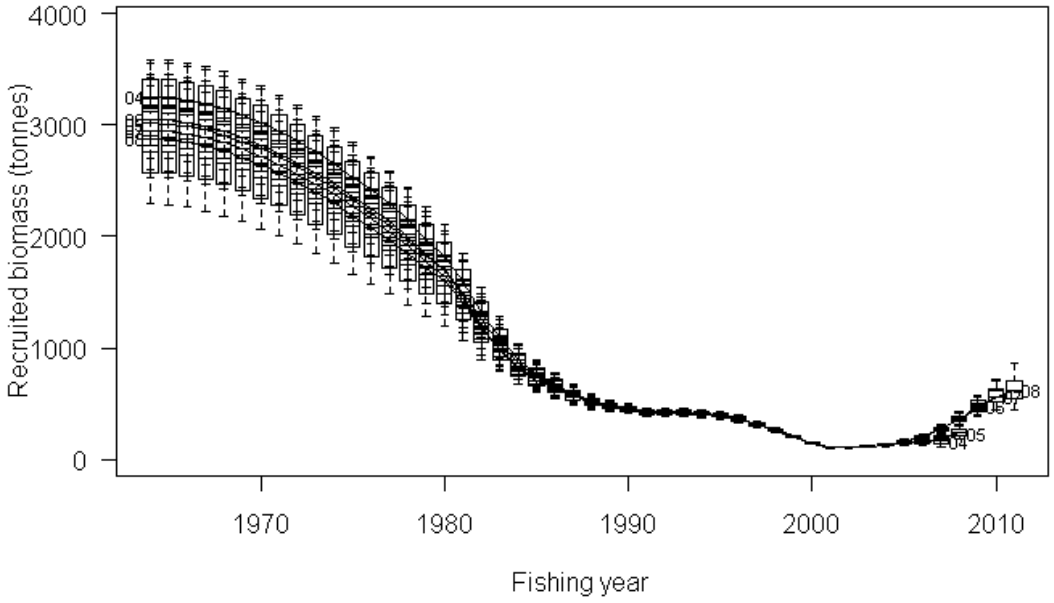

Figure 35: The posterior trajectories of recruited biomass from the MCMC retrospective sensitivity trials for PAU 7. Labels indicate the last year of data used, thus "08" is the base case.

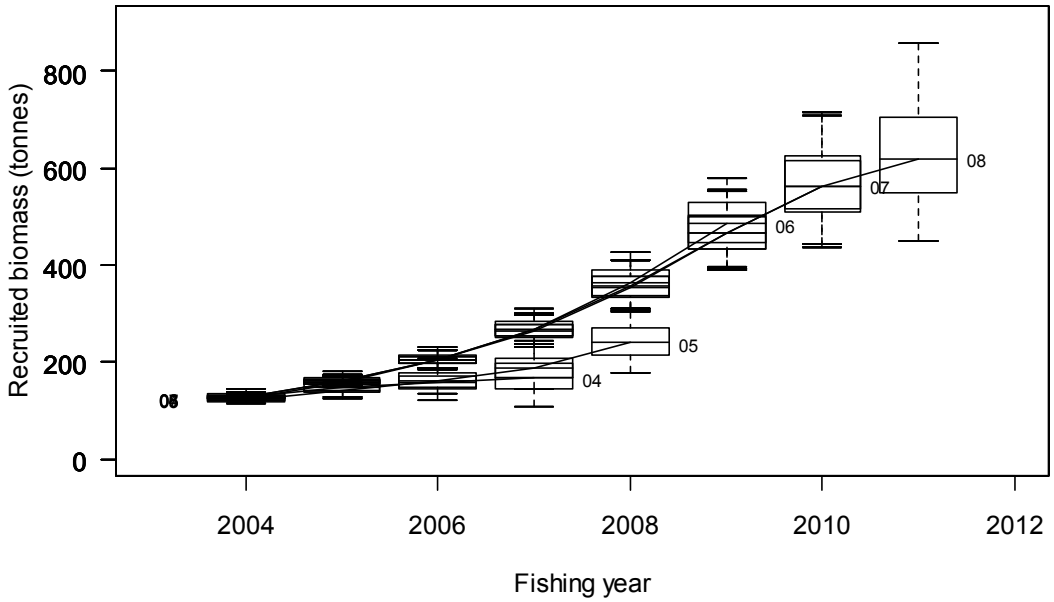

Figure 36 : For 2004 onwards, the posterior trajectories of recruited biomass from the MCMC retrospective sensitivity trials for PAU 7. Labels indicate the last year of data used, thus "08" is the base case.

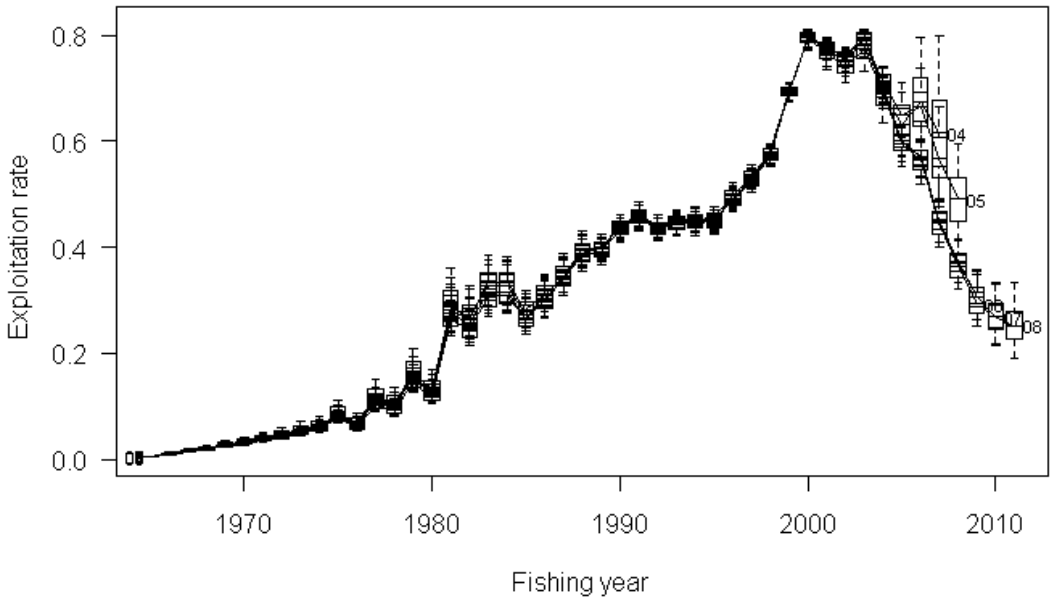

Figure 37: The posterior trajectories of exploitation rate from the MCMC retrospective sensitivity trials for PAU 7. Labels indicate the last year of data used, thus "08" is the base case.

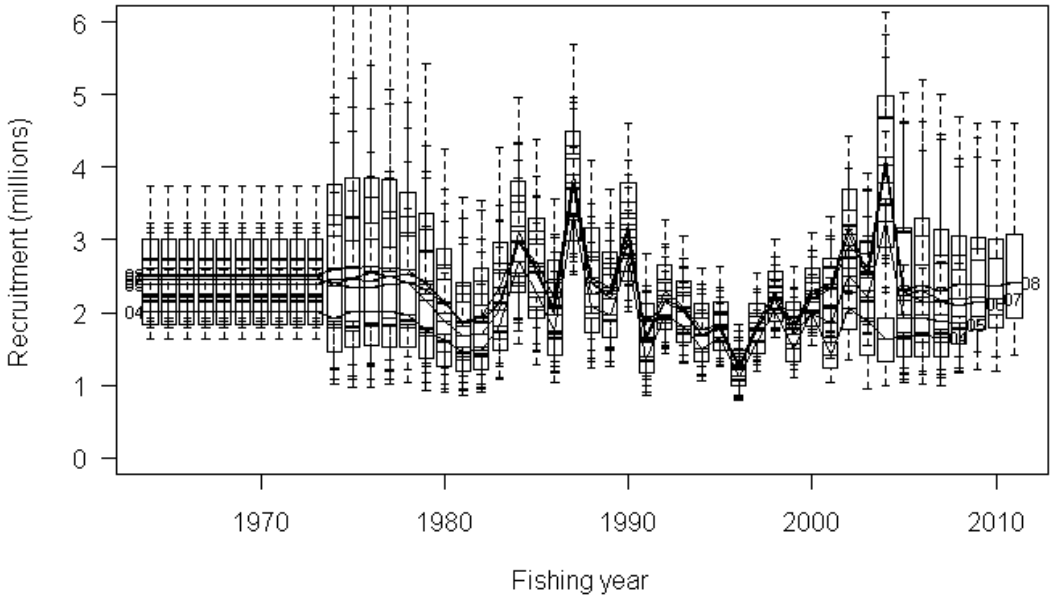

Figure 38: The posterior trajectories of recruitment from the MCMC retrospective sensitivity trials for PAU 7. Labels indicate the last year of data used, thus "08" is the base case.

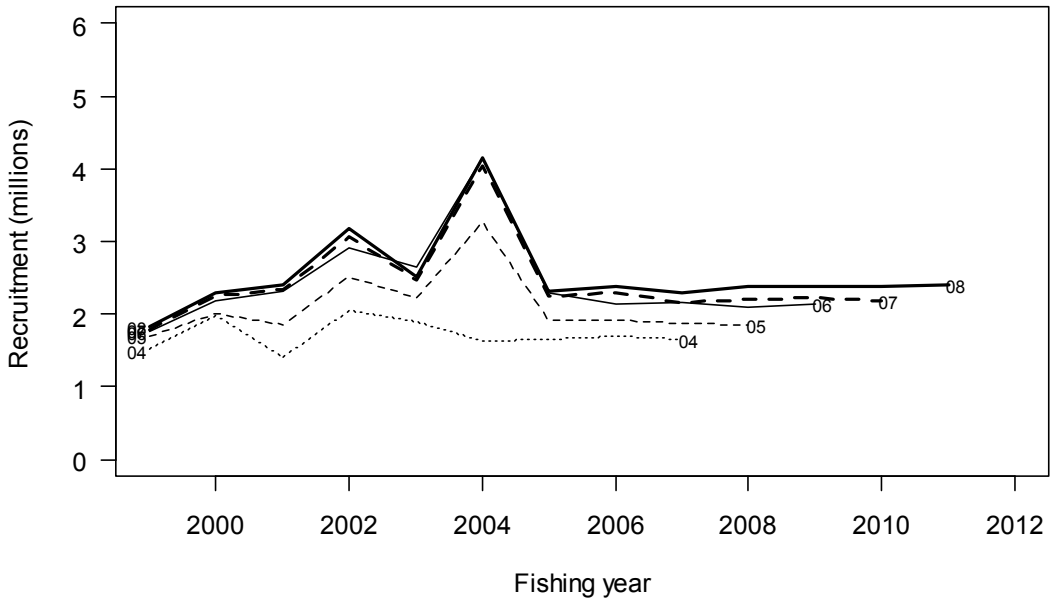

Figure 39: The medians of posterior trajectories of recruitment from the MCMC retrospective sensitivity trials for 2004 to 2008. Labels indicate the last year of data used, thus "08" is the base case.

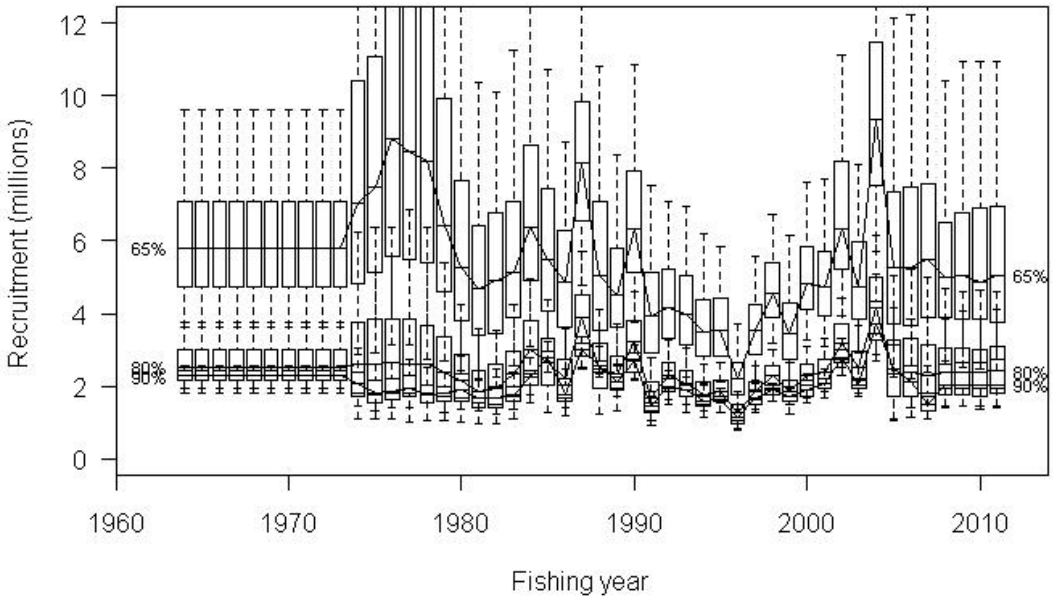

Figure 40: Posteriors of recruitment trajectories from the MCMC sensitivity trials in which maximum allowed exploitation rate was varied from 80% in the base case to 65% and 90%. The 65% trial is the highest set of box plots.

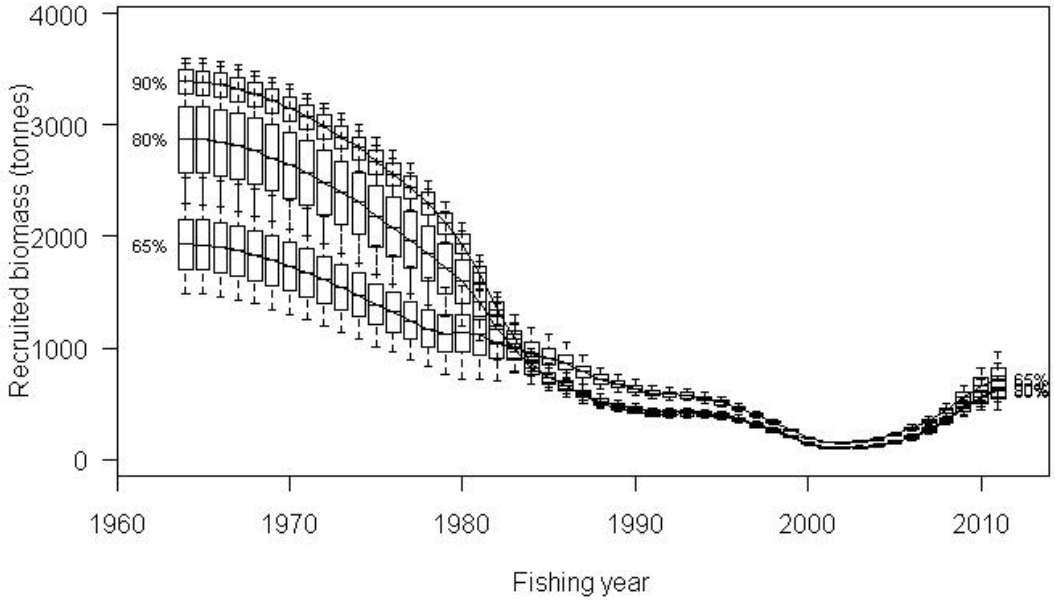

Figure 41 : Recruited biomass trajectories from the MCMC sensitivity trials in which maximum allowed exploitation rate was varied from 80% in the base case to 65% and 90%. The 65% trial is the line that is lowest on the left and highest in the early 2000s.

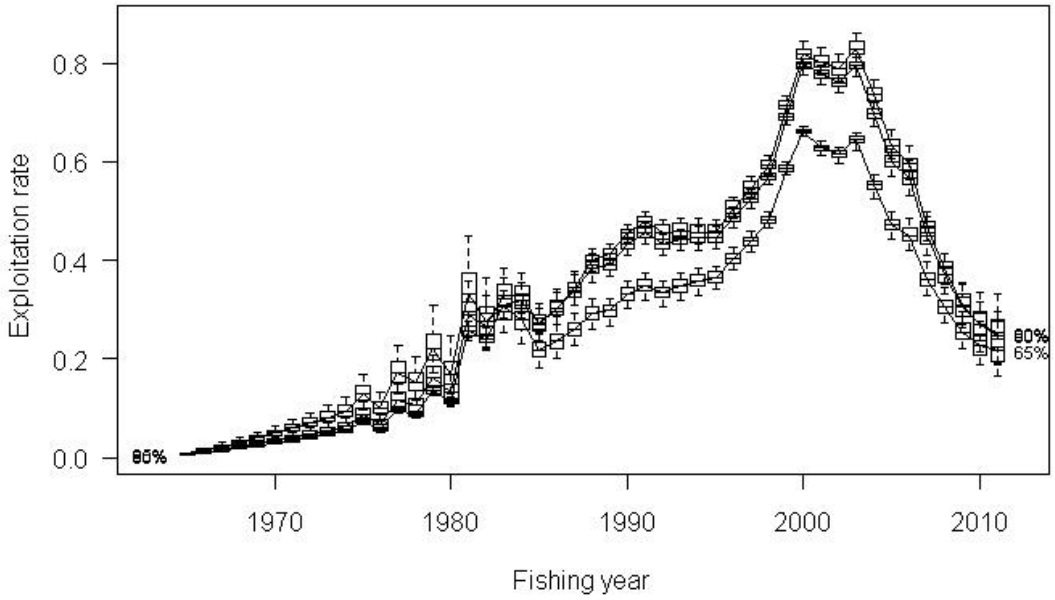

Figure 42: Posteriors of exploitation rate from the MCMC sensitivity trials in which maximum allowed exploitation rate was varied from 80% in the base case to 65% and 90%. The 65% trial is the lowest set of box plots.